NASA Technical Memorandum 81288

Final Reports of U. S. Plant and Radiation Dosimetry Experiments Flown on the Soviet Satellite Cosmos 1129

May 1981

National Aeronautics and Space Administration

NASA Technical Memorandum 81288

Final Reports of U. S. Plant and Radiation Dosimetry Experiments Flown on the Soviet Satellite Cosmos 1129

Milton R. Heinrich and Kenneth A. Souza (Editors)
Ames Research Center, Moffett Field, California

National Aeronautics and
Space Administration

Ames Research Center
Moffett Field, California 94035

TABLE OF CONTENTS

PREFACE

On September 25, 1979, the Soviet Union launched Cosmos 1129, an unmanned spacecraft carrying biological and radiation physics experiments from nine countries, including fourteen from the United States. The launch marked the third time the Soviet Union has flown US experiments aboard one of its unmanned spacecraft. The first two, Cosmos 782 and 936, were launched November 1975 and August 1977, respectively.

Cooperation between the US and USSR in the area of Space Biology and Medicine began in 1971 with the signing of the US/USSR Science and Applications Agreement. A Joint Working Group for Space Biology and Medicine was established and met periodically to exchange information obtained during spaceflights and to discuss problems and topics of mutual scientific interest. In October of 1974, during the fifth meeting of the Joint Working Group, the Soviets offered to fly US experiments aboard an unmanned spacecraft which was scheduled for launch during the winter of 1975. The US accepted this offer and submitted experiment proposals to the Soviets. A group of 11 experiments was selected and subsequently flown on Cosmos 782 which remained in orbit 19.5 days. Since Cosmos 782, the US has flown seven experiments on Cosmos 936 and fourteen experiments on the most recent joint US/USSR venture, Cosmos 1129.

Cosmos 1129, like the Cosmos 782 and 936 flights, contained experiments which were directed at determining the effects of spaceflight on a variety of biological specimens, including animals, plants, and insects. Although all three of these Cosmos flights were unmanned, many of the experiments they contained focused on problems common to both man and animals during prolonged spaceflight. Rats, for example, were used to investigate alterations in normal bone chemistry, muscle structure, and general physiology resulting from spaceflight, alterations that have been observed in both astronauts and cosmonauts during and following stays in space. Rats were also used, together with a variety of other biological and nonbiological material, to measure cosmic radiation and assess its potential hazard to man during prolonged spaceflights.

The scientific results of U.S. experiments flown on Cosmos 1129 are presented in two separate volumes; one entitled, "Final Reports of U.S. Plant and Radiation Dosimetry Experiments Flown on the Soviet Satellite, Cosmos 1129," and the other entitled, "Final Reports of U.S. Rat Experiments Flown on the Soviet Satellite, Cosmos 1129." As evidenced by the scientific results presented in these volumes, the Cosmos 1129 mission has made a substantial contribution to Space Biology and Medicine. In addition, a low-cost systematic approach to the development, testing, and utilization of experimental hardware has been established which will be applied to the preparation of US biological experiments for flight aboard the Space Shuttle. But perhaps the most important result derived from the Joint US/USSR Biological Satellite Program has been the level of international cooperation achieved. American and Soviet scientists and engineers working together overcame the difficulties of language and logistics to conduct spaceflight experiments, share the results, and discuss their significance.

It has been a pleasure to have taken part in this program and, on behalf of all members of the NASA and the scientific community who participated in the Cosmos 1129 mission, I would like to extend our sincere thanks to the Soviet government for making our participation possible and to our Soviet colleagues for their devoted assistance in the execution of our experiments.

Kenneth A. Souza
Manager, Cosmos Project
NASA-ARC

COSMOS 1129 MISSION DESCRIPTION

KENNETH A. SOUZA

MANAGER, COSMOS PROJECT

BIOSYSTEMS DIVISION

NATIONAL AERONAUTICS AND SPACE ADMINISTRATION

AMES RESEARCH CENTER

MOFFETT FIELD, CA 94035

Abstract

On September 25, 1979, the Soviet Union launched Cosmos 1129, an unmanned spacecraft carrying biology and physics experiments from 9 countries including both the Soviet Union and the U.S.A. The launch marked the third time the Soviet Union has flown U.S. experiments aboard one of its unmanned spacecraft; the first was Cosmos 782 in November 1975 and the second, Cosmos 936 in August 1977. All three flights have carried a variety of biological species and remained in orbit approximately 19 days. Aboard Cosmos 1129 were: 1) 30 young male Wistar SPF rats used for a wide range of physiological studies, 2) experiments with plants, fungi, insects, and mammalian tissue cultures; 3) radiation physics experiments; 4) a heat convection study; 5) a rat embryology experiment in which an attempt was made to breed 2 male and 5 female rats during the flight; and 6) fertile quail eggs used to determine the effects of spaceflight on avian embryogenesis. After 18.5 days in orbit the spacecraft landed in Central Asia where a Soviet recovery team began experiment operations within a few hours of landing. Specimens for US experiments were initially prepared at the recovery site or in Moscow and transferred to US laboratories for complete analyses. An overview of the mission focusing on preflight, on-orbit, and postflight activities pertinent to the fourteen US experiments aboard Cosmos 1129 is presented.

Introduction

A series of Soviet Biological Satellites has been launched at approximately 2-year intervals, beginning with Cosmos 605 in 1973. Participation of the United States began in 1975 with the third mission (Cosmos 782), by invitation of the USSR. The fifth and most recent mission, Cosmos 1129, was launched September 25 and recovered 18.5 days later on October 14, 1979 (Table I). The principal objective of the Cosmos missions is to determine the effects of spaceflight on biological materials, focusing on biomedical problems observed in both men and animals during spaceflight and those unique biological questions that cannot be answered on the earth. Areas of special interest include muscle atrophy, space sickness, bone mineral loss, radiation, and plant growth and development. Cosmos 1129 differed from previous missions in providing an opportunity to study the progeny of rats bred during spaceflight and the development of Japanese quail embryos during weightlessness*.

---

*Although the term "weightlessness" is used here and in other reports of this volume, it should be noted that complete weightlessness (the absence of all accelerations) was not achieved. The spacecraft rotated in orbit and imparted accelerations to experiments located at the edge of the spacecraft of 1.7×10^{-7} to 1.5×10^{-4} x g. Accelerations to rats were actually lower because rat holding units were located near the center of the spacecraft. These accelerations are generally thought to be below the threshold of biological sensitivity.

Nine countries participated in the Cosmos 1129 mission. In addition to experiments from the US and USSR, the mission included experiments from Czechoslovakia, France, Hungary, Poland, Rumania, Bulgaria, and the German Democratic Republic. Every attempt was made to maximize the scientific return from the mission and, to this end, investigators from the nine participating countries examined virtually every organ and piece of tissue from all the specimens flown. A short descriptive title and the sponsoring country for these experiments is given in Table 2. Table 3 lists the participating institutions from each country.

The involvement in the mission of scientists from countries other than the USSR was much the same. In nearly all cases, Soviet scientists were trained by the principal investigators to perform preflight and postflight procedures (e.g., drug injections, blood sample collection, tissue removal and preparation), required for various experiments. Following the flight, a team of Soviet scientists and engineers were transported to the satellite landing site where a portable field laboratory was set up. Experimental procedures at the recovery sites were designed to obtain and process specimens to a point where they could be frozen or preserved and subsequently sent to the principal investigators for analysis.

In the following sections of this chapter, a general description of the Cosmos 1129 mission operations, particularly those pertinent to US experiments, is presented and will provide a foundation for understanding and interpreting the reports of US experiments contained in this volume. The pre- and post-flight activities performed in support of non-US experiments, and which had no impact on them, will appear in the Soviet

final mission report and were not included here.

THE SPACECRAFT

A modified Vostok spacecraft similar to that used for previous biological satellites, Cosmos 605, 690, 782, and 936 as well as the early Soviet manned spaceflights, was used for the Cosmos 1129 mission. It was a spherical craft approximately 2.5 meters in diameter with a 900 Kg payload and a gross weight of approximately 2250 Kg (Fig. 1). During flight, the power required by the spacecraft was supplied by batteries. The atmosphere within the craft was maintained at approximate sea level conditions. Total pressure averaged 780 mm throughout the flight, with a pO_2 of 135-212 mm mercury and a pCO_2 of up to 7 mm. Relative humidity within the spacecraft during flight was 56-66%. Gaseous impurities generated within the cabin, e.g., ammonia and methane, were kept at low levels by circulating cabin air through cannisters containing absorbent materials. Ambient temperature within the spacecraft during flight ranged from 22-25.5^{o}C.

Within the spacecraft, biological specimens and experiments were contained in a variety of hardware. Of primary interest to US investigators were the rat holding units (Fig. 2). Rats were held throughout the flight in individual cages, each containing its own light, food, water, air circulating, and waste management systems. Each cylindrically shaped cage was approximately 200 mm deep and 100 mm in diameter. Light was regulated to a 12/12 hour light/dark cycle with a 2-lux intensity within each cage. Ten-gram quantities of a special paste diet were provided to the animals

four times/day at 6-hour intervals throughout the flight. This same diet was provided to both flight and ground control animals. All animals were placed on this diet approximately 10 days before launch and kept on the diet throughout the flight and 29-day recovery phases of the mission. Water was provided ad libitum at all times. Cabin air entered each cage from the rear and was dispersed from the cage ceiling through a series of holes in a plastic cage liner. The air flow passed downward over the animal, forcing animal wastes and debris into a waste collection trap which rotated to present a clean trap to the animal at 2-day intervals. Air passing through the waste trap was then circulated through activated charcoal filters and returned to the cabin. Surrounding the plastic cage liner was a wire coil through which an electric current was passed and changes in current were monitored as the animal moved through the cage and the data used to determine gross motor activity during flight.

In addition to the 30 cages described above, the spacecraft contained a rodent mating chamber which housed 5 female and 2 male rats (Fig. 3). The chamber was partitioned into two sections which segregated the males from the females until day two of flight whereupon two doors in the partition were opened, permitting males and females to mingle. The dimensions of the male chamber were 17.0 cm x 20.0 cm x 16.0 cm, and of the female chamber, 48.0 cm x 20.0 cm x 16.0 cm. Within the chamber the animals had access to 8 feeding stations each of which presented approximately 10 gram aliquots of the standard paste diet at 6 hour intervals throughout the flight. The light/dark regimen was the same as that used for the standard rat cages, 12/12 hours.

Plant specimens and radiation dosimeters were held in special containers designed, fabricated, and tested by the U.S. The hardware was loaded with biology and dosimeters in the laboratories of U.S. investigators and delivered to the Soviet Union shortly before launch. An electronic temperature recorder was developed to record the temperature within the plant experiment containers every 30 minutes throughout the duration of the flight. Detailed descriptions of the hardware and a temperature profile obtained from the electronic temperature recorders are presented in the reports of Baker and Krikorian (this volume).

Payload

The Cosmos 1129 payload consisted of:

- Rats

  Thirty male Wistar specific pathogen free (SPF) rats were obtained from the Institute of Experimental Endocrinology of the Slovakian Academy of Sciences, Bratislava, Czechoslovakia. These animals were used for a wide variety of physiological studies. The rats were approximately 85 days old and weighed an average of 300 gms at the start of the experiments.

  In addition, there were 5 female Wistar SPF rats and 2 males which constituted the rodent embryology experiment. Both males and females were proven breeders and their approximate weights at launch were 340 gms and 260 gms, respectively.

o Plants and Fungi

Carrots (Daucus carota) were used as a substrate for the growth of Crown Gall tumors and as a source of totipotent single cells and small plantlets. Tumor growth was used to assess the effects of spaceflight on the rate of cellular metabolism. The carrot cell culture was used to determine if spaceflight affected plant growth and development. Full reports of these two U.S. experiments are presented in this volume.

In Soviet experiments, small sprouts (Arabidopsis thaliana) and corn seedlings (Zea mays) were flown to investigate the growth and development of these species. A multinucleated fungus (Physarum polycephalum) was flown to determine if fungal migration over the solid surface of the growth medium was affected by weightlessness.

o Insects

A gravity-gradient experiment with the fruit fly, Drosophila melanogaster was designed by Soviet scientists to determine if a gravity preference could be detected in this species. Drosophila eggs were placed in a feeding dish at the hub of a centrifuge (Fig. 4). Connecting the hub to the perimeter of the centrifuge were four tubes inside of which were three food dishes placed along the tube so that when the centrifuge rotated at 53 rpm the gravity levels at the three dishes were 0.3g, 0.6g and 1.0g. Flies hatched on the first day of flight were free to move along the tubes and select the feeding site of

preference. Post flight the quantity of eggs and pupal cases found in each feeding dish showed that there was no gravity preference.

- Japanese Quail

Fertilized eggs of the Japanese Quail (Coturnix coturnix) were flown to determine the effects of spaceflight on avian embryological development.

- Mammalian Cell Cultures

Cultures of Chinese hamster and mouse cells were used to determine if weightlessness and/or radiation experienced during spaceflight affected their metabolism and reproduction.

- Radiation Physics Experiments

Radiation physics experiments consisted of dosimetry using biological and nonbiological materials to measure the radiation environment inside and outside the spacecraft, and radiation shielding studies to evaluate electrostatic and dielectric techniques for reducing the level of cosmic radiation within the spacecraft.

- Heat Exchange Experiment

An experiment was designed and flown to study the process of heat exchange between a heated surface and the spacecraft cabin air during spaceflight.

MISSION OPERATIONS

In support of the investigations aboard the spacecraft, two different types of ground controls were performed: the Synchronous Control and the Vivarium Control. The Synchronous Control attempted to provide an environment as similar as possible to that experienced by the biological specimens during spaceflight. A spacecraft mockup was loaded with all of the experiments and specimens were housed in the same type of hardware as that used for flight (Figure 5). Food, water, lighting, temperature, humidity, and airflow were similar for both flight and control groups.

Five days after launch, the Synchronous Control was initiated (September 30, 1979). Specimens were subjected to launch stresses similar to those experienced during the actual launch. The noise level was raised to 110 db and a vibration frequency of 50-70 Hz at an amplitude of 0.4 mm was applied to specimens for 10 minutes. Immediately following noise and vibration stresses, specimens were subjected to acceleration for a period of 10 minutes with a plateau of 4 x g for 7 minutes.

After completion of the Synchronous control on October 19, 1979, reentry stresses were applied to the plant specimens and most of the groups of rats. They were first accelerated for 5 minutes to a plateau of 6 x g for 3 minutes and subsequently subjected to an impact shock with a magnitude of 50 x g and a duration of 10 msec. Following the application of reentry stresses, the specimens were handled exactly as the flight specimens during the postflight period.

The purpose of the Vivarium control was to provide a group of minimally stressed animals for comparison with the Flight and Synchronous Control groups. Animals were housed individually in polyvinyl cages (18 x 18 x 12.5 cm) and maintained in that arrangement throughout the flight and postflight periods. Neither U.S. plant experiment utilized the Soviet vivarium for control studies; however, special controls were set up at other laboratories in Moscow and in the investigators laboratories (see final reports in this volume for details).

Prelaunch Activities

Wistar SPF male rats which comprised the reservoir of experimental animals, were shipped from the Institute of Endocrinology, Slovakian Academy of Sciences, Bratislava, Czechoslavakia to Moscow during August 1979. In Moscow the animals were placed in a vivarium at the Institute of Biomedical Problems with approximately 5 rats per cage, held at an ambient temperature of 22 $\pm$ 2°C, a relative humidity of 80 $\pm$ 5% and a 12-hour light day.

During the preflight period, radiation dosimeters were fabricated and assembled in the U.S., carrot slices were infected with crown galls and loaded into containers, and carrot tissue cultures were grown and loaded into spaceflight hardware. Plant material was shipped to the USSR in special incubators designed to maintain the specimens at 4 $\pm$ 2°C in order to retard growth and development until launch. Radiation dosimeters were handcarried to Moscow, loaded together with Soviet dosimeters into special containers and mounted inside and outside the spacecraft. Three days before launch, plant and dosimetry material was placed onboard the

spacecraft.

On-Orbit Activities

On September 25, 1979, at 6:30 p.m. (Moscow time), Cosmos 1129 was launched into an elliptical orbit with a perigee of 226 km, an apogee of 406 km, an orbital inclination of 62.8°, and a period of 90.5 minutes. Five days later, on September 30, the Synchronous Control was initiated.

During the 18.5 day flight, animals were fed 10g quantities of the paste diet four times daily and given water ad libitum. Total gross body movement of the Flight and Synchronous Control animals was monitored for 2 hour blocks of time on odd-numbered days throughout the flight phase of the mission. Body temperature was obtained from the animals by bio-telemetry on even-numbered flight days. On the second day of the flight, the divider separating male and female rats in the rat embryology experiment was opened and remained opened throughout the remainder of the mission. On the seventh day of flight the temperature of the quail egg incubator was elevated from the spacecraft ambient of 22-25°C to approximately 37°C. Simultaneously, the relative humidity in the incubator was raised to about 80%. Unfortunately, the humidity control system failed in the flight incubator on day thirteen of flight resulting in a serious drop in the humidity which detrimentally affected the developing embryos.

On flight day 10, the light/dark cycle was reversed in the cages of 5 animals. The reversal was accomplished by subjecting the animals to 24 hours of darkness. This shift in the light/dark cycle was performed as

part of a study to determine if spaceflight affected the biorhythm of these animals and their ability to adapt to an altered day/night cycle. After the flight, these animals were maintained at the inverted light regime.

Postflight Activities

On October 14, 1979, at 7:59 a.m. (Moscow time), Cosmos 1129 touched down near the central Asian city of Kustanay. Within several hours a recovery team consisting of Soviet scientists and engineers arrived at the scene and began assembling a field laboratory (Figs. 6 and 7). The general condition of animals and other biological material postflight was good. The rats gained an average of 47 gms during the flight as compared to 54 and 59 gms for Synchronous and Vivarium control animals, respectively.

Only 7 rats were autopsied at the recovery site. Autopsies began at 1:50 p.m. and each autopsy took approximately 30 minutes. All scientific studies including removal and processing of plant material and dosimeters were completed in less than 18 hours whereupon the recovery team, specimens, and equipment departed the recovery site and arrived in Moscow in the afternoon of October 15.

On October 19, the flight phase of the Synchronous control was completed and the same recovery team that processed the flight specimens also processed the controls. Autopsies of the animals were begun at 10:04 a.m. and completed by 4:42 p.m. (Moscow time) and the experimental procedures employed at the recovery site were again followed. Animals not sacrificed at this time were transferred to the Vivarium and treated like the flight

animals throughout the readaptation period.

Upon completion of the unique operations at the recovery site required by the animal, plant and radiation dosimetry investigators, the specimens were packed for shipment to the appropriate U.S. laboratories according to procedures worked out in advance between Soviet and US mission managers: specimens were packed in dry ice, immersed in a preservative, or brought back alive at $4^{o}C$ (plants). Specially designed shipping containers were developed to maintain the temperature requirements and integrity of the specimens during transit. On October 29, US specimens and scientists arrived in San Francisco and specimens were transferred to the laboratories of US investigators.

Two weeks after the arrival of the specimens in the US, a second group of US scientists was sent to Moscow to attend the autopsies and experimental operations of the animals allowed to readapt to terrestrial gravity. The same autopsy procedures and team members were utilized for both recovery and readaptation studies. Autopsies of the Flight, Synchronous Control and Vivarium Control animals occurred on November 12, 17, and 12, respectively. Samples were again escorted by US scientists back to the US and arrived in San Francisco on November 20, 1979. Temperature recorders contained in all shipping containers indicated that the temperature in all but one container remained within specifications throughout both recovery trips. The exception occurred in a container of preserved Group 4 specimens of some bone and nasal mucosae. In this case a small quantity of dry ice was added to the shipping container by overzealous cargo handlers in Tokyo. This resulted in the temperature dropping below the specified $0^{o}C$ for a few

hours during the Tokyo to San Francisco flight. Fortunately, damage to the specimens was minimal.

With the return of the experimental samples and materials on November 20, the mission operations phase was brought to an end. For the many investigators involved in the US experiments aboard Cosmos 1129, their work was just beginning, the results of which are contained in the reports which follow.

Acknowledgements

A special thanks is owed to the many individuals who contributed to the success of the US experiments flown on Cosmos 1129, especially to the extremely cooperative group of principal investigators and their experiment teams who worked so diligently in the preparation and execution of their experiments, the small but dedicated group of US Project personnel whose careful attention to detail overcame the tremendous logistics and management problems inherent in an international mission of this nature, and lastly to our Soviet colleagues for their superb assistance in the execution of the US experiments.

TABLE 1

SOVIET BIOLOGICAL SATELLITE MISSIONS

MISSION PARAMETERS	COSMOS-605	COSMOS-690	COSMOS-782*	COSMOS-936*	COSMOS 1129*
LAUNCH DATE	31 OCT '73	22 OCT '74	25 NOV '75	3 AUG '77	25 SEP '79
RECOVERY DATE	22 NOV '73	12 NOV '74	15 DEC '75	22 AUG '77	14 OCT '79
MISSION LENGTH	22 DAYS	20.5 DAYS	19.5 DAYS	18.5 DAYS	18.5 DAYS
PERIOD OF REVOLUTION	90 MIN.	89.6 MIN.	90.5 MIN.	90.7 MIN.	90.5 MIN.
APOGEE	424 KM	389 KM	405 KM	419 KM	406 KM
	(261 MI)	(241 MI)	(251 MI)	(260 MI)	(252 MI)
PERIGEE	221 KM	223 KM	226 KM	224 KM	226 KM
	(135 MI)	(137 MI)	(140 MI)	(139 MI)	(140 MI)
ORBITAL INCLINATION	62.8^{o}	62.8^{o}	62.8^{o}	62.8^{o}	62.8^{o}

*U.S. PARTICIPATION IN MISSION

TABLE 2

DESCRIPTIVE TITLES, SPONSORING COUNTRIES, AND PRINCIPAL INVESTIGATORS FOR THE EXPERIMENTS OF COSMOS 1129

	TITLE	COUNTRY/PRINCIPAL INVESTIGATOR
I.	EXPERIMENTS WITH RATS	
	1. Whole Body Composition	USSR/A. Ushakov USA/G. Pitts
	2. Studies of the Central Nervous System	Czechoslovakia/S. Baransky USSR/R. Tigranyan
	3. Endocrine Studies	Czechoslovakia/R. Kvetnansky USSR/R. Tigranyan Bulgaria/*
	4. Studies of the Cardiovascular System	Czechoslovakia/S. Baransky USSR/R. Tigranyan
	5. Studies of the Musculo-Skeletal System	USSR/V. Oganov S. Oganesyan V. Nesterov E. Kovalenko G. Stupakov A. Prokhonchukov R. Tigranyan USA/ E. Morey Wolton L. Kazarian D. Simmons C. Cann Hungary/T. Szilagyi
	6. Blood and Bone Marrow Studies	Czechoslovakia/N. Ahlers E. Mishurova N. Chernaya I. Alers A. Bacek USSR/R. Tigranyan L. Serova V. Korol'kov Bulgaria/*

*Principal Investigator not known

TABLE 2 (Continued)

7.	Studies of Lymphoid Organs	Czechoslovakia/I. Alers E. Mishurova USSR/I. Egorov L. Serova
8.	Studies of Connective Tissue	USSR/L. Serova Bulgaria/*
9.	Studies of the Hepatic System	USA/ S. Abraham USSR/R. Tigranyan I. Egorov Czechoslovakia/I. Alers
10.	Excretory System Studies	USSR/M. Natochin A. Pankova
11.	Adipose Tissue Studies	Czechoslovakia/I. Alers USSR/R. Tigranyan
12.	Studies of the Gastrointestinal Tract	USSR/K. Smirnov Rumania/P. Groza
13.	Studies of Sensory Organs and Mucosae	USSR/F. Sushkov USA/ L. Kraft
14.	Embryological Studies	USSR/L. Serova N. Chel'naya V. Yagodovsky V. Oganov Yu. Natochin Z. Apanasenko
15.	Embryological Studies	USA/ J. Keefe S. Abraham E. Sabelman Bulgaria/A. Vyglenov Poland/V. Stodolnik-Baranskaya S. Kozlovsky K. Ostrovsky

II. EXPERIMENTS WITH PLANTS

1.	Studies of Carrot Crown Gall Tumor Growth	USA/ R. Baker USSR/M. Gusev
2.	Studies of Carrot Tissue Culture Morphogenesis	USA/ A. Krikorian

*Principal Investigator not known

TABLE 2 (Continued)

	3. Studies of Higher Plant Morphogenesis	USSR/M. Tairbekov
	4. Studies of Fungal Surface Migration	USSR/M. Tairbekov
III.	EXPERIMENTS WITH INSECTS	
	1. *Drosophila melanogaster* Gravity Preference	USSR/*
IV.	EXPERIMENTS WITH BIRDS	
	1. Study of Embryogenesis in the Japanese Quail	USSR/Y. Shepelev USA /J. Keefe
V.	EXPERIMENTS WITH MAMMALIAN CELL CULTURES	
	1. Cytological Studies of Mammalian Cell Cultures	USSR/*
VI.	RADIOBIOLOGICAL RESEARCH	
	1. Bioblock Studies	USSR/E. Kovalev France/Planel
	2. Radiation Dosimetry	USSR/E. Kovalev USA/ E. Benton

*Principal Investigator not known

TABLE 3

LIST OF SCIENTIFIC INSTITUTIONS PARTICIPATING IN THE EXPERIMENTS OF COSMOS 1129

INSTITUTION	COUNTRY
NASA-Ames Research Center	USA
Colorado State University	USA
University of Delaware	USA
State University of New York, Stony Brook	USA
University of California, San Francisco	USA
Veterans Administration Hospital, American Lake	USA
University of Utah	USA
Baylor University Medical Center	USA
University of the Pacific Dental School	USA
Columbia University	USA
Wright-Patterson Air Force Base	USA
University of Southern California Medical Center	USA
Jet Propulsion Laboratory	USA
University of San Francisco	USA
Washington University School of Medicine	USA
Yale University	USA
Children's Hospital Medical Center, Oakland	USA
Biospace Incorporated, Ohio	USA
University of Virginia	USA
University of California, Berkeley	USA
University of California, Davis	USA
Institute of Medical and Biological Problems, USSR Ministry of Health	USSR
Institute of Evolutionary Physiology and Biochemistry, USSR Academy of Sciences	USSR
Bach Institute of Biochemistry, USSR Academy of Sciences	USSR
Pavlov Institute of Physiology, USSR Academy of Sciences	USSR
Central Dental Research Institute, USSR Ministry of Health	USSR
Priorov Central Institute of Traumatology and Orthopedics Research, USSR Ministry of Health	USSR
Central Institute of Gastroenterology Research, Moscow Municipal Executive Committee of the Council of Workers' Deputies	USSR
Institute of Medical Radiology, USSR Academy of Medical Sciences	USSR
Institute of Nutrition, USSR Academy of Medical Sciences	USSR
Sklifasovsky Central First Aid Institute, RSFSR Ministry of Health	USSR
Institute of Cardiology, Armenian SSR Ministry of Health	USSR
Bratislava Institute of Experimental Endocrinology, Slovakian Academy of Sciences	Czechoslovakia
Shafarik State University, Kosice	Czechoslovakia
Military Institute of Aviation Medicine, Warsaw	Poland

TABLE 3 (Continued)

INSTITUTION	COUNTRY
Bucharest Institute of Physiology	Romania
Institute of Roentgenology and Radiobiology, Sofia Medical Academy	Bulgaria
Institute of Physiology, Debrecen Medical College	Hungary
Institute of Pathophysiology, Debrecen Medical College	Hungary
Szeged Institute of Biochemistry	Hungary
Humboldt University	GDR

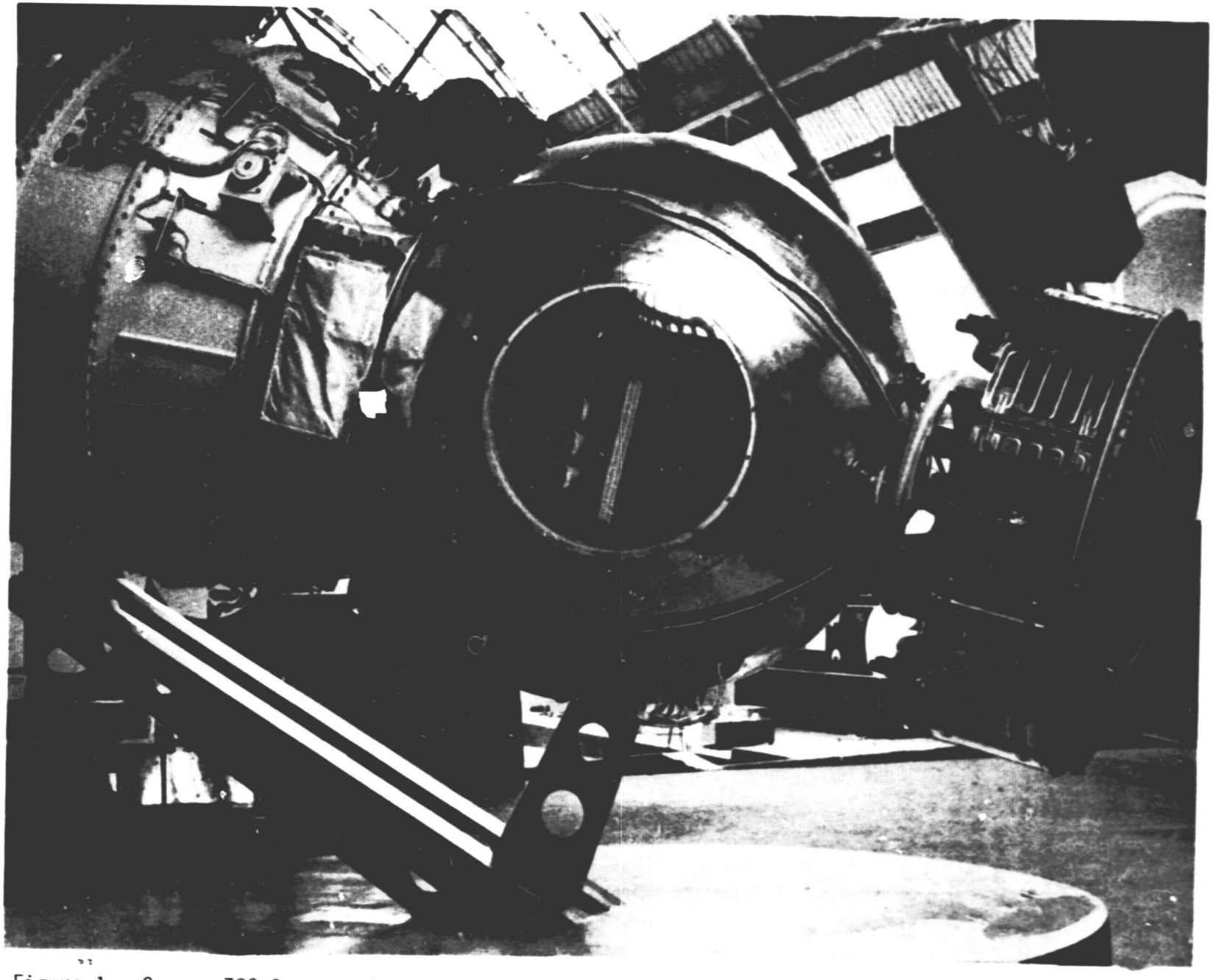

Figure 1. Cosmos 782 Spacecraft on display in the Space Museum. Astakeno, USSR. A circular viewport was installed in the spherical craft when placed on display in the museum.

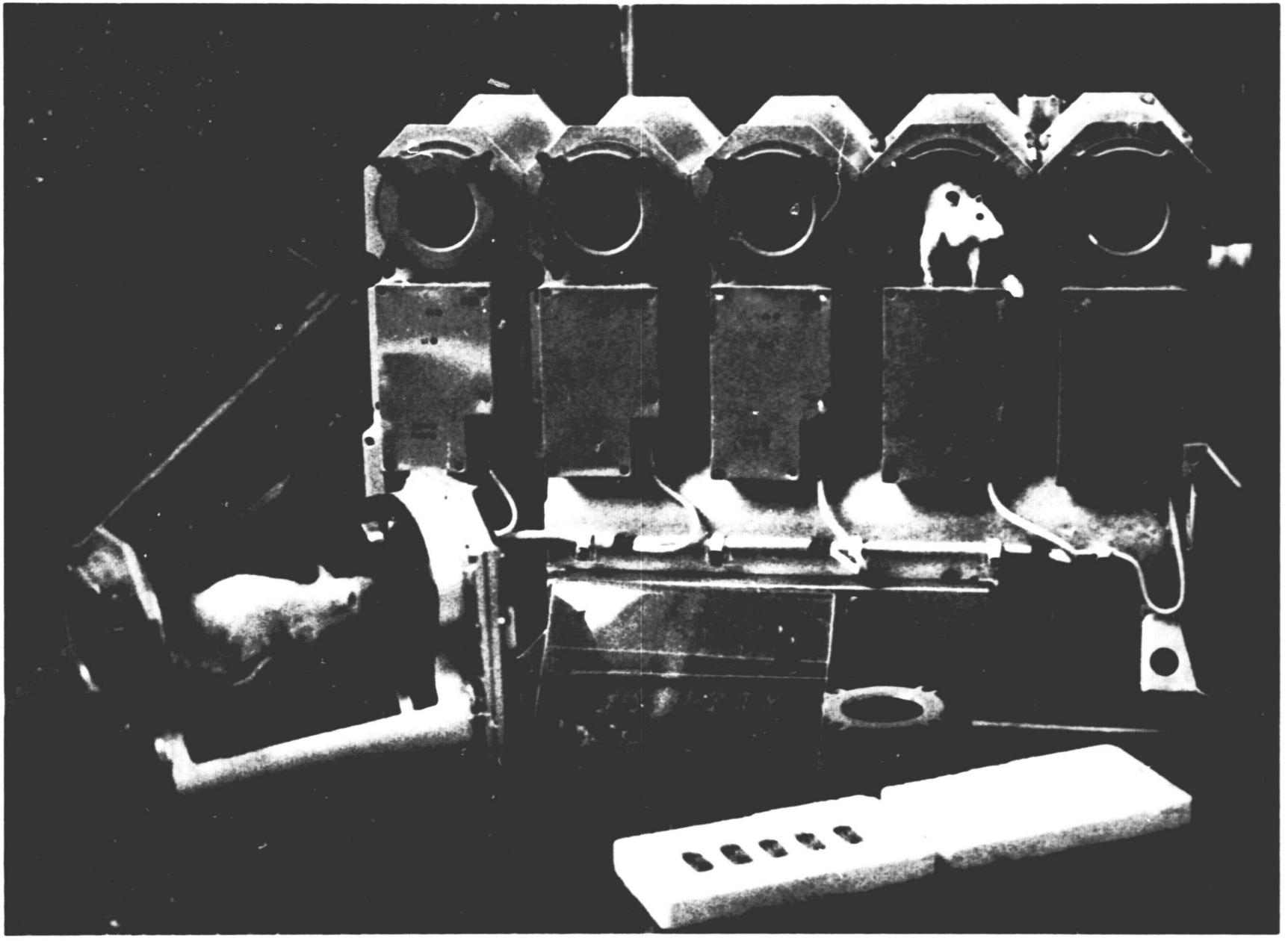

Figure 2. Rat cages of the type flown on Cosmos 1129. Cages are placed aboard the spacecraft in blocks of five cages. The cages in a block share food and water reservoirs.

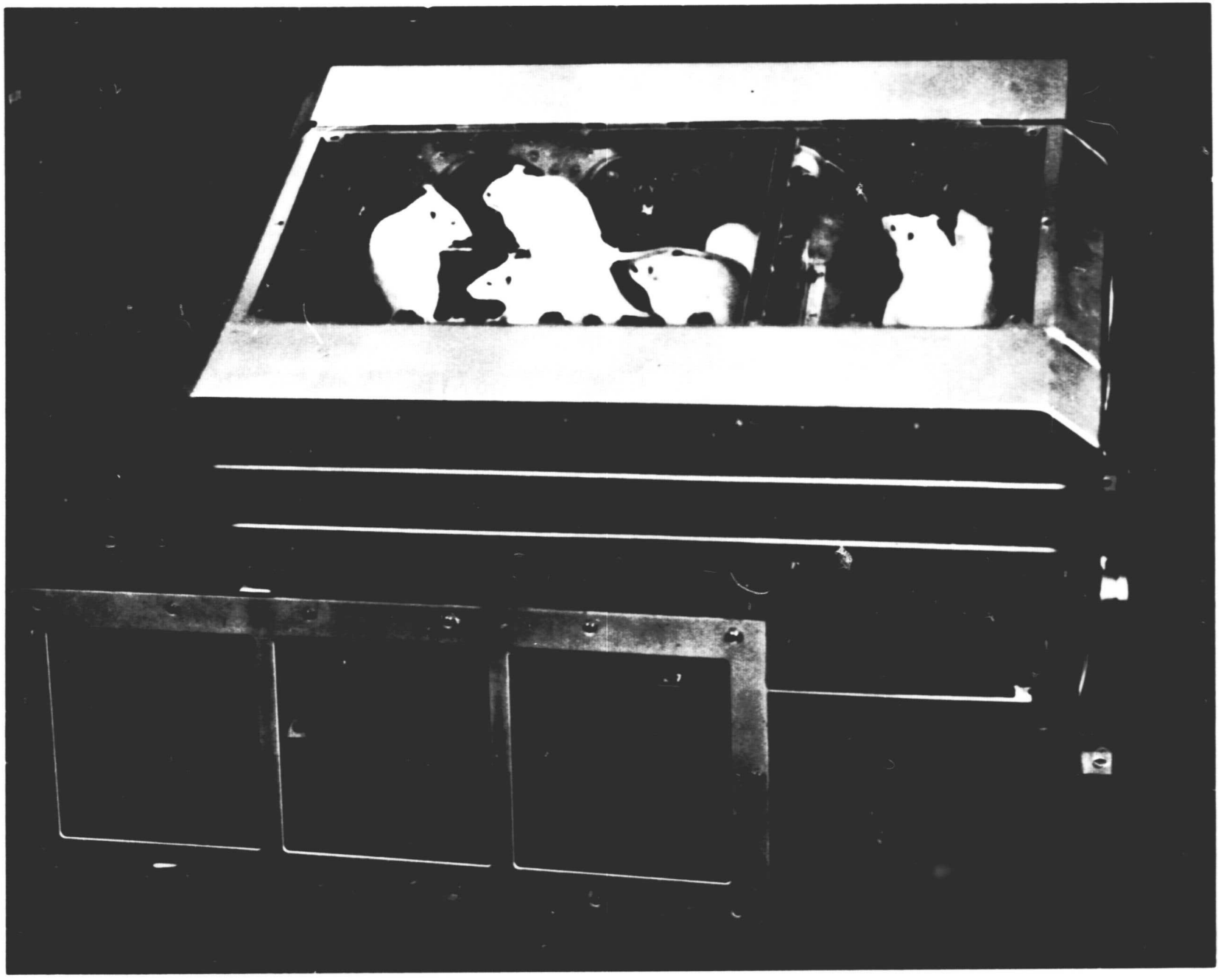

Figure 3. Rat breeding chamber of the type flown on Cosmos 1129.

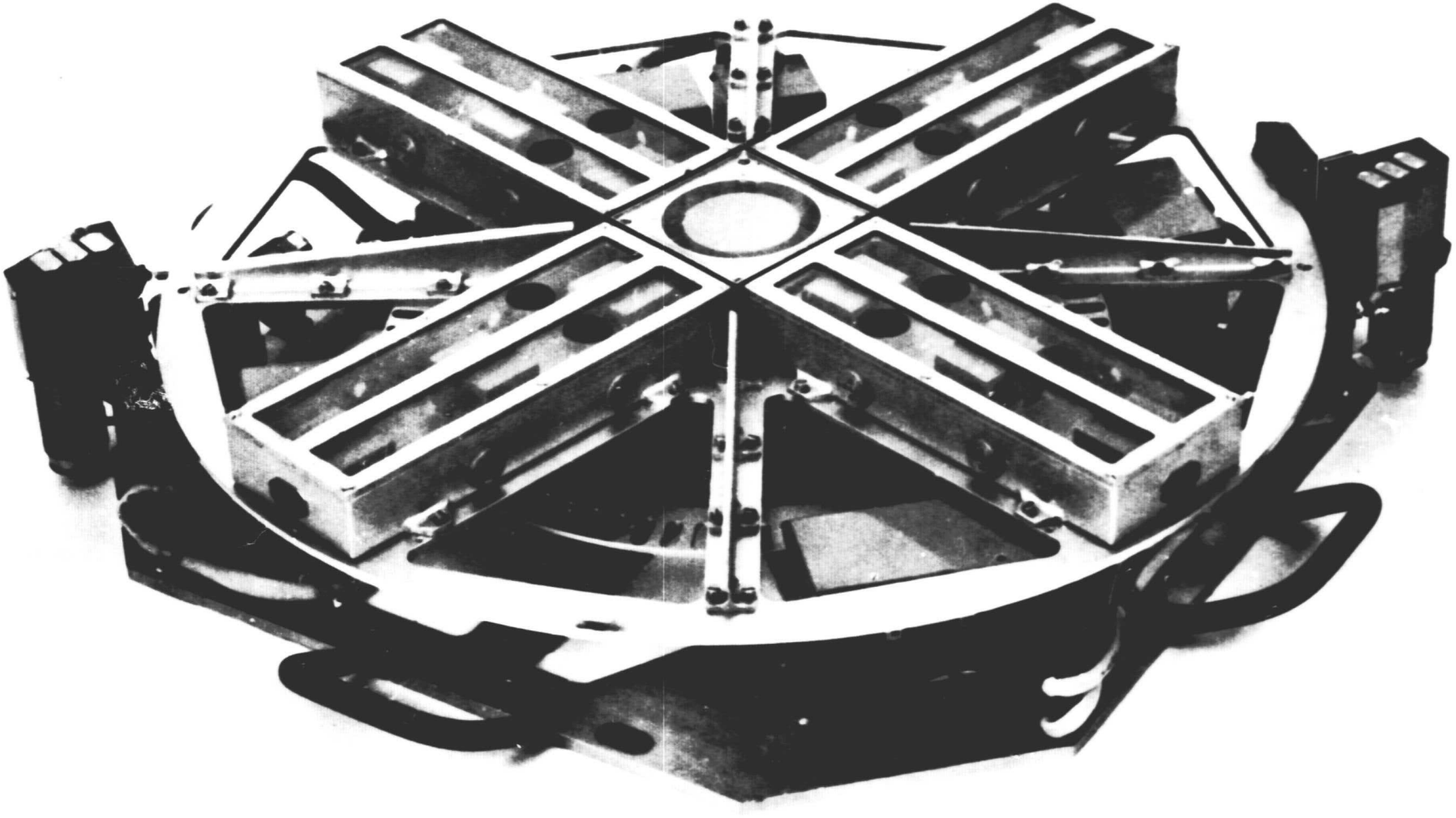

Figure 4. Cosmos 1129 centrifuge used to create a gravity gradient for an experiment with the fruit fly, Drosophila melanogaster.

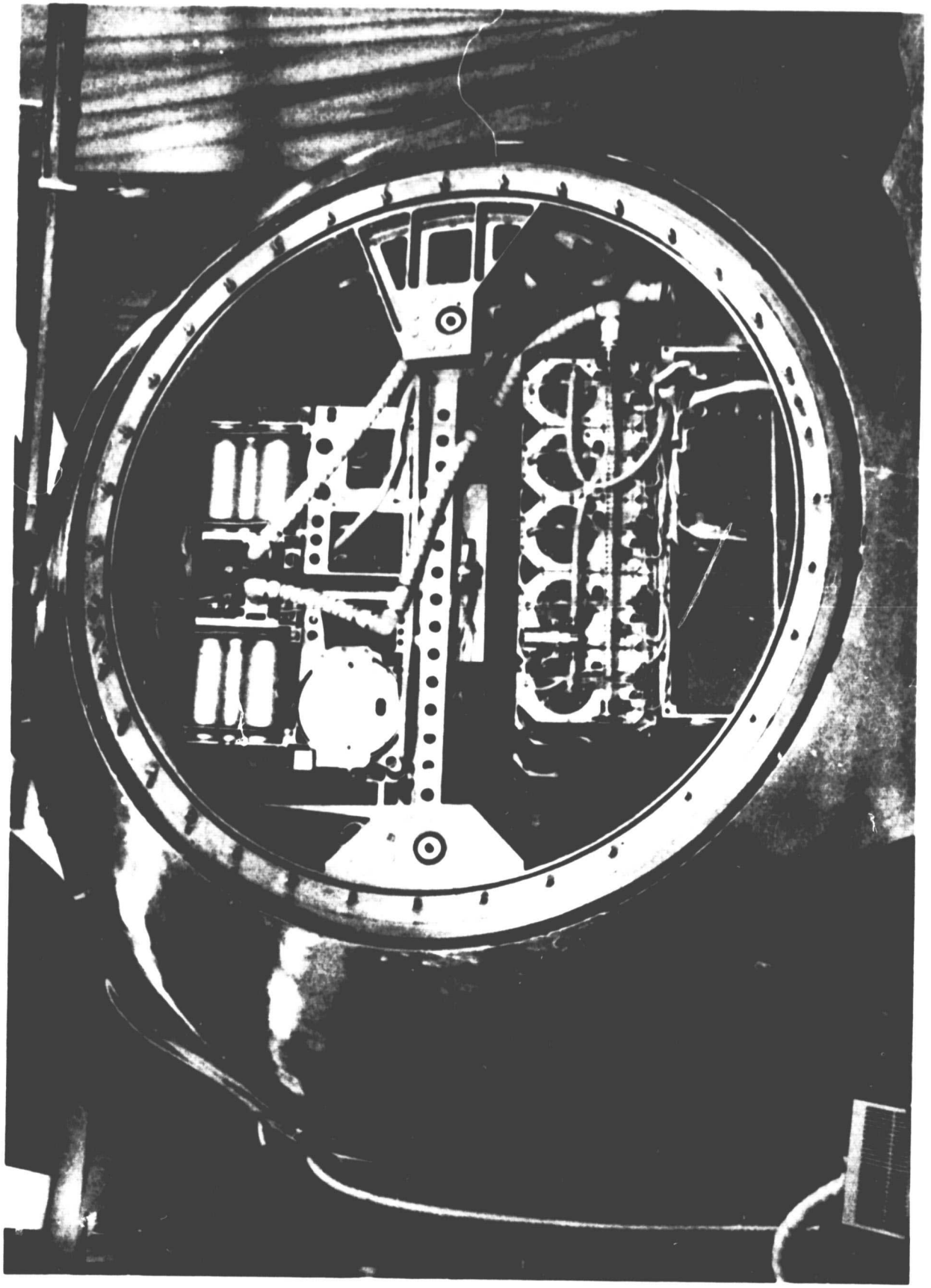

Figure 5. Spacecraft mockup used to conduct the Synchronous ground control.

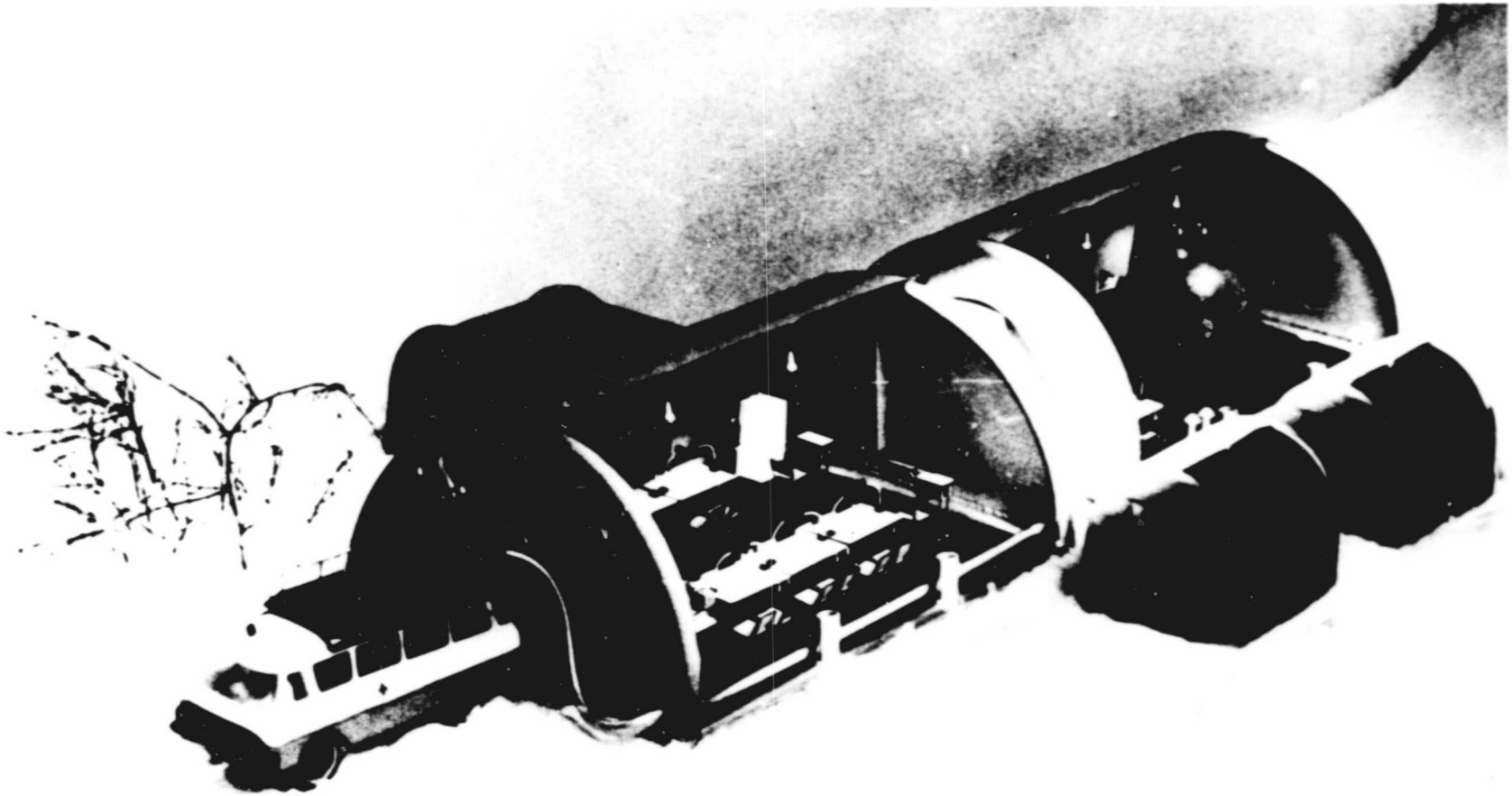

Figure 6 - Model of the field laboratory set up at the spacecraft recovery site. Electric generators and environmental control equipment provide the necessary conditions for the initial observation and examinations of biological specimens.

Figure 7 - Recovery team in the process of performing an autopsy and experimental procedures following the completion of the Synchronous Control experiment.

Experiment Number K301

LONG-TERM EFFECTS OF WEIGHTLESSNESS ON A BIOLOGICAL SYSTEM

Ralph Baker

Botany and Plant Pathology Department

Colorado State University

Fort Collins, CO 80523

John Hendrix

Botany and Plant Pathology Department

Colorado State University

Fort Collins, CO 80523

Charles R. Curtis

Plant Science Department

University of Delaware

Newark, DE 19711

SUMMARY

Tumors of crown gall were generated in the space environment. Weights of tumors produced on the spacecraft were not significantly different from those developing at 1 g. Gravity compensated tumors, however, were significantly larger, which confirms previous experimentation. This suggests that subjecting plant material to clinostat rotation does not simulate weightlessness. Carbohydrate analysis of the disks supporting the growth of the tumors under various gravity treatments also suggests that gravity compensation is not comparable to weightlessness.

INTRODUCTION

Plants orient to the direction of the gravitational field and contain supporting structures made necessary by the presence of gravity. Even so, only two gross responses of plants to gravity are known. The first is geotropism. It is difficult to construct a rationale for performing experiments in expensive biosatellites to elucidate this phenomenon. The principal unknown factor in this discipline is the nature of gravity perception, and basic research on related questions (e.g. threshold response) can and has been performed adequately in ground-based experiments. The second response is related to the increased metabolic activity associated with gravity compensation (3). This is thought to be due to the orientation of protoplasmic inclusions in a g force field. These inclusions (starch grains) are precipitated and so concentrated in a 1 g force field that metabolic, rate limiting concentration gradients occur. Rotation on a clinostat, however, results in more uniform spatial distribution of gravity perceptible inclusions, and limitation of metabolic rate by concentration gradients in the cells is minimized. This results in increased metabolic activity when plant

material is gravity compensated. Gordon and Shen-Miller (4) in reviewing this hypothesis reserved judgement until unknown effects of reorientation shear (due to sagging of shoots on the clinostat during rotation) are known. Our work with rigid carrot material (7, 11), however, suggests that stress phenomena associated with rotation are not entirely responsible for enhanced metabolism.

It has been hypothesized that a weightless environment might be simulated on earth by rotating plants slowly on clinostats so that gravity compensation occurs. Characteristics observed in plants on clinostats (4, 10) include changes in sensitivity to geo- or photostimulation, redistribution of cellular organelles, changes in metabolism, twisting and other abnormal effects on gross morphology, decrease of incubation period for bean rust (2) and effects on cellular and tissue (7) morphogenesis.

Are clinostat responses identical to those observed under conditions of weightlessness? An answer to this question was considered to be of high priority for evaluation of expected responses to weightlessness (9). Certainly different responses would be expected for whole plants on clinostats because of mechanical stresses placed on leaves and stems during rotation (10), but does this method of gravity compensation simulate weightlessness at the cellular level or in a rigid plant system, e.g. a tissue culture?

With these questions in mind, we undertook the development of a biological system with the capacity to answer the most pertinent questions being considered (9) regarding the long-term effects of weightlessness on plant metabolism, cellular and tissue morphology, and physiology. A system involving the generation of crown gall tumors induced by Agrobacterium tumefaciens (E. F. Sm. & Towns.) Conn. on root disks of carrot (Daucus carota L. var.

sativa DC) was developed (11) which was responsive to gravity treatments (5, 7). Thus, measurable parameters of responses to gravity compensation could be established in ground-based experiments. In addition, there were other advantages that made the system desirable for use in biosatellite experiments. It was flexible, insensitive (within broad limits) to launch holds, capable of being stored for long periods with little reduction in experimental efficiency, required no attention during flight, operated without spacecraft power or telemetry (other than monitoring of environmental factors), and was impervious to the physical insults associated with launch and recovery.

MATERIALS AND METHODS

Carrots were cross-sectioned and suspended aseptically with gnotobiotic techniques (8). In addition two pieces of each carrot, one apical and one basipetal to the experimental pieces, were retained to establish the original carbohydrate concentrations in each carrot separately. These are referred to elsewhere as "untreated." In these experiments, the top surface of the carrot disks was the apical facing surface in all cases. Water agar was poured on plastic support plates of the flight canister (Fig. 1) to maintain a high relative humidity and to seal the suspended carrot sections. The top surfaces of the sections were inoculated with bacterial suspensions (1×10^8 cells/mℓ) of Agrobacterium tumefaciens grown on Stoner's glutamate medium. Each disk received 0.2 mℓ of suspension. Four dishes were stacked in each canister and there were four carrot disks in each dish. The inoculated disks in the canisters were incubated at 25 C for 72 hr to allow initiation of tumors. At the end of this period, they were placed in environmental chambers maintained at 4 C for transport to the Soviet Union. This temperature

was maintained until shortly before launch. Each treatment consisted of two canisters (a total of 32 carrot disks) contained within a specially prepared box designed for placement in the spacecraft (Fig. 2).

As controls, canisters comparable to those in flight were oriented vertically or horizontally with respect to gravity, or rotated on "single axis" clinostats either vertically or horizontally (gravity compensated) at Colorado State University, Fort Collins, CO. Ground controls (hereafter designated as synchronous controls) also were located in a mock-up spacecraft in the Soviet Union. Upon recovery from the spacecraft in the Soviet Union or from ground controls, tumors and disks were either quick-frozen for isozyme and carbohydrate studies or (after transport to the U.S. at 4 C) killed and fixed with formalin-alcohol-acetic acid (FAA) fixative for anatomical studies. Frozen tumors were lyophilized, weighed and stored at -20 C until assayed.

Each carrot disk was separated into stele and cortex, freeze-dried, and weighed. Half of each of these disk pieces were retained at C.S.U. for carbohydrate studies. The remainder went to the University of Delaware for isozyme analysis.

Carbohydrate Analysis. The freeze-dried carrot disk pieces were extracted with 20 mℓ of 80% ETOH in a microsoxhlet extractor for 3 hr. It was determined earlier that 3 hr was sufficient for extraction of sugars.

A reducing sugar analysis was run by the method of Avigad (1). The extraction liquid was diluted with 80% ETOH as necessary to obtain a concentration of reducing sugars within the sensitivity range of the procedure. The dilution factor and the weight of the disk were accounted for when calculating the final concentration of reducing sugars present in the carrot disk.

A second aliquot of extractive solution was used for nonreducing sugar analysis. It was hydrolyzed to reducing sugars by drying 1 mℓ aliquots of diluted aliquot of the extraction and adding 1 mℓ of 2 M trifluoroacetic acid to each sample (6). The resultant solution was air dried. The dry sugars were dissolved in 2 mℓ water. This was divided into two equal parts for replicate analyses using the methods described above for reducing sugars. To obtain the values for nonreducing sugars, the values obtained for each sample for reducing sugars was subtracted from the results obtained in this step.

To measure the amount of starch present, small pieces (.001-.006 g) of the freeze dried disks were cut and shredded with a scalpel. These were placed in individual test tubes containing 5 mℓ of a suspension of α amylase (4.5 units/mℓ) in 0.03 M sodium phosphate buffer at pH 5.8. The carrot pieces were then vacuum infiltrated. Samples were held at 35 C in a water bath and were stirred continuously by micro magnetic stirring bars. After 72 hr, aliquots were taken, diluted, and analyzed for reducing sugars as described above. Dilution factors and weight of the shredded sample were accounted for when calculating the final concentration of starch in the sample.

RESULTS

Experimental material generated on the flight and received at CSU was not uniformly in good condition. There was some contamination and also evidence of drying in the upper dish from which tumors for anatomical studies were to be taken. Thus, this phase of the study was abandoned. In other cases some of the 1 g treatments were eliminated when there was insufficient tissue for analysis; however, there was always one ground control treatment

available for comparisons.

There was no significant (P = 0.05) difference between the weight of tumors produced at 1 g and in flight (Fig. 3). Gravity compensation, however, induced tumors with significantly increased weight compared with flight-generated tumors.

The values exhibited in Fig. 4 and 5 were obtained in the following manner. For each piece of carrot tissue, the "reducing sugars to starch" and "nonreducing sugars to starch" ratios were determined. The ratio so obtained for untreated disks of each carrot was subtracted from the similar ratio for the treated disk of the same carrot. This yielded the change in these ratios for each carrot from the start until the end of each experiment. Statistical analysis was done on the values so obtained. If the value was positive, the soluble components were depleted by the treatment, proportionately more than the starch. However, if the value was negative, starch was depleted proportionately more than the soluble component. Data are reported only for the cortex portions of each disk because no differences were found for the stele portions.

Using these comparisons, the change in ratio for reducing sugars/starch for the horizontal stationary is significantly different from those ratios for the flight material and horizontal rotated (gravity compensated) at the 5% level of confidence. However, the ratios for these latter two are not significantly different.

For nonreducing sugars/starch, the change in ratio for the flight material is significantly different from the horizontal stationary at the 5% level of confidence. The change in ratios for the horizontal rotated and horizontal stationary are statistically different only at the 10% level

of confidence. Again, no difference was found between the flight and the horizontal rotated.

Carbohydrate data were collected for other treatments, but were not reported because either tumor growth was minimal, so no interpretation could be made, or, in one case (synchronous control), the wrong package was used so we had no zero time tissue for comparison.

DISCUSSION

In the Kosmos 782 experiments, tumors developing in the weightless environment were smaller than those generated on a 1 g centrifuge in space. In repeated experiments on the ground (11), tumor weights were consistently greater under gravity compensation than at 1 g. While the present experiment did not have a centrifuge treatment in the spacecraft, trends were essentially the same, that is, tumors generated in weightlessness were significantly smaller than those under gravity compensation. Gravity compensation is believed to induce increased metabolic activity (3) due to the orientation of cellular substrates. While orientation of cellular organelles in weightlessness may be comparable to those in cells being gravity compensated, the results of the tests indicate that there is no increase in metabolic activity (as reflected in tumor size) when tumors are generated in the space environment as compared with those developing at 1 g. There is no current body of theory to explain this result.

Unlike the results for tumor growth, the analyses of the change in carbohydrate levels are similar for the horizontal rotated and the flight material. This is surprising, for soluble carbohydrates must have been supplied to the tumors for growth. In addition to the statistical difference indicated above, it is also of interest that the change in ratios for the

horizontal rotated and the flight material were both positive, indicating the soluble components were depleted relatively more than the starch. However, the results for the horizontal stationary are negative, indicating that the starch was proportionately more depleted by the treatment than the soluble sugars.

This lack of correspondence between the results for tumor growth and carbohydrate utilization is not understood, but does indicate that one should be cautious in assuming that one, or a few tests can indicate the validity of using a clinostat in simulating weightlessness. It is our conclusion that weightlessness is not simulated by a clinostat. This conclusion is supported by the results from the previous flight experiment.

LITERATURE CITED

1. Avigad, G. Colorimetric ultramicro assay for reducing sugars. From W. A. Wood, ed. Vol. XLI Part B. Methods in Enzymology. Academic Press. 1975.
2. Curtis, C. R. Bean rust development in relation to gravity. Phytopathology 57:1025-1027. 1967.
3. Dedolph, R. R., D. A. Oemick, B. R. Wilson, and G. R. Smith. Causal basis of gravity stimulus nullification by clinostat rotation. Plant Physiol. 42:1373-1383. 1967
4. Gordon, S. A., and J. Shen-Miller. Simulated weightlessness studies by compensation. In: Gravity and the Organism, edited by S. A. Gordon and M. J. Cohen. The University of Chicago Press, p. 415-426. 1971.
5. Hanchey, P., B. L. Baker, and R. Baker. Isozyme patterns in gravity-compensated crown gall tissue. Phytopathology 65:1136-1138. 1975.
6. Karr, A. L., and P. Abersheim. Polysaccharide-degrading enzymes are unable to attack plant cell walls without prior action of a "wall-modifying enzyme." Plant Physiol. 46:69-80. 1970.
7. Kleinschuster, S. J., B. L. Baker, and R. Baker. Responses of crown gall tissue to gravity compensation. Phytopathology 65:931-935. 1975.
8. Kreutzer, W. A., and R. Baker. Gnotobiotic assessment of plant health. In: Biology and Control of Soil-Borne Plant Pathogens, p. 11-21, G. W. Bruehl, ed. American Phytopathologic Society, St. Paul. 1974.
9. Salisbury, F. B. Expected responses to weightlessness. Bioscience 19:407-410. 1969.
10. Tabbitts, J. W., and W. M. Hertzberg. Growth and epinasty of marigold plants maintained from emergence on horizontal clinostats. Plant

Physiol. 61:199-203. 1978.

11. Wells, T. R., and R. Baker. Gravity compensation and crown gall development. Nature 233:734-735. 1969.

Figure 2. Assembly of flight unit in preparation for insertion into box to be placed in the spacecraft.

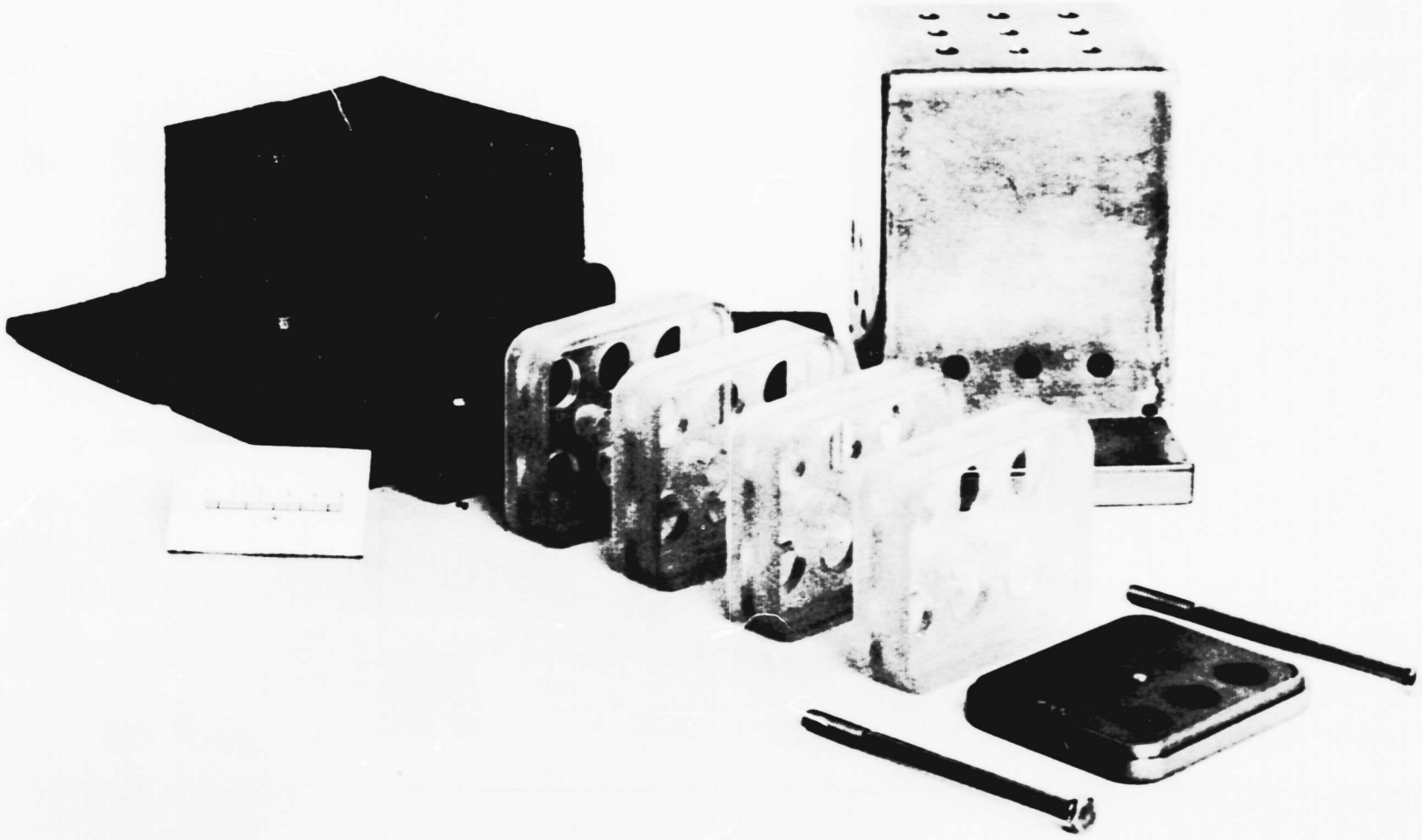

Figure 1. Flight unit (expanded view) showing dishes which supported carrot disks in the holes.

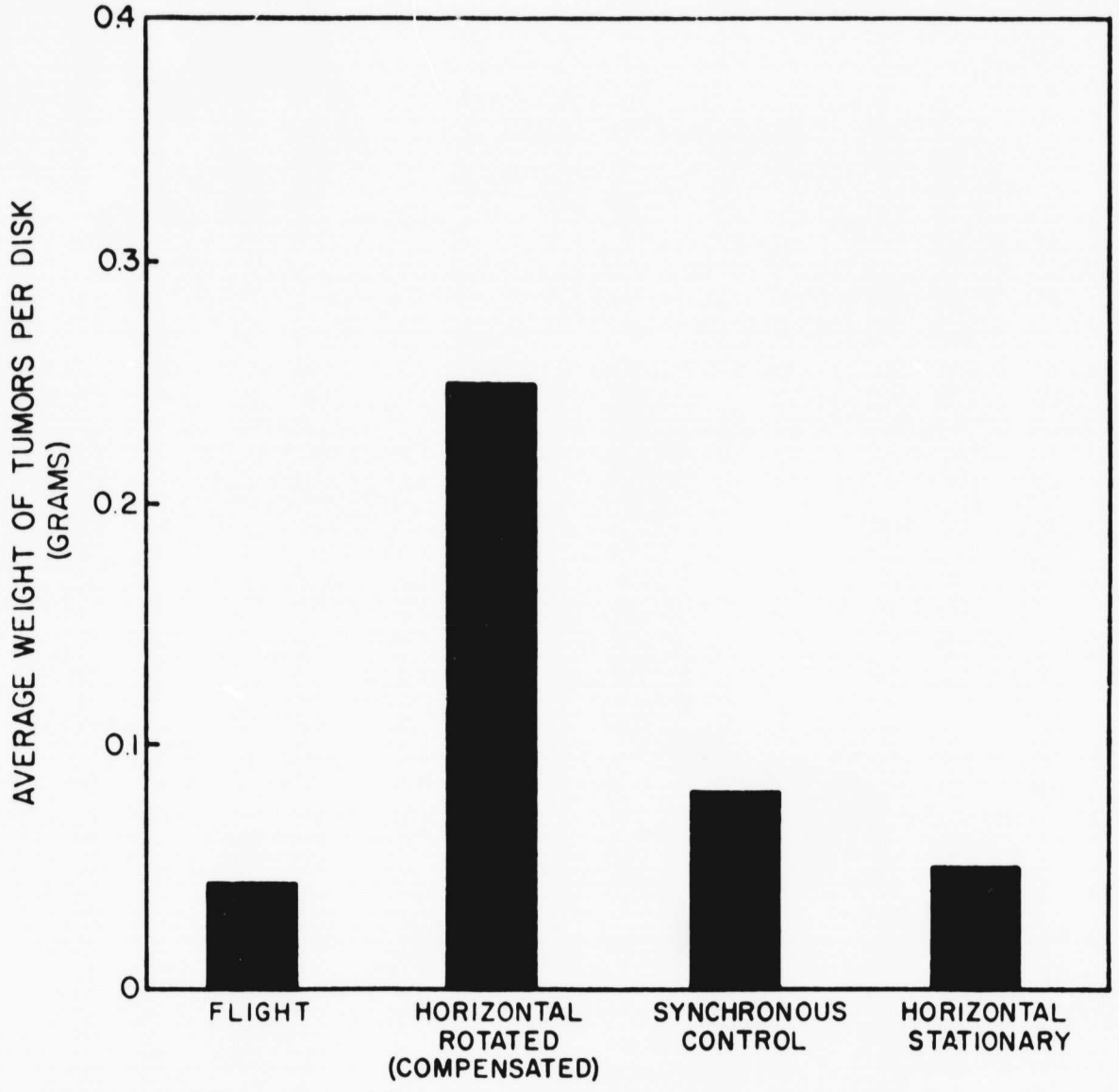

Figure 3. Fresh weights of tumors induced by Agrobacterium tumefaciens. Least significant difference (5%) = 0.1990 .

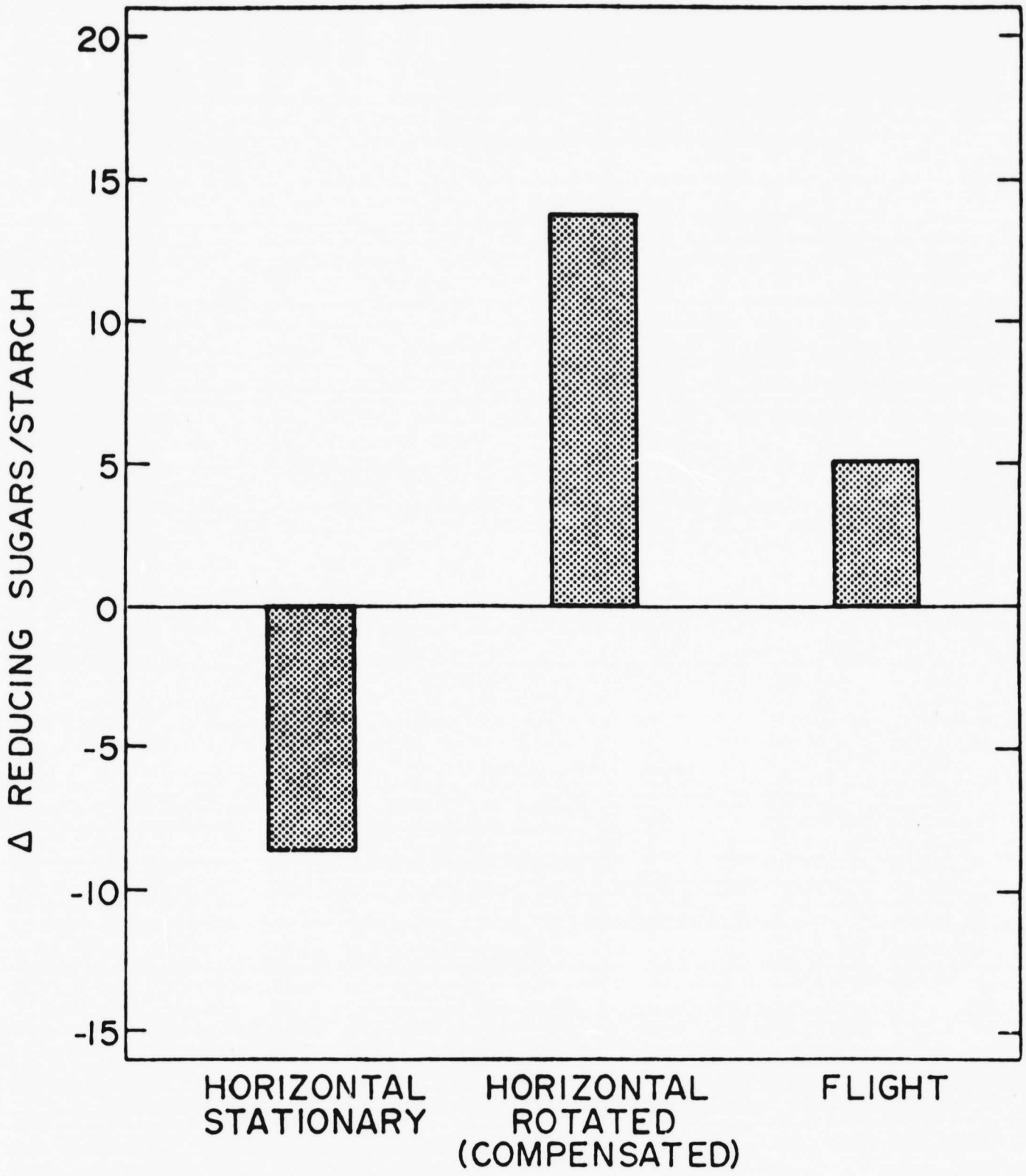

Figure 4. Change in reducing sugar/starch ratios. Positive values indicate sugars were proportionately more depleted by the treatments than starch; negative values indicate the opposite. Least significant difference (5%) = 13.77 .

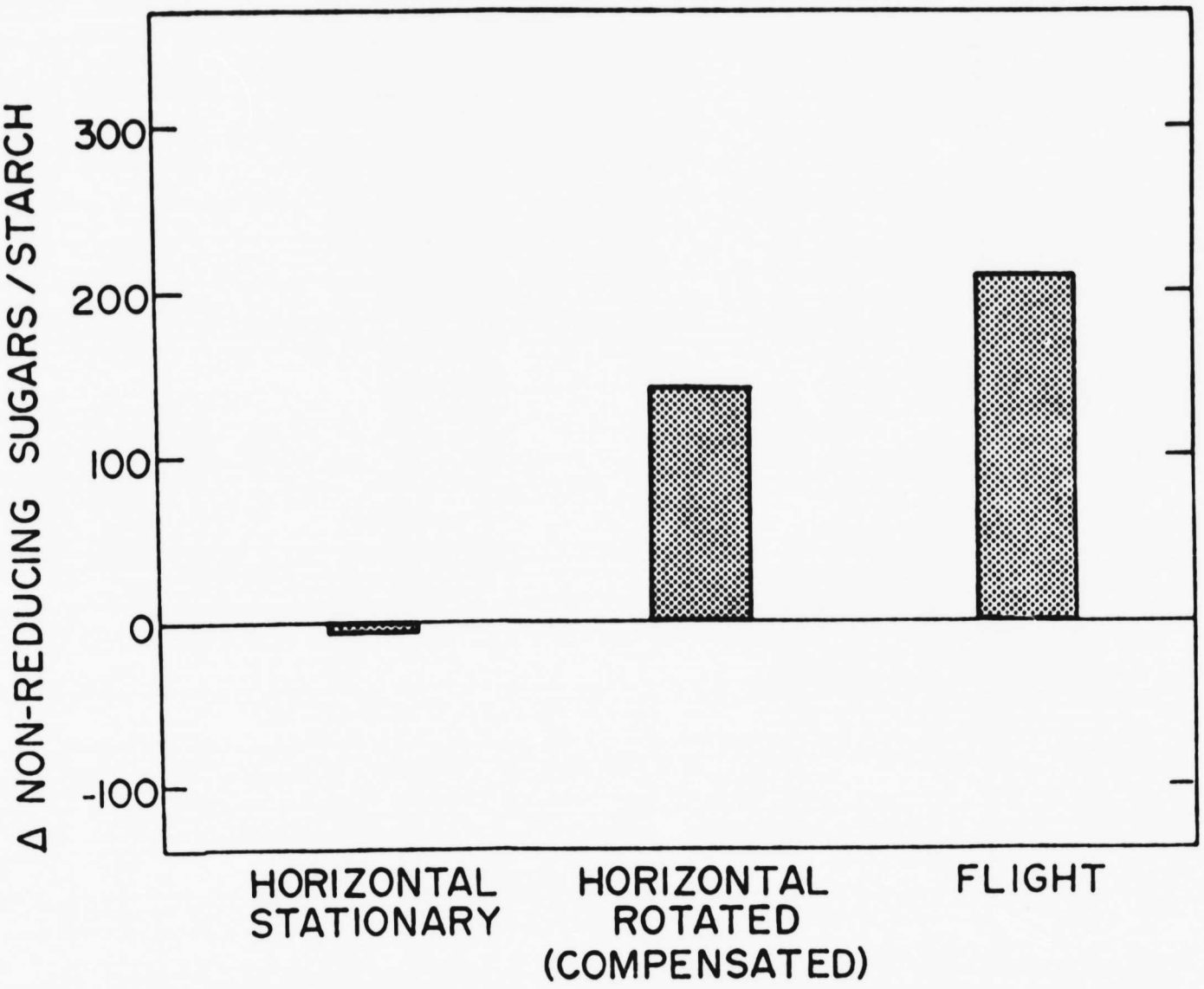

Figure 5. Change in nonreducing sugar/starch ratios. Positive values indicate sugars were proportionately more depleted by the treatments than starch; negative values indicate the opposite. Least significant difference (5%) = 169.90; least significant difference (10%) = 138.45 .

Experiment Number K301

Supplemental Report Number 1

LONG TERM EFFECTS OF WEIGHTLESSNESS ON A BIOLOGICAL SYSTEM-ISOENZYME ANALYSIS

Charles R. Curtis, Edward V. Podleckis and Caroline M. Golt
Department of Plant Science, University of Delaware
Newark, Delaware, 19711

SUMMARY

Proteins were extracted from tumors, cortex and stele carrot tissue and subjected to electrophoretic analyses. Six major bands of esterase activity were found in all tissues. The gravity treatments did not appear to affect the esterase enzyme pattern.

INTRODUCTION

The main objective of the gel electrophoresis study was to determine if weightlessness or other gravity treatments altered the isoenzyme profile of crown gall tumors. This objective was extended to include non-tumored cortex and stele tissue after the experimental material was received at Colorado State University.

Some of the experimental material was received in poor condition and tumors were either not present or not plentiful. Although tumor growth in the weightless state was minimal, and the amount of material for study was extremely limited, it was decided to proceed with electrophoretic analysis where a sufficient amount of tumor tissue was available. In addition, to maximize data yield it was requested that a portion of the non-tumored carrot disk be sent to our laboratory for analysis after it was separated into cortex and stele tissue.

A system was developed (8) involving the generation of crown gall tumors induced by Agrobacterium tumefaciens (E. F. Sm. & Towns.) Conn. on root disks of carrot (Daucus carota L. var. sativa DC) which was responsive to gravity treatments (5,7). The advantages in using this system for biosatellite experiments are described in a separate report (1).

MATERIAL AND METHODS

The details of carrot tissue preparation, inoculation, enviromental conditions, protocol and treatments administered during the experiment were provided in a separate report (1).

After recovery and transport of all flight material from the Soviet Union to Colorado State University, frozen tumors and frozen-lyophilized cortex and stele tissues were transported at 4 C to our laboratory for electrophoretic analysis.

The following treatments were received from Colorado State University. It should be mentioned that not all inoculated carrot disks developed tumors.

Excised Tumors	Disks (separated into cortex and stele)
Flight disks with tumors	Flight disks with tumors
Synchronous control with tumors	Flight disks without tumors*
Horizontal stationary with tumors	Synchronous control with tumor
Horizontal rotated with tumors	Synchronous control without tumor*
Vertical stationary with tumors*	Horizontal stationary
Vertical rotated with tumors*	Horizontal rotated
	Vertical stationary
	Vertical rotated

*insufficent tissue for analysis

*non-inoculated disks

Extraction and Protein Assay

Lyophilized carrot disk samples and frozen tumor samples were individually weighed and then ground in a chilled mortar with 0.2M Tris (tris(hydroxmethyl)aminomethane)-HCl containing 10% sucrose, 0.1% cysteine-HCl and 0.1% ascorbic acid, pH 7.6. The homogenate was centrifuged at 30,000 x g at 4 C for 30 minutes. The supernatant served as the sample for electrophoresis. The protein concentration

in each sample was estimated by a spectrophotometric protein assay method (2). The assay solution contained four parts distilled water to one part dye reagent concentrate. Fifty µl aliquots of sample were added to 2.5 ml of assay solution, mixed, and measured spectrophotometrically. Protein concentration was determined from absorbance changes measured at 595 nm with bovine gamma globulin as the standard.

Isoelectric Focusing

Isoenzyme patterns were examined after isoelectric focusing of samples in polyacrylamide gel cylinders (cf. 3,4). Samples from 75 to 170 µl containing 60 µg of protein were placed on a 5% cylinder and overlayered with a solution containing 3% sucrose and 1% ampholine. The cathodal electrode chamber was filled with 300 ml of 2.5% v/v phosphoric acid. An initial current of 2 mA per gel was applied with the power supply set on the constant voltage mode. The current was allowed to decrease for approximately two hours. After this time, the voltage was increased to 250V for an additional two hours. Electrofocusing of protein in the gels was completed following this sequence.

In the case of tumor tissue, sufficient material was available for at least one extraction per electrophoretic run with three separate gel-replicates per treatment. A total of five complete electrophoretic runs were made with 18 gels per run for a total of 90 gels. For the more plentiful disk tissue, a total of 24 complete runs were made with 18 gels per run for a total of 432 gels.

Staining Procedures

1. General Proteins. Gels to be stained for general proteins were placed in a solution of 12.5% w/v trichloroacetic acid (TCA) immediately following electrofocusing. After 30 to 60 minutes in TCA the gels were rinsed with distilled water and stained overnight in a solution containing 46 mg Coomassie Brilliant Blue R-250 dissolved in 5 ml 70% v/v perchloric acid and brought to 100 ml with distilled water (9). Destaining consisted of immersing gels into a solution containing 80 ml acetic acid, 250 ml 95% ethanol and 670 ml distilled water (v/v/v) until the background was clear. Destained gels were transferred to 7.5% acetic acid v/v and scanned at 550 nm using a Gilford Model 2400 spectrophotometer equipped with a linear gel transport system. The slit width was 0.2 mm with a full scale absorption usually set at 3.0. The scanning rate was set at 2 cm per minute.

2. Esterase. Immediately after electrofocusing the gels were incubated for 20 minutes at room temperature in a freshly prepared mixture of 40 mg Fast Red TR salt, 40 ml 0.1 M potassium phosphate buffer, pH 7.2, 0.6 ml 1% β-naphthyl acetate (w/v in 50:50 water: acetone) and 0.6 ml 1% α-naphthyl acetate (w:v, 50:50 acetone:water). The gels were transferred then to 7.5% v/v acetic acid and scanned at 540 nm.

3. Acid phosphatase. Immediately after electrofocusing, gels were incubated for 40 minutes at room temperature in a freshly prepared solution containing 60 ml 0.1 M acetate buffer, 60 mg α-naphthyl

phosphate, 60 mg Fast Blue RR (dissolved in several drops of acetone), 1.2 g NaCl, 12 drops 10% $MgCl_2$(w:v) and 300 mg polyvinylpyrollidone. Following incubation the gels were transferred to 7.5% acetic acid v/v and scanned at 600 nm.

4. Peroxidase. Immediately after electrofocusing, gels were incubated from 20 to 30 minutes at room temperature in a freshly prepared mixture of 50 mg 3-amino-9-ethyl carbazole dissolved in 5 ml of dimethylformamide, 100 ml of 2 M sodium acetate buffer, pH 5.0, and 0.5 ml of 3.0% (v:v) hydrogen peroxide (6). Following incubation, the gels were rinsed with distilled water, transferred to 7.5% acetic acid and scanned at 600 nm.

RESULTS

Several repeated electrophoretic trials failed to yield consistent results with general protein stains. Although a basic pattern could be seen for some treatments the variations within and among treatments were too great for meaningful conclusions. An explanation for the variability may be the non-uniform condition of the experimental material as previously noted (1).

Similarly, peroxidase isoenzyme patterns were difficult to assay because of a high degree of background interference in the gels. Smearing was encountered which was not overcome by altering the extraction techniques or using alternate staining methods. A similar result was obtained with acid phosphatase, however, a recurrent pattern was observed for some treatments.

Because of the difficulties with the experimental material and interference, we did not consider these results sufficiently clear to provide a definite conclusion.

The most consistent results were obtained with the esterase staining procedure. Gels stained for esterase activity were free from background interference and reproducible in their esterase pattern. The pattern was remarkably similar for 6 major bands of activity for all treatments.

Table 1 lists the average distance in mm moved from the origin by each band for tumored tissue. There appears to be no difference among the treatments based on the distance moved by each esterase band. The pattern noted for tumor tissue was observed with disk tissue as well. Although the disk tissue was separated into cortex and stele the esterase pattern was unchanged.

Figure 1 presents data on the approximate isoelectric points for each band and an interpretative diagram of the esterase pattern. The approximate pI values were determined from 1 mm sliced gels following the electrophoretic run. The pH line shown in Figure 1 was determined from gels in which no sample was applied. If a linear regression is calculated for the points in Figure 1, the pH values for each band change slightly to 5.36, 5.24, 4.87, 4.75, 4.63 and 4.38.

DISCUSSION

Six major bands of esterase activity were found in tumored tissue as well as cortex and stele tissue for all treatments. In a previous study (5) the esterases were similar but were separated by a different electrophoretic technique. Definite conclusions could not be made on the band intensity because of highly variable results among the treatments. An exception to this was found with the two bands having the highest pI values 5.52 and 5.40. As indicated in the diagram of Figure 1, these two bands always stained less intensely. These data support the conclusion that there were no differences among tissues or treatments in terms of esterase activity. No other conclusions could be made from the protein, peroxidase and acid phosphatase data because of a lack of sufficient material for complete analysis, non-uniform condition of the experimental material and inconsistent results.

LITERATURE CITED

1. Baker, R., J. Hendrix and C. R. Curtis. Long term effects of weightlessness on a biological system. Final Reports of U. S. Plant and Radiation Dosimetry Experiments Flown on the Soviet Satellite Cosmos 1129. Joint US/USSR Biological Satellite Program. 1981 (this volume).
2. Bio-Rad Protein Assay. Bio-Rad Laboratories, Chemical Division. Technical Bulletin 1051. 1977.
3. Curtis, C. R., R. K. Howell, and D. Kremer. Soybean peroxidase from ozone injury. Environ. Pollut. 11:189-194. 1976.
4. Curtis, C. R., and L. H. Weinstein. Chapter 16: Special Techniques A. Electrophoresis, p. 16-1 to 16-10. In W. W. Heck, S. V. Krupa and S. N. Linzon (eds.) Methodology for the Assessment of Air Pollution Effects on Vegetation. Air Pollution Control Association, Pittsburgh, Pa. 1979.
5. Hanchey, P., B. L. Baker, and R. Baker. Isoenzyme patterns in gravity - compensated crown gall tissue. Phytopathology 65:1136-1138. 1975.
6. Hoyle, M. Illustrated Handbook for High Resolution of IAA - Peroxidase Isoenzymes by Isoelectricfocusing in Slabs of Polyacrylamide Gel. Forest Service General Technical Report NE-37. Forest Service USDA Northeastern For. Exp. Sta., Broomall, Pa. 1978
7. Kleinschuster, S. J., B. L. Baker, and R. Baker. Responses of crown gall tissue to gravity compensation. Phytopathology 65:931-935. 1975

8. Wells, T. R., and R. Baker. Gravity compensation and crown gall development. Nature 233:734-735. 1969 .

9. Wrigley, C. W. and J. M. McCausland. Variety Identification by Laboratory Methods:Instruction Manual for Barley, Wheat and Other Cereals. CSIRO Wheat Research Unit Technical Publication No. 4. New South Wales, Australia. 1977.

Table 1. Approximate average distance moved from the origin (in mm) by tumor tissue esterases.

Esterase Band Number	Treatment			
	Flight	Synchronous Control	Horizontal Stationary	Horizontal Rotated
1	32.50	30.33	33.50	32.50
2	33.25	31.50	34.50	33.50
3	35.25	34.67	36.50	35.83
4	36.50	35.83	38.00	37.17
5	38.25	36.83	39.00	38.33
6	39.25	38.33	40.00	39.67
gel replicates	2	3	1	3
electrophoretic runs	2	1	1	2

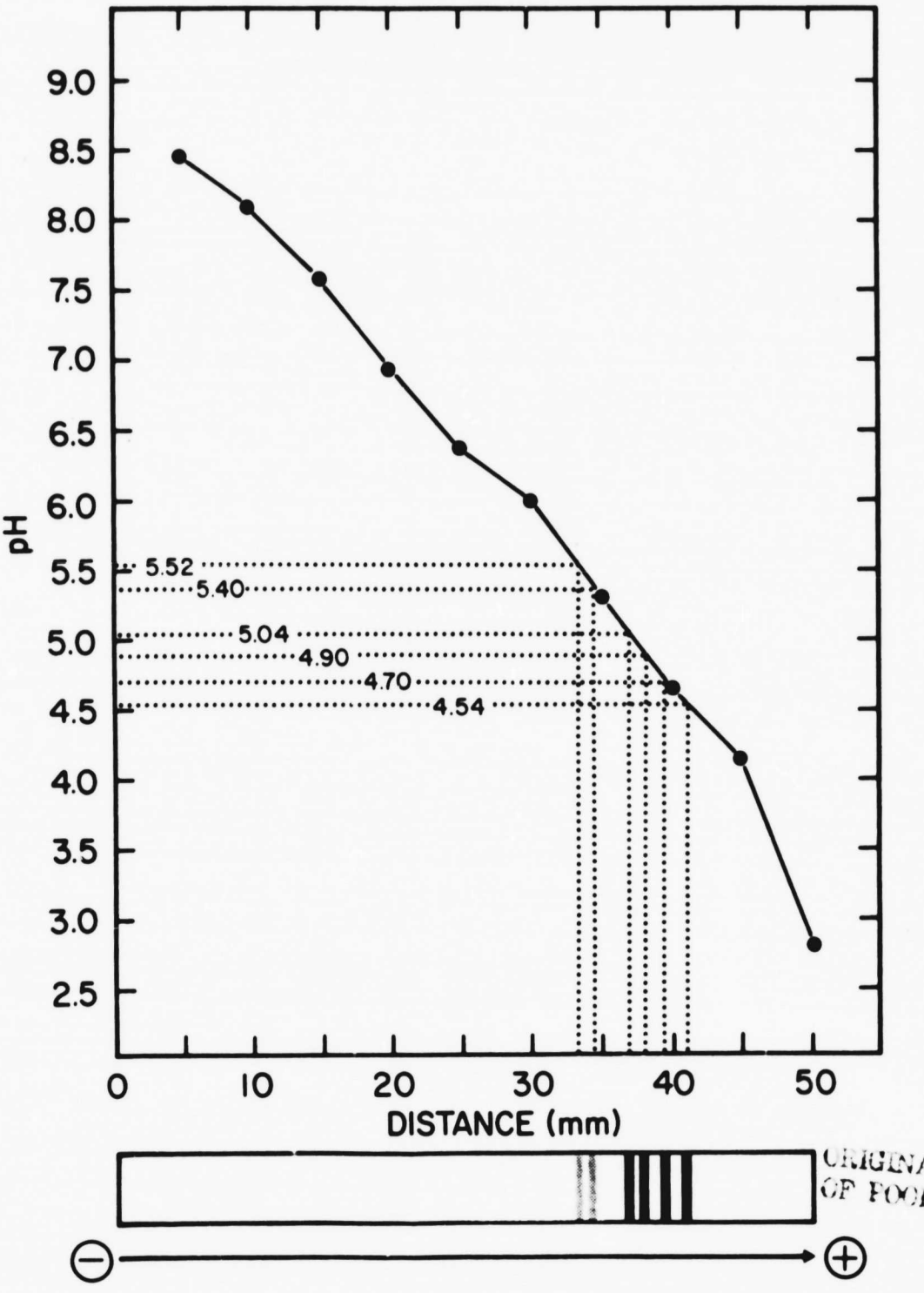

Figure 1. Representative esterase pattern obtained after isoelectric focusing of experimental material in polyacrylamide gel cylinders. The approximate isoelectric point of each esterase band is indicated by the dotted line in the graph.

Growth and Development of Carrot Cells and Embryos in Space--K302

A.D. Krikorian, F. Ronald Dutcher, Carol E. Quinn and F.C. Steward
Department of Biology, State University of New York at
Stony Brook, Stony Brook, New York 11794

SUMMARY

Morphogenetically competent proembryonic cells and well-developed somatic embryos of carrot at two levels of organization were exposed for 18.5 days to a hypogravity environment aboard the Soviet Biosatellite Cosmos 1129. It was confirmed that cultured totipotent cells of carrot can give rise to embryos with well-developed roots and minimally developed shoots. It was also shown that the space hypogravity environment could support the further growth of already-organized later somatic embryonic stages and give rise to fully developed embryo-plantlets with roots and shoots.

INTRODUCTION

A major area of research in space biology has been to ascertain whether plant development can proceed normally and consecutively in the weightless state, especially that salient feature of it in which a cell gives rise to a multicellular unit and thence to an embryo with shoot and root growing regions, which in their turn, give rise to all the tissues and organs of the plant body including functional flowers (1). An opportunity to carry out a preliminary experiment to test whether cultured carrot cells, capable of organized development, could undergo somatic embryogenesis at near-0 gravity arose in 1975. A carrot cell experiment designated "K-102" was aboard the unmanned Soviet Vostok biosatellite Cosmos 782 which was launched on November 25, 1975 in the USSR. The principal mission of the K-102 experiment was to test whether cells of a higher plant, such as the carrot, could develop normally under conditions of weightlessness in space and emulate their known ability on earth to multiply and develop, forming organs, embryoids and normal plantlets.

The Soviet Satellite carried Daucus carota var. carota cells in petri dishes in special canisters and for 19.5 days in space exposed them to both weightlessness (near-0 g) and, by means of a centrifuge that was on board the spacecraft, exposed them to a gravitational force equivalent to that on earth (1 g). The petri dishes contained actively growing somatic cells distributed in thin layers in an agar culture medium which allowed the cells to grow heterotrophically in darkness. To ensure proper controls for the experiment, comparable dishes were maintained at NASA Ames Research Center,

Stony Brook and in the USSR. Canisters were kept at 4°C ± 2°C for the entire period following preparation of the cells at Stony Brook until just before launch in the Soviet Union and until "synchronous controls" were performed. It has been determined by prior experimentation that such chilling precludes cell division and development and it was anticipated that once on board the spacecraft and at the temperature of flight (20 to 24° C), metabolic activity and growth would resume and morphogenetic potential could be expressed if the flight conditions so permitted.

In the final outcome viable biological material was recovered from all treatments except those that were to simulate lift-off, flight and recovery on the ground in the USSR. However, as the complete record (based on photographs of the dishes, the number of developed structures they contained, and photographs of "embryos" at different stages of their development) showed (2,3), the useful result was that even the dishes exposed in flight at near-0 g produced viable embryos in large numbers, that they did not differ significantly from those exposed in flight to 1 g and, in consequence, the various other controls were not needed to test the reality of any observed quantitative differences between the responses observed at near-0 g and 1 g in flight.

The particular clone of carrot cells used in the K-102 experiment contained units which, under the conditions and duration of the experiment, varied greatly in the level of development they achieved. These were arbitrarily classified by size and complexity into many categories and their frequency in the populations on the dishes was established by actual counts. Representative samples of the different stages of developed embryos were

obtained for photography and microscopic examination. However, the large numbers of initial units on the dishes and the number of replicate dishes enabled it to be established that the near-0 g and 1 g treatments did not result even in significantly different proportions of embryos at the different stages of development into which they were classified.

The level of development achieved from cell units around 74 μm in size in 19.5 days in darkness produced somatic embryos at various levels of heart, torpedo and early cotyledonary development. Where embryos were larger, their increased size or complexity was in the length of primary root (which could be substantial) and in the development of hypocotyls. Shoot development tended, however, to be arrested. Nevertheless, the leaf primordia and shoot apices had become sufficiently established during space flight at both near-0 g and 1 g, so that when somatic embryos from the spacecraft were exposed to 1 g and to light, their shoots developed rapidly and normally into plantlets. Such plantlets were grown to maturity on earth and their subsequent growth and development observed.

The main conclusion from the Cosmos 782 experiment was that totipotent somatic cells could undergo morphogenesis to produce viable and fully competent embryos at near-0 g, apparently as effectively as at 1 g. There were, however, two reservations. First, the imposed conditions, i.e. total darkness and duration of the experiment, did not preclude the possibility that the later rapid development of shoots with the concomitant tissue differentiation might be more sensitive to near-0 g than the initial induction of embryonic form. Secondly it was an open question whether the cells as used in the experiment had through their pre-treatment retained some consequences

of asymmetric 1 g stimulus so that, when they did develop at near-0 g in space, they could respond as to a 1 g "presentation time", i.e. to an existing "memory" of prior 1 g conditions.

In short, the generally satisfying outcome of the K-102 carrot cell culture experiment raised more questions than it answered. It was recognized that the test of the competency of the near-0 g environment to support normal growth and development would not be convincing until it could be repeated. It was also hoped that an opportunity would arise one day to extend the experiment to address the question of the potential for the further growth of the embryonic shoot. Because of the relatively short duration of the flight, the question whether a "second generation" of cells, produced from plantlets which had developed in an organized way in space, could undergo morphogenesis, somatic or zygotic embryogenesis, as readily as cells which were isolated and grown in prior culture at 1 g, remained unanswered. It was emphasized that repeated tests would eventually have to be made to dispose of any possibility that the carrot cells that organized in space into embryos needed to have a recent "experience" or "memory" of growth and development under 1 g conditions for their later successful development at near-0 g. Finally, it was stressed that higher plants, whether carrot or other species, ultimately would have to be grown to sufficient maturity in space so they flower and set seed and this would have to be repeated through as many generations as possible.

It was welcome news, therefore, that an opportunity would be available through Cosoms 1129 to confirm and possibly extend the conclusion drawn from our studies from Cosmos 782. One of the first considerations that was given

in planning another experiment after the possibility of access to space on Cosmos 1129 arose, was that of the line of cultured carrots to be used. Indeed, due to the line of carrot cells used in the Cosmos 782 experiment, and also from our ground based studies, it was known that much of the embryonic development from the cells occurred during the first 14 days of flight (3). Unfortunately, it could not simultaneously be tested whether the weightless space environment could support the further development of leafy shoots. Since we started with cell units that had no organized growing regions, the flight period was not sufficient to allow for extensive plantlet development. On Cosmos 1129 the plan would be to use cultured carrot materials with different degrees of prior organization and development ranging from embryos down to morphogenetically competent cell units. In that way we planned to utilize experimental material with as much pre-exposure to conditions conducive to shoot development as possible. Even so, it was recognized that the imposed periods of darkness during flight at metabolically permissive temperatures could possibly re-"set" already developing shoots upon the trend of embryos that have not caused their developed growing points to actively expand or "push". Additionally, although it was known that there would be no access to light or a 1 g control centrifuge, it was hoped that the results from a successful mission would far outweigh any possible reservations.

MATERIALS AND METHODS

Morphogenetically competent populations of carrot cells were grown in liquid suspension culture in a basal medium containing salts, sucrose, vitamins and napthaleneacetic acid (NAA), utilizing techniques developed in

this laboratory (4). These suspensions were graded by filtration through stainless-steel sieves of known dimension. The final size of the filtered units ranged between 38 and 74 μm. Populations of somatic embryos were also grown to provide material at more advanced stages of development. The embryos were developed in a medium identical to that described for the cells, except NAA was omitted. The final size of the somatic embryos prepared ranged between 234 and 406 μm in one case, and 406 and 864 μm in the other. Since the details of preparation of the cells and embryos is critical to a full appreciation of the development and morphogenesis which occurred in space, the specifics are presented in Appendix 1. The cells and the two fractions of embryos were distributed separately at an appropriate density in 5 mls of agar culture medium in 50 mm diameter snap-lid plastic petri dishes (Falcon 1006). Dishes contained an average of 5,000 unorganized cell units per plate and an average of 100 and 122 somatic embryos per dish for the larger and smaller fractions respectively. The plastic dishes were loaded into acrylic tubes and covered with anodyzed aluminum end-caps. HEPA filters were used to help maintain sterility (cf. Figs. 1 and 2). To prevent further development before lift-off and the beginning of the experiment, the cultures were chilled to 4°C to arrest growth. Precautions were taken to ensure that this chilled state was maintained until flight time. The chilling effect is, however, reversible, and it was anticipated that growth would resume once orbit was achieved if the conditions permitted. Table 1 provides a list of the 12 canisters that were prepared and their disposition. Material was taken to NASA Ames Research Center in a biotransporter maintained around 4°C. (Biomaterials were taken to the USSR and to the launch site in

Table 1. Final hardware disposition of materials from K-302 experiment.

	GRAVITY CONDITION	NUMBER OF UNITS	EXPERIMENTAL CANISTER UNIT NUMBER
Flight[1]	O G	1	KF-1
Flight[1]	O G	1	KF-2
Not Returned - intended as "back-ups"		1	KF-3
Not Returned - intended as "back-ups"		1	KF-4
Returned from Ames Research Center		1	KF-5
Returned from Ames Research Center		1	KF-6
Synchronous Control[2] (Ground Control)	1 G	1	KF-7
Synchronous Control[2] (Ground Control)	1 G	1	KF-8
Stationary Synchronous[3]	1 G	1	KF-9
Stationary Synchronous[3]	1 G	1	KF-10
Stationary Synchronous[3]	1 G	1	KF-11
Stationary Synchronous[3]	1 G	1	KF-12
Total Canisters		12	

Footnotes to Table 1.

[1]Flight - (KF-1, KF-2) Two canisters which were aboard the Soviet satellite for 18.5 days at 24°C.

Started: September 25, 1979 at 6:40 p.m. (Moscow time).

Finished: October 14, 1979 at 8:00 a.m. (Moscow time).

Canisters were placed in the biotransporter on October 14, 1979 at 2:00 p.m. (Moscow time), at a temperature of 4°C.

[2]Synchronous Control (Ground Control) - (KF-7, KF-8) Those 2 canisters were used to simulate flight conditions. Dishes were maintained at 24°C for 18.5 days and then placed in the biotransporter at 4°C on October 19, 1979. There was a 5 day lag time here before the start of this material.

Started: September 30, 1979 at 6:40 p.m. (Moscow time).

Finished: October 19, 1979 at 8:00 a.m. (Moscow time).

[3]Stationary Synchronous - (KF-9, KF-10, KF-11, KF-12) Those canisters were kept at 24°C for the length of the flight, 18.5 days. There was, however, a 5 day lag time before the start of the material. The canisters were held stationary, (i.e. no flight simulation involved) in Moscow. Every other day 3 dishes, one of each fraction, cells, smaller and larger embryos were removed for fixation.

Started: September 30, 1979 at 6:40 p.m. (Moscow time).

Finished: October 19, 1979 at 8:00 a.m. (Moscow time).

Those canisters were hand carried back on an airplane from Moscow at 24°C.

an identical biotransporter.) One of us (A.D.K.) left New York City for San Francisco on 14 September 1979 and departed on September 15 with Mr. Peter Chetirkin of NASA Ames Research Center for Moscow via Tokyo (16 September, arriving Moscow 16 September at 3:10 p.m. On 18 September at 3:40 p.m. Moscow time, the continuous reading temperature recorders were activated and inserted into position in the foam blocks earmarked for flight and the synchronous controls. The maximum-minimum temperature recorders and dosimeters were also inserted (cf. Fig. 3). The biomaterials left the Institute of Biomedical Problems in Moscow at 10:47 a.m. Moscow time on 19 September for the launch site in Plesetsk. Appendix 2 provides a detailed record of subsequent handling of relevant flight, synchronous control and ground control units. This record is especially important since it includes temperature data, and this confirms that ambient temperatures permissive for development were not reached for very long periods. Launch occurred 25 September at 6:30 p.m. Moscow time; recovery in Kustanai area of Khazakstan was Sunday 14 October 8:00 a.m. Moscow time. The duration in orbit thus was 18.5 days. On Tuesday 16 October material from KF's 1 and 2 were examined, photographed and fixed as necessary by A.D.K.. Dishes KF 1-2, 1-5 and 1-8 and KF 2-1, 2-4 and 2-7 were fixed with glutaraldehyde (cf. ref. 3). The remaining dishes were refrigerated at 4°C. On Friday 19 October material from KF-7 was examined, photographed and fixed as necessary. Dishes KF 7-2, 7-5 and 7-8 were fixed with glutaraldehyde. The remaining dishes were refrigerated at 4°C. Additional procedural details will be provided under RESULTS. The methods of counting and scoring embryonic units, and rearing of plantlets to maturity, etc. which were followed have all been discussed in detail and

hence will not be given here.

RESULTS

Fig. 4 provides a graphic representation of the time course of events associated with the K-302 experiment with special emphasis on the temperature of the cells and embryos even as they were being prepared and processed at Stony Brook. The precise computer record of temperature taken every half hour by the temperature recorder in the flight and synchronous control containers (number 6, flight; number 3, synchronous) are available through NASA Ames Research Center and will not be provided here. The crucial feature of this figure is that only for a brief period of time after the final preparation of the cells and embryos did the biomaterials attain a temperature at which metabolic activities could resume and development proceed. Material was in the space capsule 3 days prior to launch and the temperature in the flight container averaged around 21°C. Apparently the packaging maintained a fairly constant temperature although the ambient temperature in the capsule was said to have on occasion been as low as 10-12°C. In any case, it may be stated categorically that the period of time at permissive temperatures could in no way compromise interpretation of the observations made. Figs. 5 through 10 show the degree of development that morphogenetically competent populations of carrot proembryonic cell units underwent. The satisfying feature of these photographs is that they provide a "before" and "after" record of all of the dishes that were exposed to the space environment. Figs. 11 through 16 show the degree of development that well-developed somatic embryos ranging in size from 406 to 864 μm underwent. Figs. 17 through 22 show the degree of development that less-developed, but

nevertheless fully competent, somatic embryos ranging in size from 234 to 406 μm underwent. Presentation of the photographic evidence follows the placement of dishes in the canisters, i.e., the smallest and least developed units in the first three positions, the largest and most developed somatic embryos in the next three and the intermediate stage somatic embryos in the last three. In this way, it is hoped that ready comparison may be made between the top and lower panels, representing "before" and "after", respectively as well as between dishes with varying degrees of prior development before and after exposure to space conditions. Note the numerous embryonic forms in KF's 1 and 2, dishes 1 through 3. The relatively low magnification and the fact that the crop of embryos is dispersed within as well as on the agar make it difficult to distinguish all the forms, but typical globular, heart-shaped, torpedo and mature embryonic structures were present. In KF's 1 and 2, dishes 4 through 6, the degree of development is particularly dramatic and the organized forms are clearly recognizable as plantlets; in KF's 1 and 2, dishes 7 through 9, the degree of development is also very dramatic, and the organized forms are also recognizable as plantlets, although not quite to the same degree as those in dishes 4 through 6. Fig. 23 provides a photographic record of the course of growth of carrot units in nutrient agar medium in 50 mm diameter petri dishes. The growth visible to the naked eye only becomes apparent at around 11 days although the embryos are well developed from a morphological viewpoint much earlier (cf. ref. 3). Figs. 24 and 25 provide a similar photographic record of the course of growth of the two categories of somatic embryos. These well-defined embryos and plantlets illustrate that development could proceed

under hypogravity conditions. Some dishes were used as sources of material to test the subsequent viability and growth responses of the crops of embryos and plantlets that developed in space. Organized forms were allowed to continue their growth in fresh media...sometimes in tubes, other times in jars and still later in pots under greenhouse conditions. Growth was also continued into the field to maturity--i.e. flowering. Figs. 26 and 27 provide a photograph record of representative stages of growth from aseptically cultured embryos to plants in pots in the greenhouse. The figures show:-- (a) through (d), on the left-hand side of the figures, the sequential growth of a plantlet developed in space, removed from its culture dish and reared to pot size. (e) through (h), on the right-hand side of the figures, the sequential growth of a plantlet developed on earth, removed from its culture dish and reared to pot size.

There was no detectable difference between the subsequent ability of any of the stages of embryos or plantlets which had developed under space conditions at near-0 g to continue their course of growth and development. The plantlets were all within the range of variability for the material as grown. Indeed, the plants at the time of this writing are in the field and look nearly identical for they are the products of a now well-established cloning procedure (4,5).

DISCUSSION

This report emphasizes the gross morphological aspects of the embryos and plantlets recovered from flight and ground controls. It stresses that at the gross morphological level, at least, there were no major detectable

differences between plantlets developed in space and their control counterparts (cf. Figs. 28 and 29). Insofar as the objectives referred to in the INTRODUCTION are concerned, the findings from Cosmos 782 were confirmed and extended. It is very satisfying that despite the unique scope of the experimental conditions, namely the space environment and transport and return of materials to and from the USSR, the experiment could be repeated. The precise extent to which subtle, but nonetheless real, differences may obtain between materials developed at hypogravity and on earth has been deferred in this "final" report since the data are still being critically evaluated and analyzed. For this reason, quantitative data have also been omitted in this report. This has, in part, been necessitated by the concentrated effort placed on rearing large numbers of embryos and plantlets to maturity under field conditions. But it also reflects a conservative stand taken by us to refrain from interpreting results that have not yet been completely analyzed. It also is appropriate to point out here that although the use of cultured higher plant cells provides a number of advantages to investigators interested in pursuing the study of plant development in space (1), there are, not unexpectedly, very real problems of interpreting growth responses. Responses to environmental parameters which are familiar on earth are made much more difficult to evaluate in the context of the completely new setting of space since the consequences of their possible interaction are still unexplored.

It would be a mistake at this juncture to interpret broadly the findings from Cosmos 782 and 1129 as incontestible evidence that plant development can proceed normally in hypogravity. No higher plant had yet been reared to

maturity under space conditions. Although it seems clear that very early stages of plant embryogenesis and young plantlet development can proceed with a minimum of disturbance in terms of gross morphology, no evidence exists that still later stages of growth can proceed normally--this is especially true of those stages immediately prior to, during and after flowering. It should also be emphasized that the carrot materials flown necessarily had prior extended exposure to 1 g conditions and the criticisms presented in the INTRODUCTION concerning Cosmos 782 still apply for Cosmos 1129. Tests must be made to dispose of any possibility that free cells that organize in space into embryos and embryos into plantlets need to have had a recent "experience" and consequent "memory" of growth and development under 1 g conditions for their later successful development at near-0 g.

ACKNOWLEDGEMENTS

Supported by NASA contract NAS2-10150 "Carrot Embryo Development during Space Flight" and NASA grant NSG7270 "Cells, Embryos and Development in Space". We are indebted to the Institute of Biomedical Problems (Dr. Oleg Gazenko, Director) and the K.A. Timiriazev Institute of Plant Physiology (Dr. A.L. Kursanov, Director) for all their help. In the latter Institute we are especially grateful to Dr. Raisa G. Butenko and her associates, Dr. Natasha Dimitriaeva and Dr. Vidoyatsi Ongko for needed laboratory facilities and assistance.

REFERENCES

1. Krikorian, A.D., and F.C. Steward. 1979. Is gravity a morphological determinant in plants at the cellular level? In Life Sciences and Space Research 17:271-284. Ed. by W.R. Holmquist. Pergamon Press.
2. Krikorian, A.D., and F.C. Steward. The morphogenetic responses of cultured totipotent cells of wild carrot at zero gravity. Science 200: 67-68 (1972).
3. Steward, F.C., and A.D. Krikorian. 1978. The morphogenetic responses of cultured totipotent cells of carrot (Daucus carota L.) at zero gravity. In Final Reports of U.S. Experiments Flown on the Soviet Satellite Cosmos 782. pp. 71-159. Ed. by Susan N. Rosenzweig and Kenneth A. Souza. NASA Technical Memorandum 78525.
4. Steward, F.C., H.W. Israel, R.L. Mott, H.J. Wilson, and A.D. Krikorian. Observation on growth and morphogenesis using cultured cells of carrot. Phil. Trans. Royal Society London 273:33-53 (1975).
5. Steward, F.C., and Krikorian, A.D. 1979. Problems and potentialities of cultured plant cells in retrospect and prospect. In Plant Cell and Tissue Culture: Principles and Applications. pp. 221-262. (Ohio State University Biosciences Colloquia No. 4). Ed. by W.R. Sharp, P.O. Larsen, E.F. Paddock, and V. Raghavan. Columbus Ohio State University Press.

Appendix 1.

METHOD OF CELL PREPARATION

Six nipple culture flasks containing suspensions of a 10 day old line of carrot (76/A2A1) were chosen to provide morphogenetically competent units at the proembryonic cell stage of development. The cultures had been growing at 22°C in darkness on a basal medium (B_{MS}) plus NAA 2 mg/l. The contents of each nipple flask were poured through first a single and then a double layer of cheesecloth and then through a graded series of stainless steel sieves: mesh sizes were #100 (140 µm), #200 (74 µm) and #400 (38 µm). The fractions collected were cells in the size range of 74-140 µm, 38-74 µm, and < 38 µm. Each fraction was placed in a separate centrifuge tube and a small aliquot from each was taken for microscopic observation. The 38 µm-74 µm size range was chosen for plating. The centrifuge tubes containing the units were centrifuged for ten minutes at 300 rpm and the supernatant was decanted. Twenty mls of basal medium (B_{MS}) was added to each of the tubes and four of the six tubes were combined in a 500 ml erlenmeyer flask. (Two tubes were eliminated because four tubes contained enough material for the experiment and thus the possibility of contamination was reduced by combining only four tubes instead of six.)

Five mls of the combined suspension in the flask were removed for counting using a Fuchs Rosenthal microchamber. The density of the cells in the erlenmeyer flask was 41,093 cellular aggregates per milliliter and 100,859 cells per millileter. To obtain a density of approximately 5,000 aggregates per ml, 20 mls of cells were taken from the flask and were brought up to 164 ml with basal medium. The cells were then distributed among four

centrifuge tubes prior to plating in cooled agar medium (approximately 48°C). This distribution of the cells in agar was achieved by pipetting six mls of cells into a small flask containing twenty-four mls of basal medium with 1% agar, gently swirling the flask, and pouring five mls of agar medium per dish into six plastic (FALCON #1006) petri dishes. A total of ninety dishes were prepared. Plates were allowed to cool to room temperature (22°C) for one hour and then placed in a 4°C dark chamber.

Embryo Preparation

Four nipple flasks of carrot embryo suspensions (line 76/A2A3) were used to provide morphogenetically competent material at the embryo state of development. The culture flasks contained embryos grown in basal medium and had been growing for four days in darkness at 22°C. Material from each flask was poured through a series of stainless steel sieves (#20, #40, #60, #80 and #100) and each sieve was rinsed with basal medium. Embryos were retained on each sieve and were collected between the #20-#40 (406 µm-864 µm), #40-60 (234 µm-406 µm), #60-80 (177 µm-234 µm), #80-100 (140 µm-177 µm) and less than #100 (140 µm) sieves. Each fraction was poured into a centrifuge tube and an aliquot was removed from each for observation under a binocular dissecting microscope. Embryos in the #20-40 mesh (406 µm-864 µm) and #40-60 mesh (234 µm-406 µm) size range were chosen for the experiment. The following manipulations were carried out with each fraction kept separate and manipulated by one worker.

The embryos in four centrifuge tubes of each fraction were allowed to settle, the supernatant was decanted and twenty milliliters of fresh basal medium were added to each tube. The material from each fraction in the

respective centrifuge tubes was then combined according to size into a 250 ml erlenmeyer flask. The embryos in each flask were thoroughly mixed and two 1 ml samples were removed from each flask and placed in separate dishes for counting. The number of embryos in these aliquots was counted by placing the petri dishes over a grid under a dissecting microscope. The average density for the larger and smaller embryo fractions was 176 and 173 embryos/ml respectively. The embryos of the larger fraction in the erlenmeyer flask were diluted from approximately 80 ml to approximately 115 ml with basal medium yielding a density of approximately 122 embryos per ml. Similarly, the smaller sized embryos were diluted from 80 to 100 ml to obtain a density of approximately 138 embryos per ml. The embryos in each flask were then distributed evenly among four centrifuge tubes. Distribution of the embryos in 1% agar medium in plastic petri dishes was done in the same manner as that described for the cells. Ninety dishes were made from each fraction of the embryos. The dishes were allowed to cool to room temperature for about one hour and then were placed in darkness at 4°C.

Selected individual dishes were exactly scored by counting the number of embryos (see Appendix Tables 1 and 2).

Appendix Table 1. Counts of embryos in each dish. The embryos were within the #20-40 mesh size range.

Dish Designation	Embryos/dish
KF-1-6	97
KF 1-5	106
KF 1-4	112
KF 2-6	83
KF 2-5	81
KF 2-4	116
KF 5-6	101
KF 5-5	97
KF 5-4	106
KF 6-6	98
KF 6-5	107
KF 6-4	100
Average number of embryos/dish	1204/12 100.3

Appendix Table 2. Counts of embryos in each dish. The embryos were within the #40-60 mesh size range.

Dish Designation	Embryos/dish
KF 1-7	159
KF 1-8	108
KF 1-9	191
KF 2-7	87
KF 2-8	94
KF 2-9	186
KF 5-7	101
KF 5-8	119
KF 5-9	96
KF 6-7	89
KF 6-8	86
KF 6-9	151
Average number of embryos/dish	1467/12 122.3

Appendix 2, Procedure list for K-302 from Dr. Mourad Tiarbechov, Institute for Biomedical Problems, Moscow.

Variant	
Flight	2 units taken from biotransporter at 2 p.m. on September 22, 1979 (t = 4.8°C) and fastened to Bios IV in container N 16 at 8 p.m. (weight 1100 g) 2 units placed in biotransporter on October 14, 1979 at 2 p.m. (t = 4°C)
Synchronous Control*	2 units taken out from refrigerator at 4 p.m. on September 27, 1979 (t C = 4°C) and fastened to Bios IV in container N18 at 4:30 p.m. on September 30, 1979 2 units placed in biotransporter on October 19, 1979 (t = 4°C)
Ground Control	2 units stored at 24°C during 18.5 day flight

*The temperature in the synchronous units during flight incubation period varied between 23.5 - 24°C.

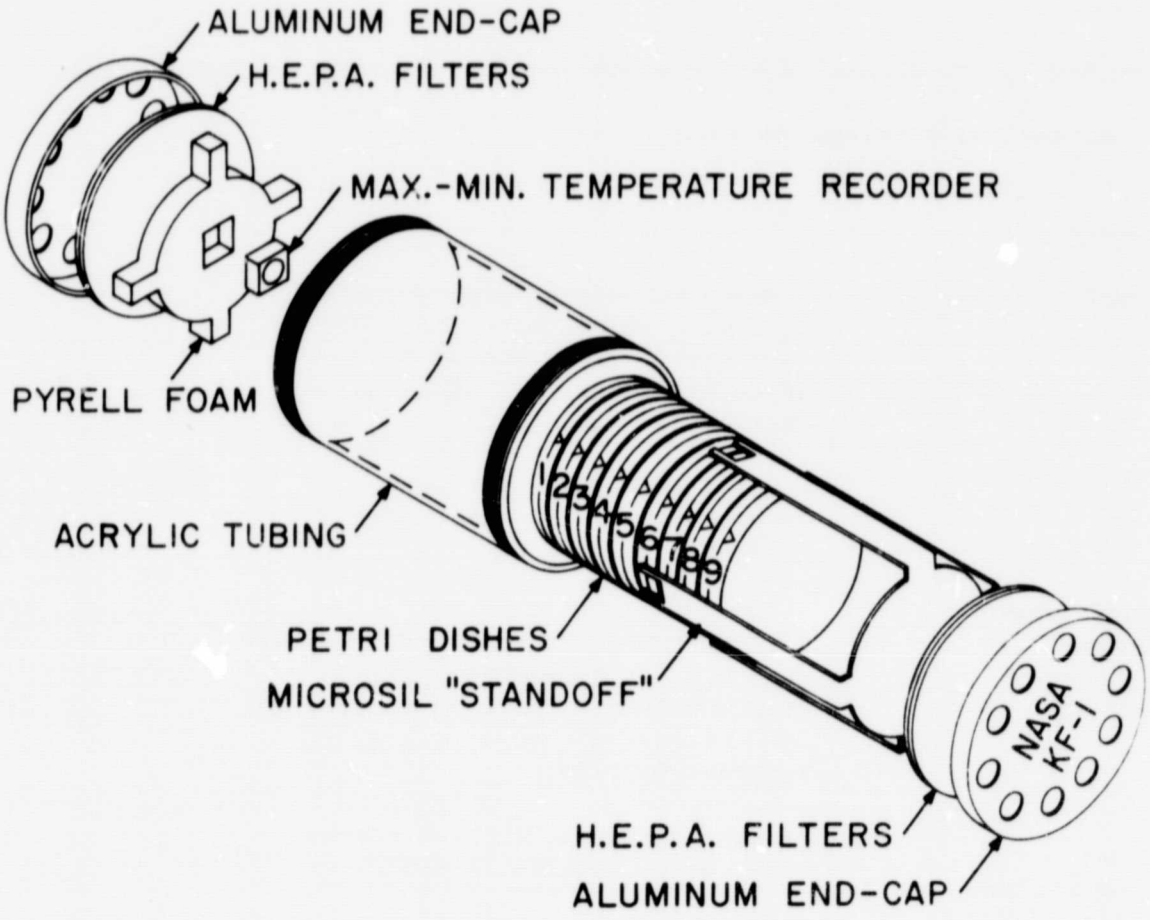

Fig. 1. Diagram of flight canister in partially assembled perspective showing petri dishes, etc. The numbers on the petri dishes represent position in the canister, 1 is at the top, 9 is at the bottom.

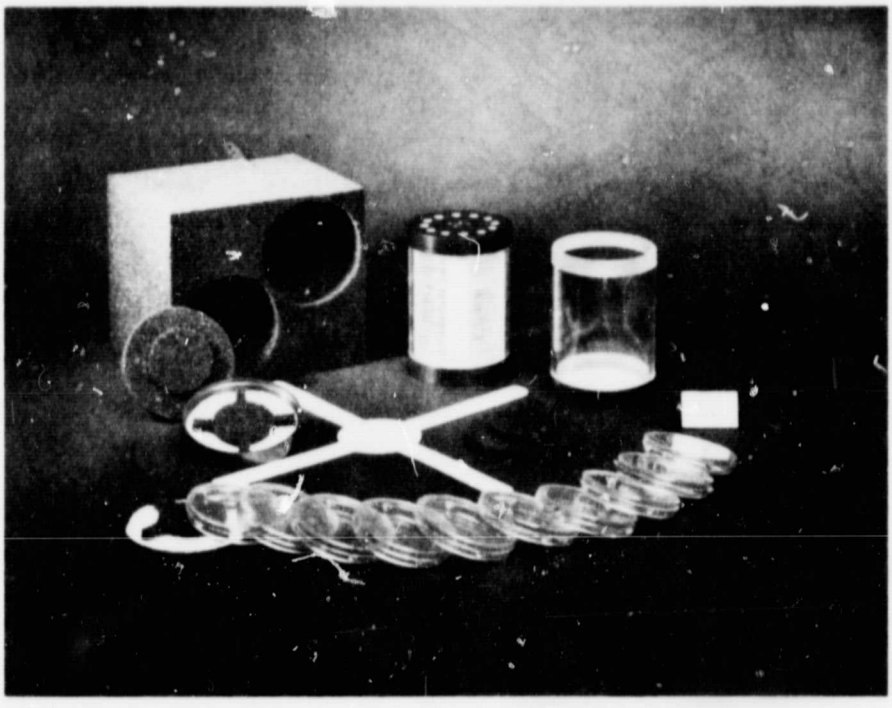

Fig. 2. Photograph of a canister in assembled (center) and disassembled (right) perspective. The plastic petri dishes are stacked on a microsil "standoff", pyrel foam cushions are placed in position and HEPA filters are placed in the anodyzed aluminum end-caps. The canisters are then inserted into a foam block. Scale bar, slightly below center right, is 1/2 inch or 1.27 cm.

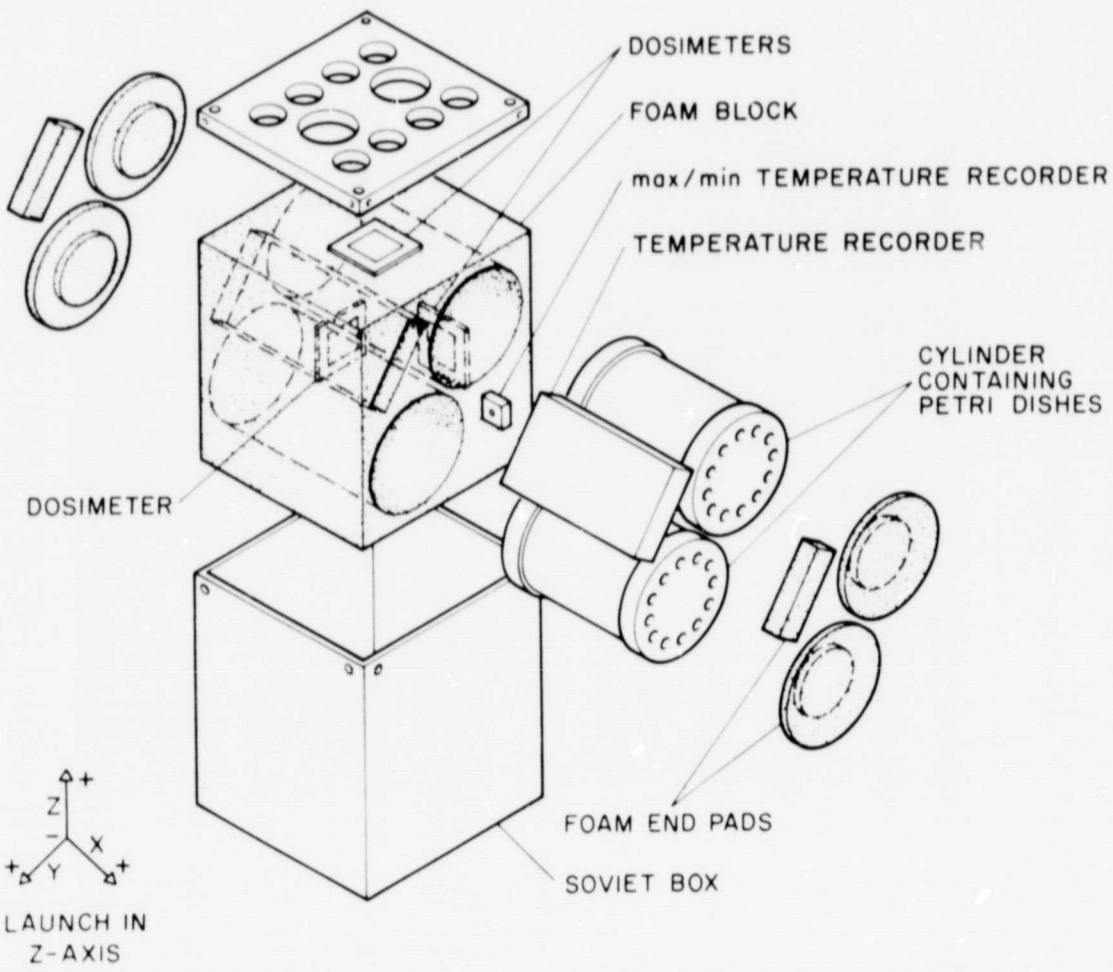

Fig. 3. Diagrammatic representation of flight hardware configuration. The lower left hand side of the diagram shows the orientation of the package as launched, i.e. the lids of the petri dishes were in the X+ position and the orientation of the units relative to gravity was in the Z- position. Not clearly shown in this diagram are all the holes (diameter 10 mm, 4 on the "top", 2 on each of the other sides) drilled in the flight container.

Fig. 4. Time course of events associated with K-302 experiment with special emphasis on temperature. 1, indicates cells and embryos maintained in liquid suspension culture at 22°C up to August 30; 2, cells prepared and distributed in agar at 48°C (note "spike") and placed in 4°C; 3, dishes with cells (KF's 1 through 12) at 22°C for several hours for inscribing and photography and returned to 4°C; 4, embryos prepared and distributed in agar at 48°C (note "spike") and placed in 4°C; 5, dishes with embryos at 22°C for several hours for inscribing and photography. Dishes with cells and embryos were then loaded into canisters, placed in biotransporter sample compartment and placed in 4°C; 6, dishes of cells and embryos (KF's 13 through 20) at 22°C for a few hours for inscribing and returned to 4°C; 7 and 8, dishes for KF's 13 through 20 at 22°C for several hours for counting and photography and returned to 4°C; 9, canisters loaded in Moscow into flight hardware. Temperature recorders for KF's 1,2, 7 and 8 activated; 10, lift-off with KF's 1 and 2; 11, recovery of KF's 1 and 2. Canisters placed in biotransporter at 4°C; 12, KF's 1,2 and 7,8, canisters returned to Stony Brook and placed in 4°C.

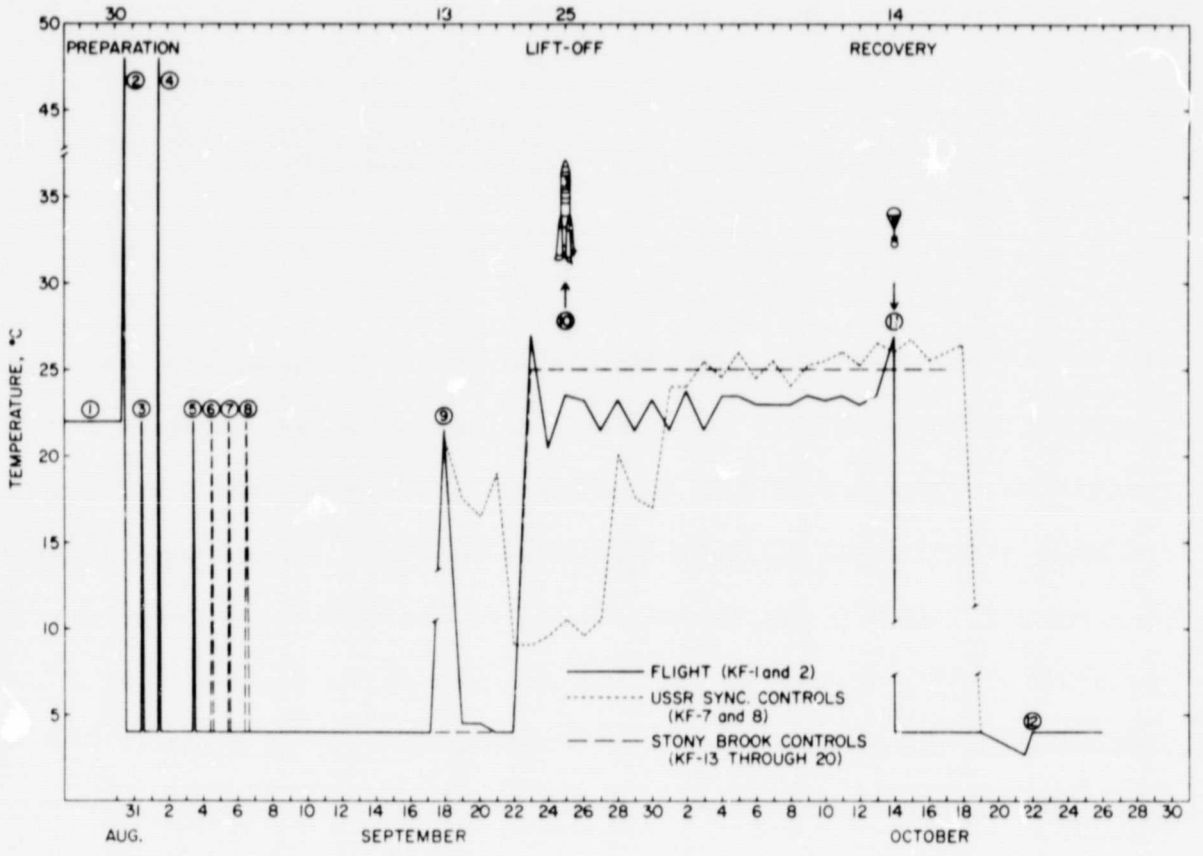

Figure 4

Figs. 5 to 10. Comparative degree of organization in carrot cells in 50 mm diameter plastic petri dishes before (a) and after (b) flight. The top panel in each of the following six figures show the dish with morphogenetically competent cellular units (sizes ranging from 38 to 74 μm) prepared for flight. There is no growth discernible to the naked eye. The lower panel in each shows discrete organized forms developed after 18.5 days at near-0 g. The designation KF 1-1, 1-2, 1-3 or KF 2-1, 2-2, 2-3 indicates the canister number, i.e. one or two, and the second digit indicates that the dish was in the first, second or third position in the canister (cf. Fig. 1).

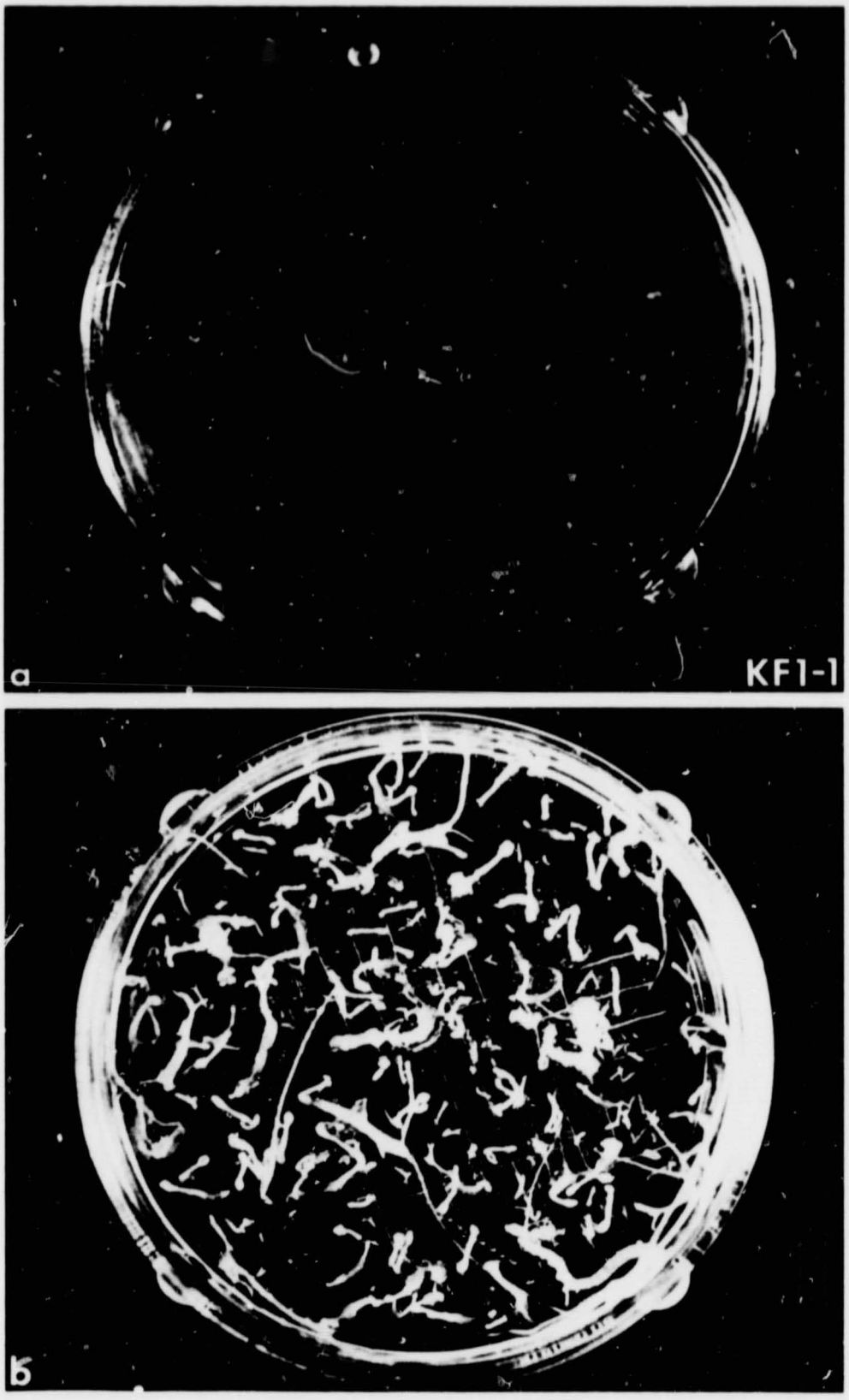

Figure 5

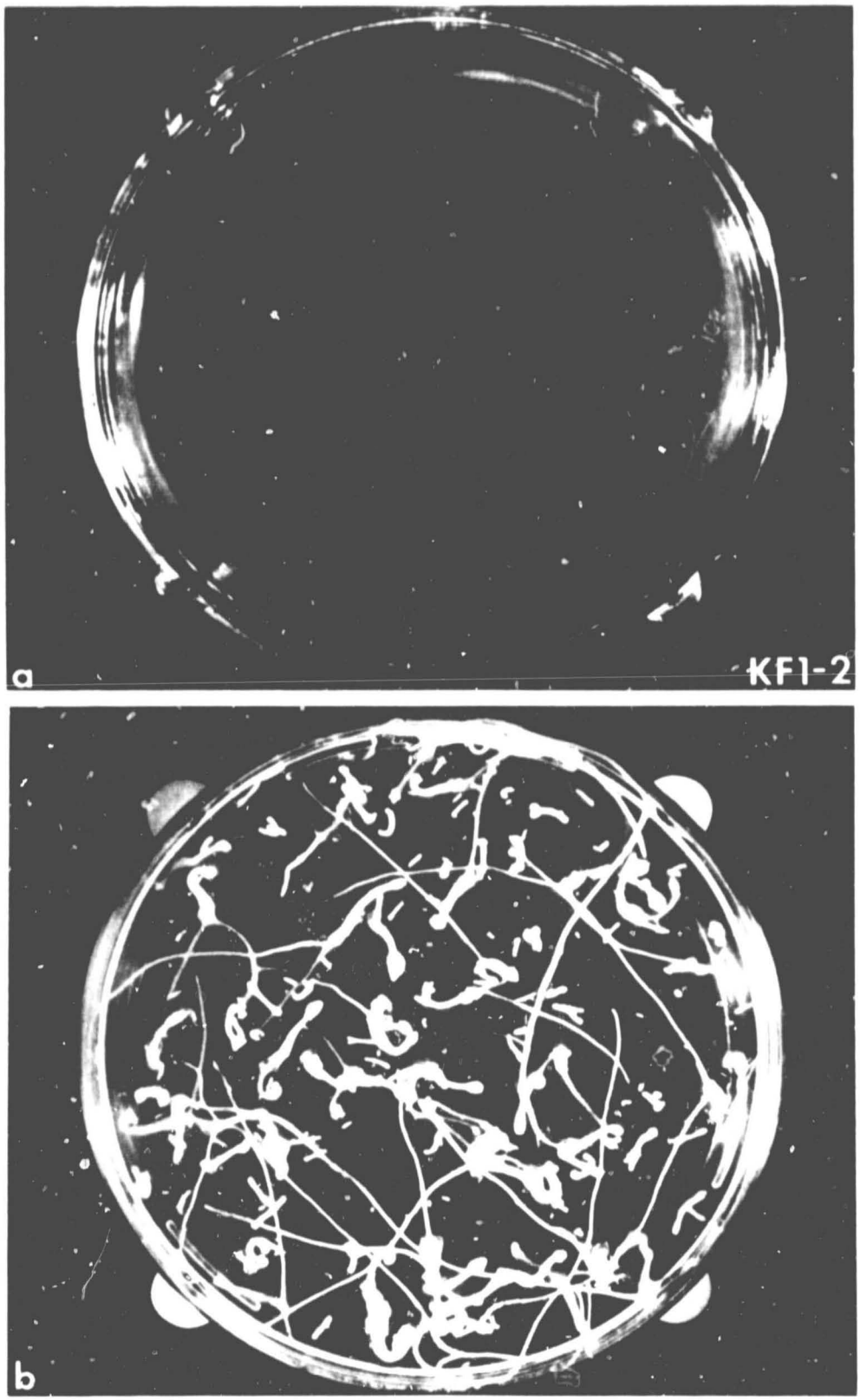

Figure 6

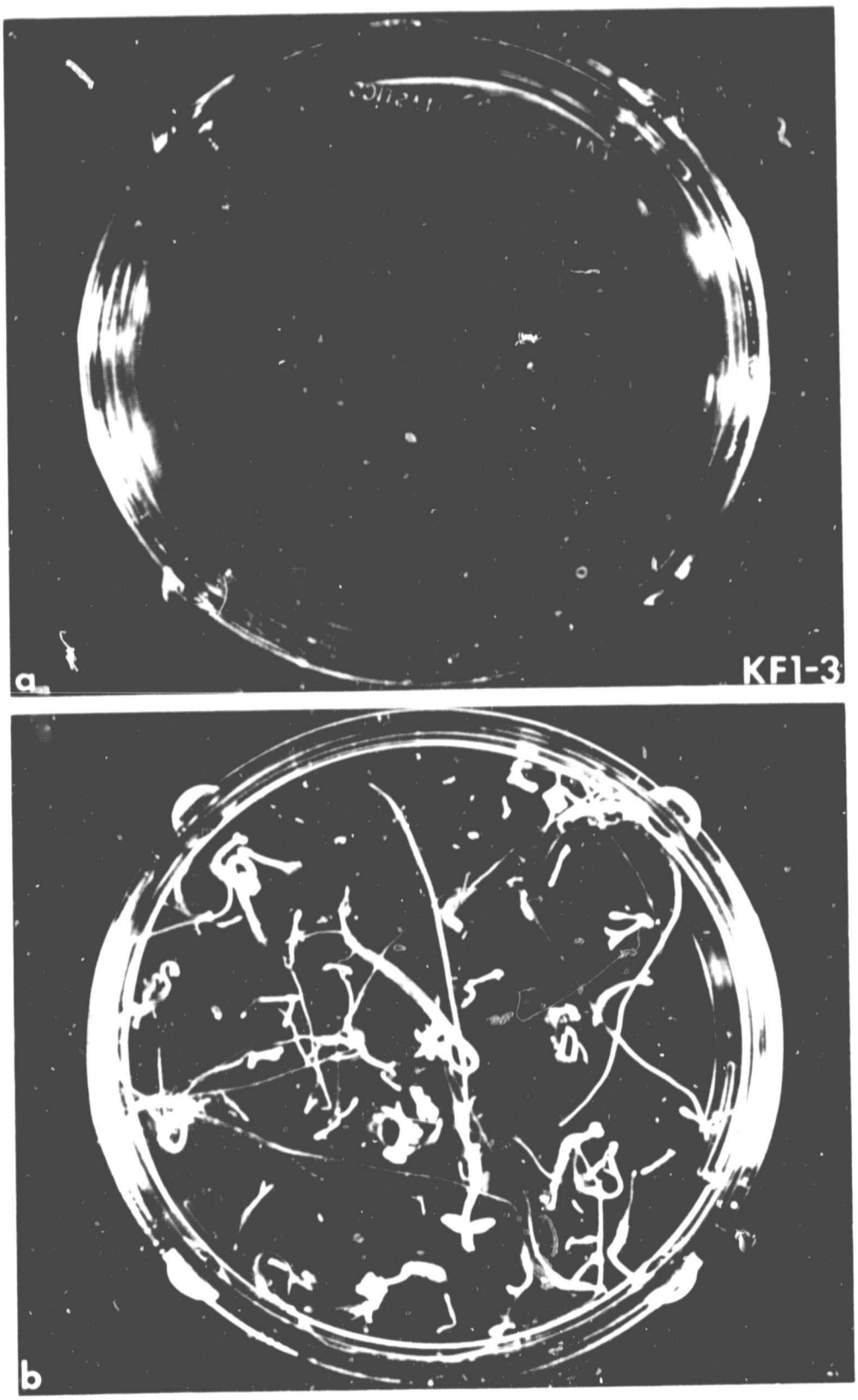

Figure 7

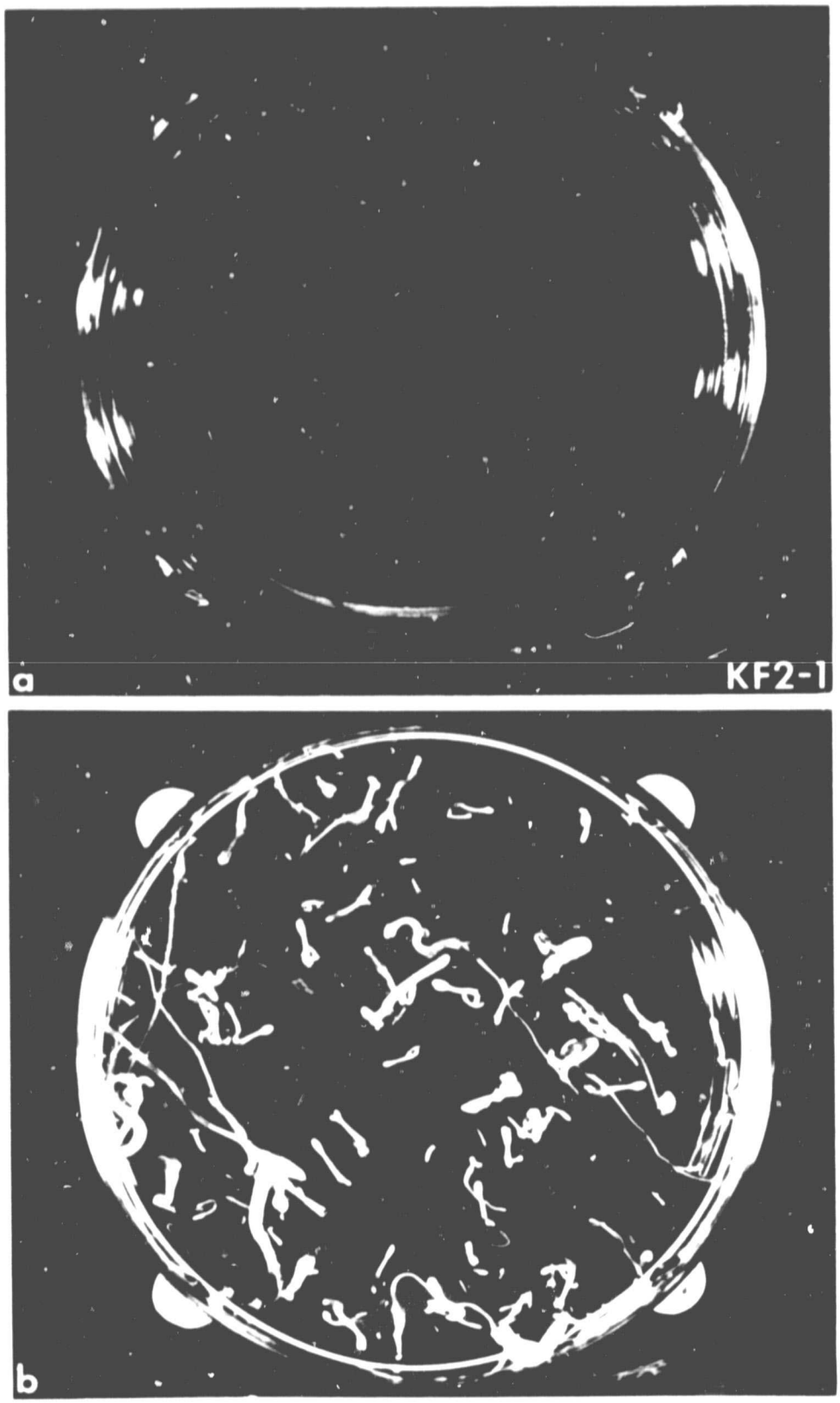

Figure 8

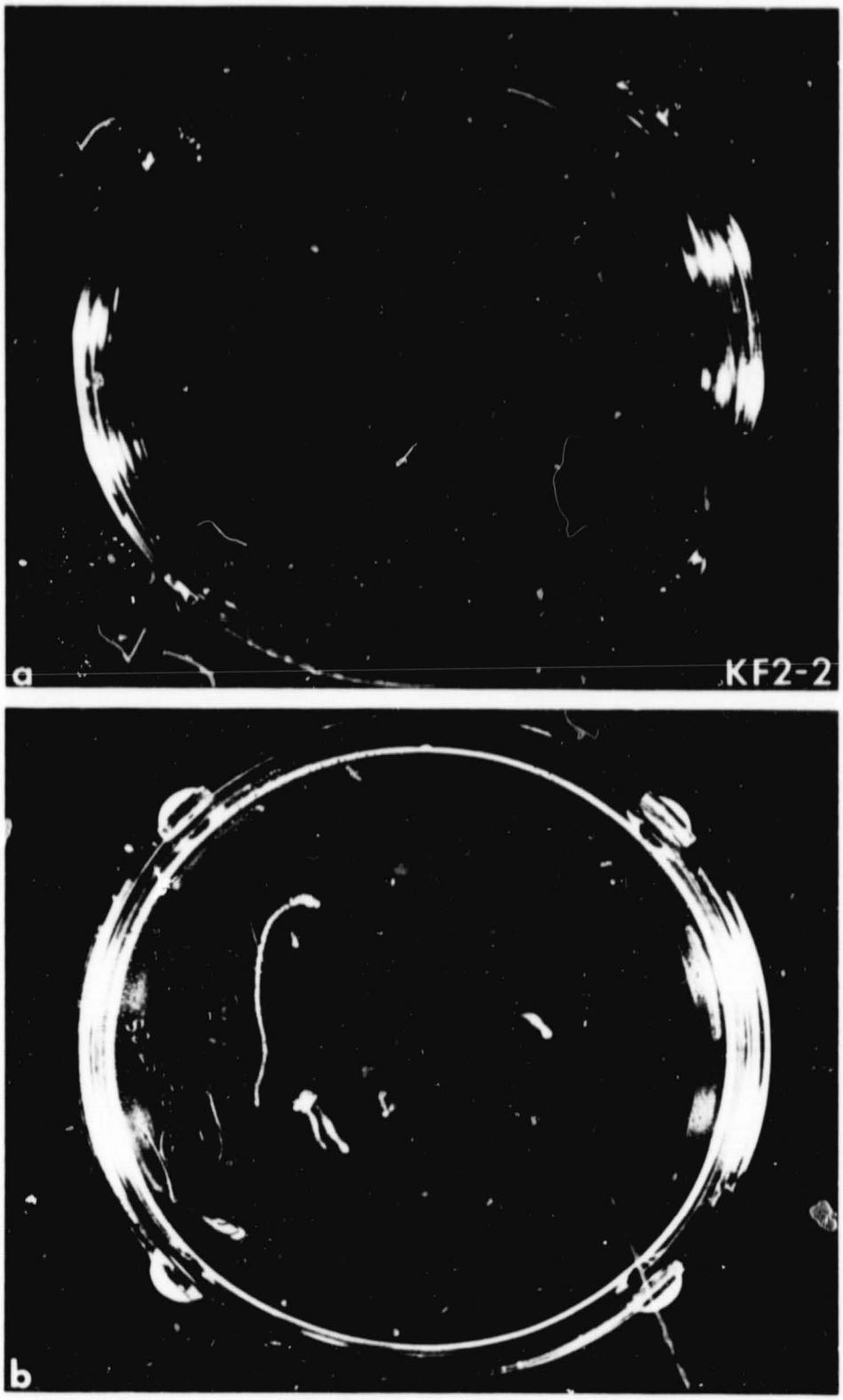

Figure 9

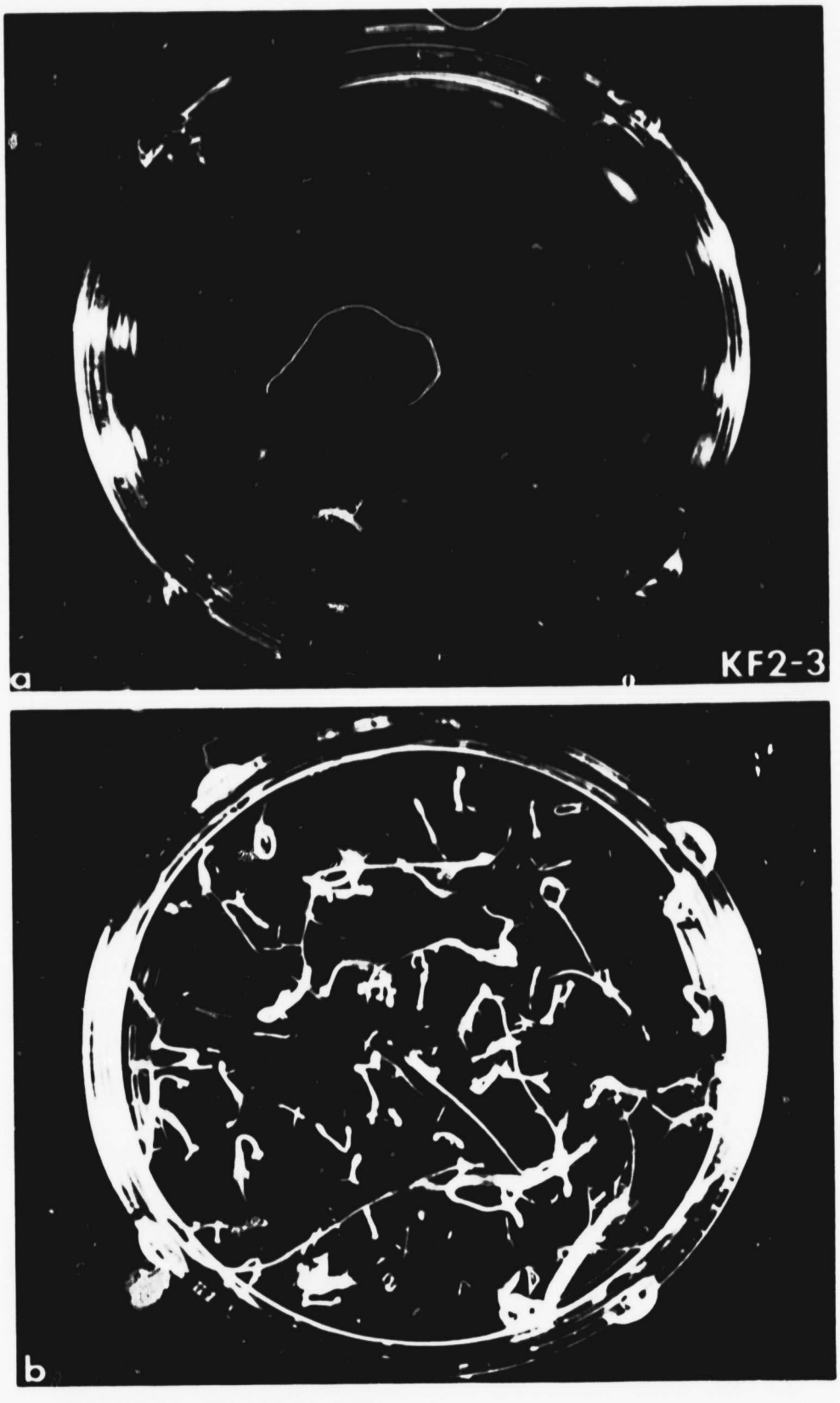

Figure 10

Figs. 11 to 16. Comparative degree of organization in carrot embryos in 50 mm diameter plastic petri dishes before (a) and after (b) flight. The top panel in each of the following six figures show the dish with somatic embryos (sizes ranging from 406 to 864 μm) prepared for flight. The embryos are well developed and have clearly identifiable root and shoot apices. The lower panel in each shows plantlets developed after 18.5 days at near-0 g. The designation KF 1-4, 1-5, 1-6 or KF 2-4, 2-5, 2-6 indicates the canister number, i.e. one or two, and the second digit indicates that the dish was in the fourth, fifth or sixth position in the canister (cf. Fig. 1).

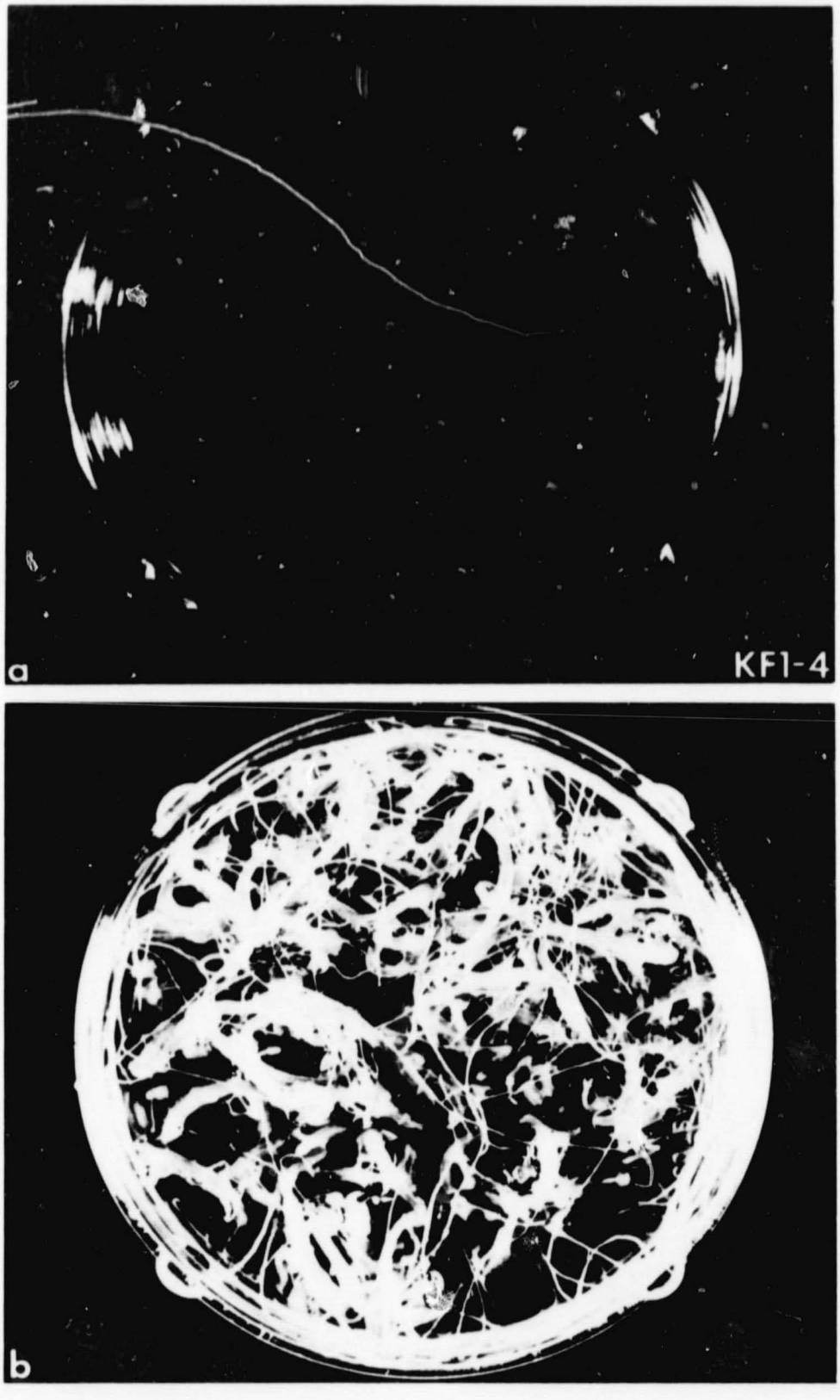

Figure 11

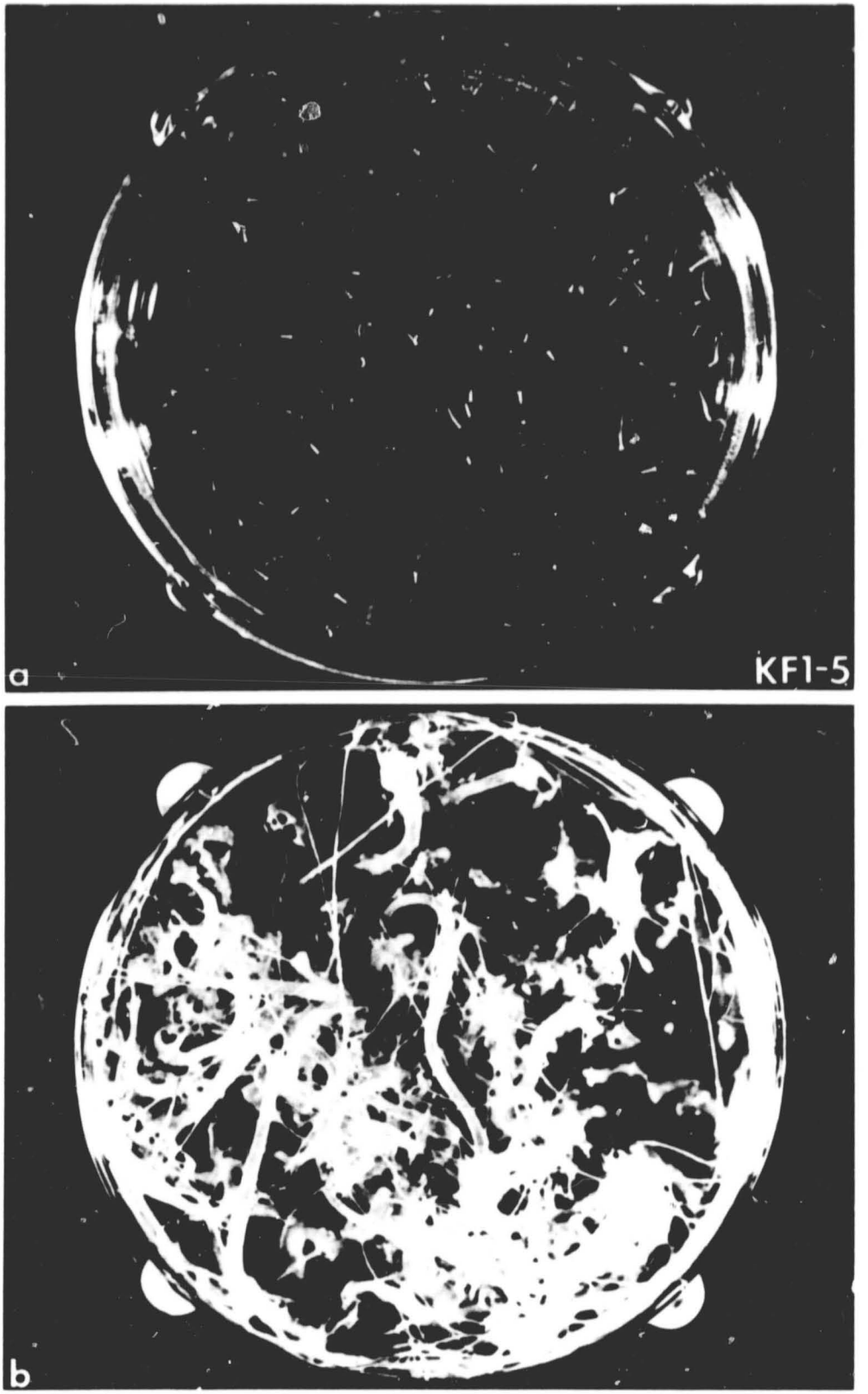

Figure 12

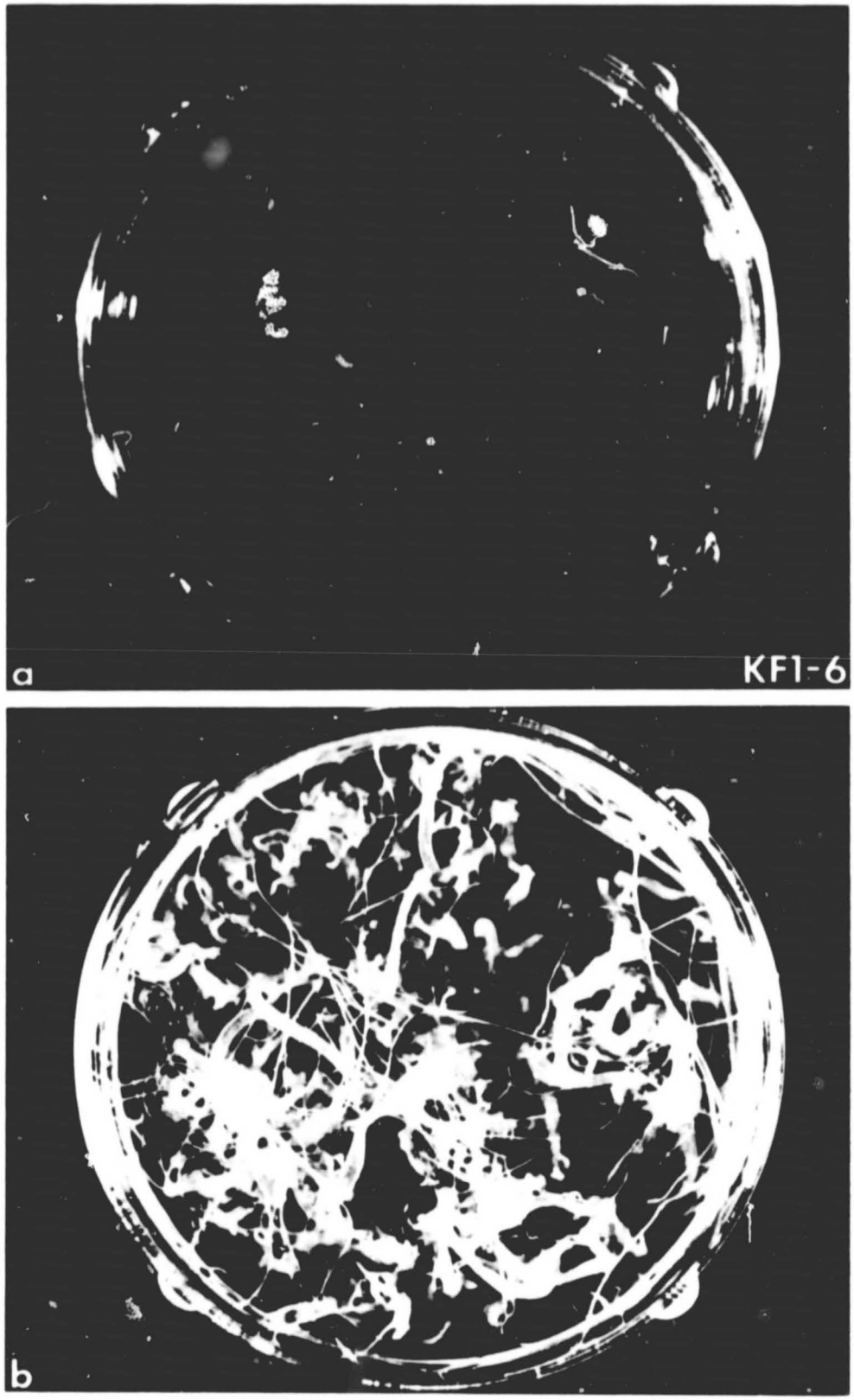

Figure 13

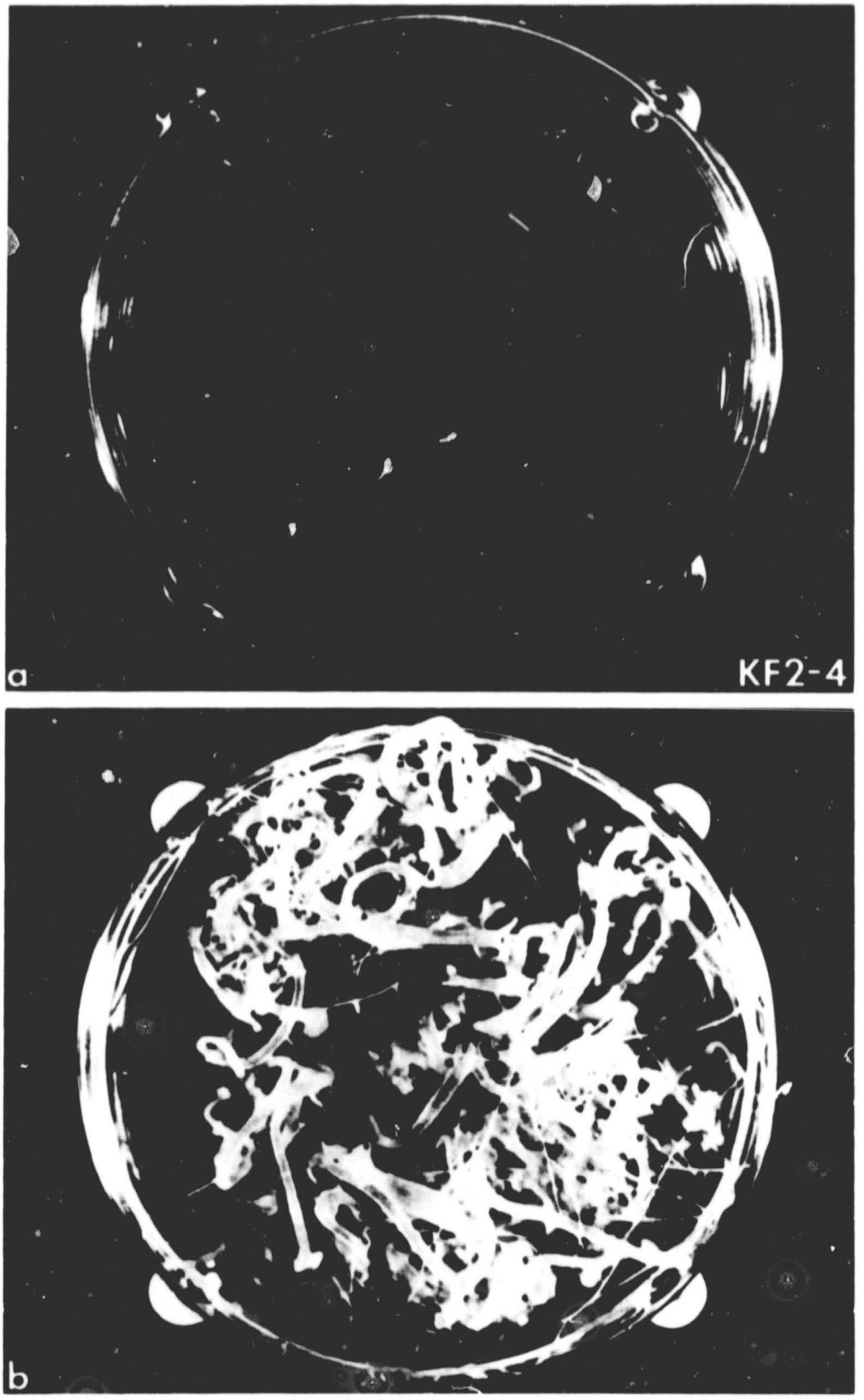

Figure 14

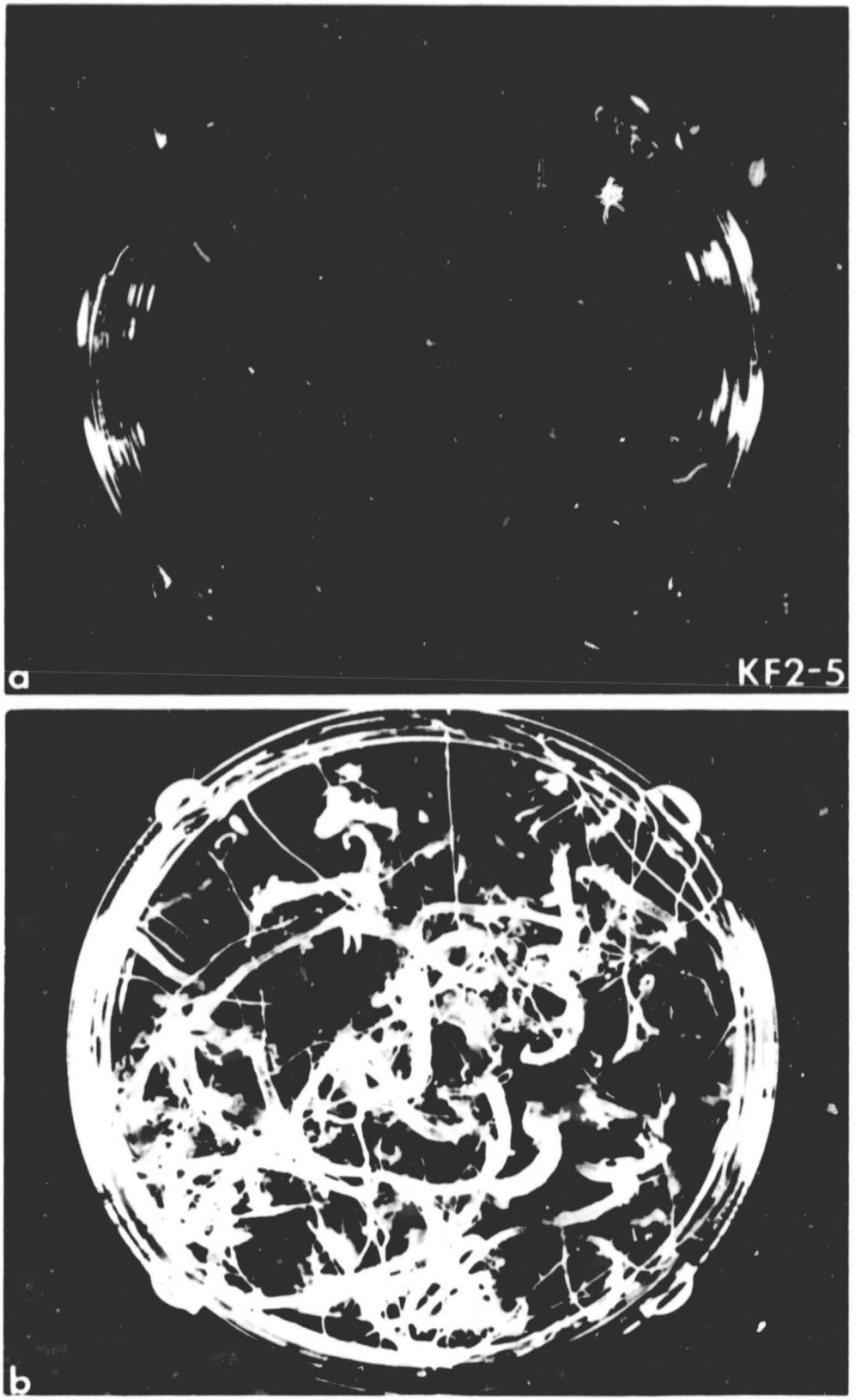

Figure 15

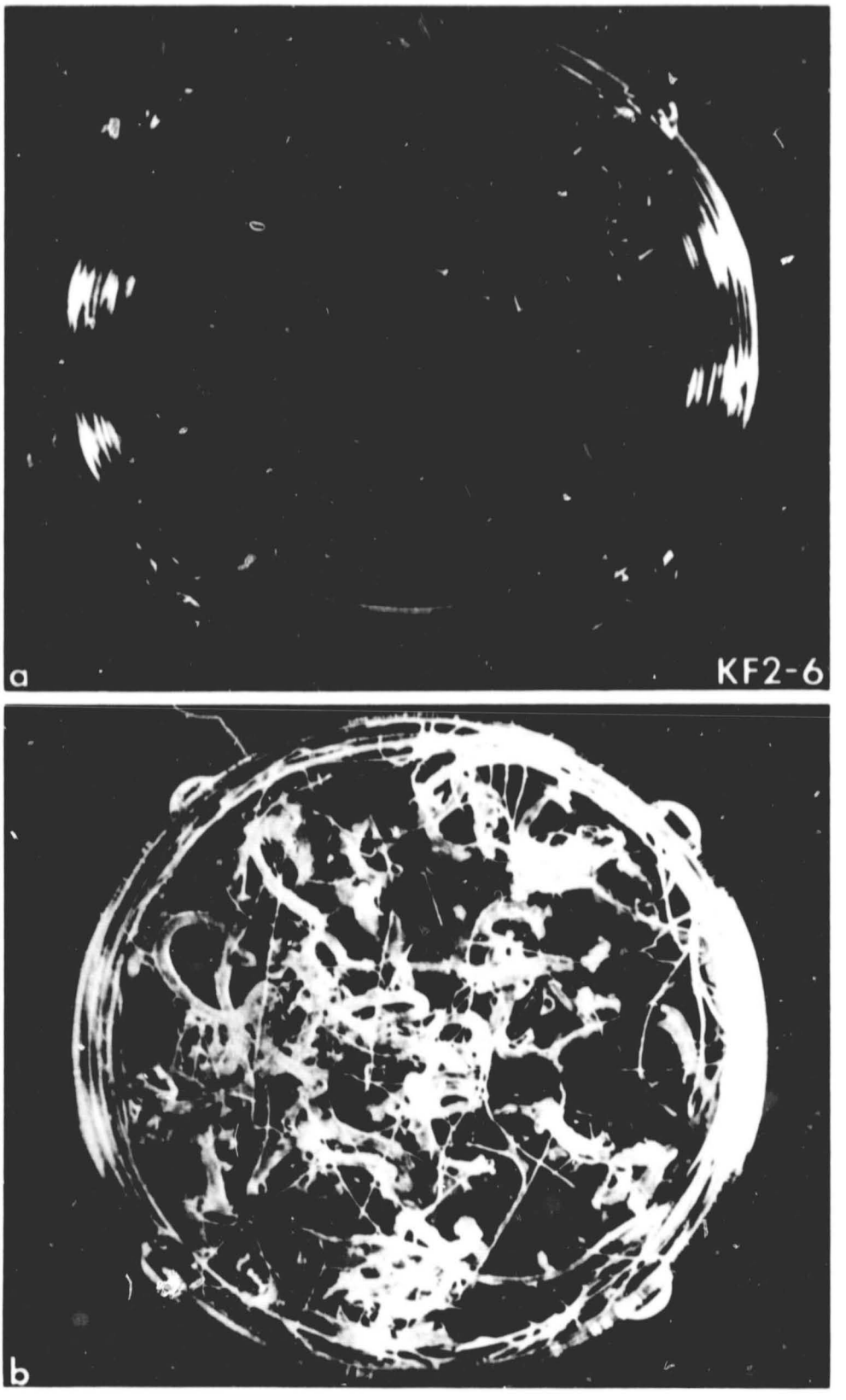

Figure 16

Figs. 17 to 22. Comparative degree of organization in carrot embryos in 50 mm diameter plastic petri dishes before (a) and after (b) flight. The top panel in each of the following six figures shows the dish with somatic embryos (sizes ranging from 234 to 406 μm) prepared for flight. The embryos, although substantially less developed and smaller than those in dishes KF 1 and 2, 4, 5 and 6, are easily recognizable. The lower panel in each shows plantlets developed after 18.5 days at near-0 g. The designation KF 1-7, 1-8, 1-9 or KF 2-7, 2-8, 2-9 indicates the canister number, i.e. one or two, and the second digit indicates that the dish was in the seventh, eighth or ninth position in the canister (cf. Fig. 1).

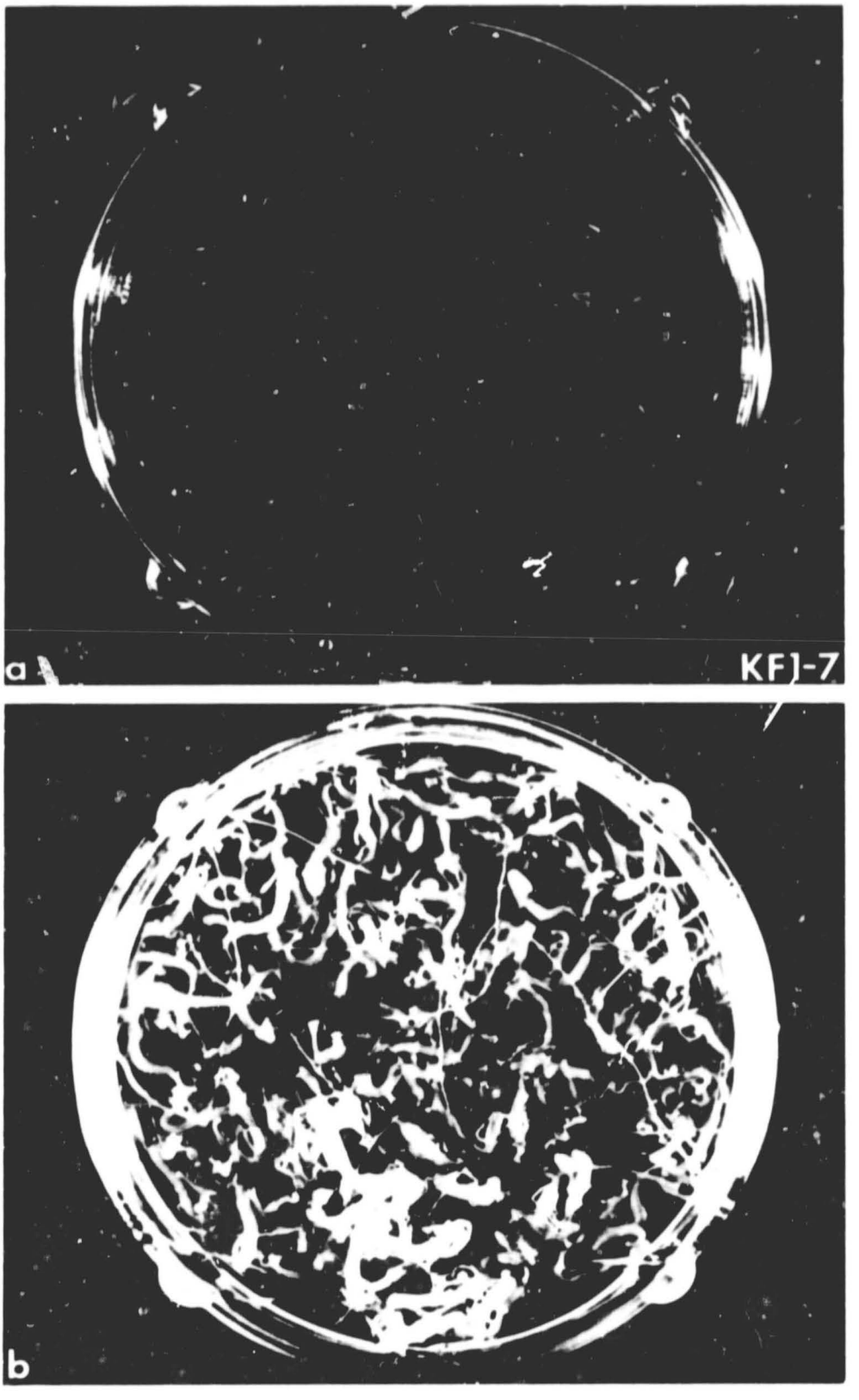

Figure 17

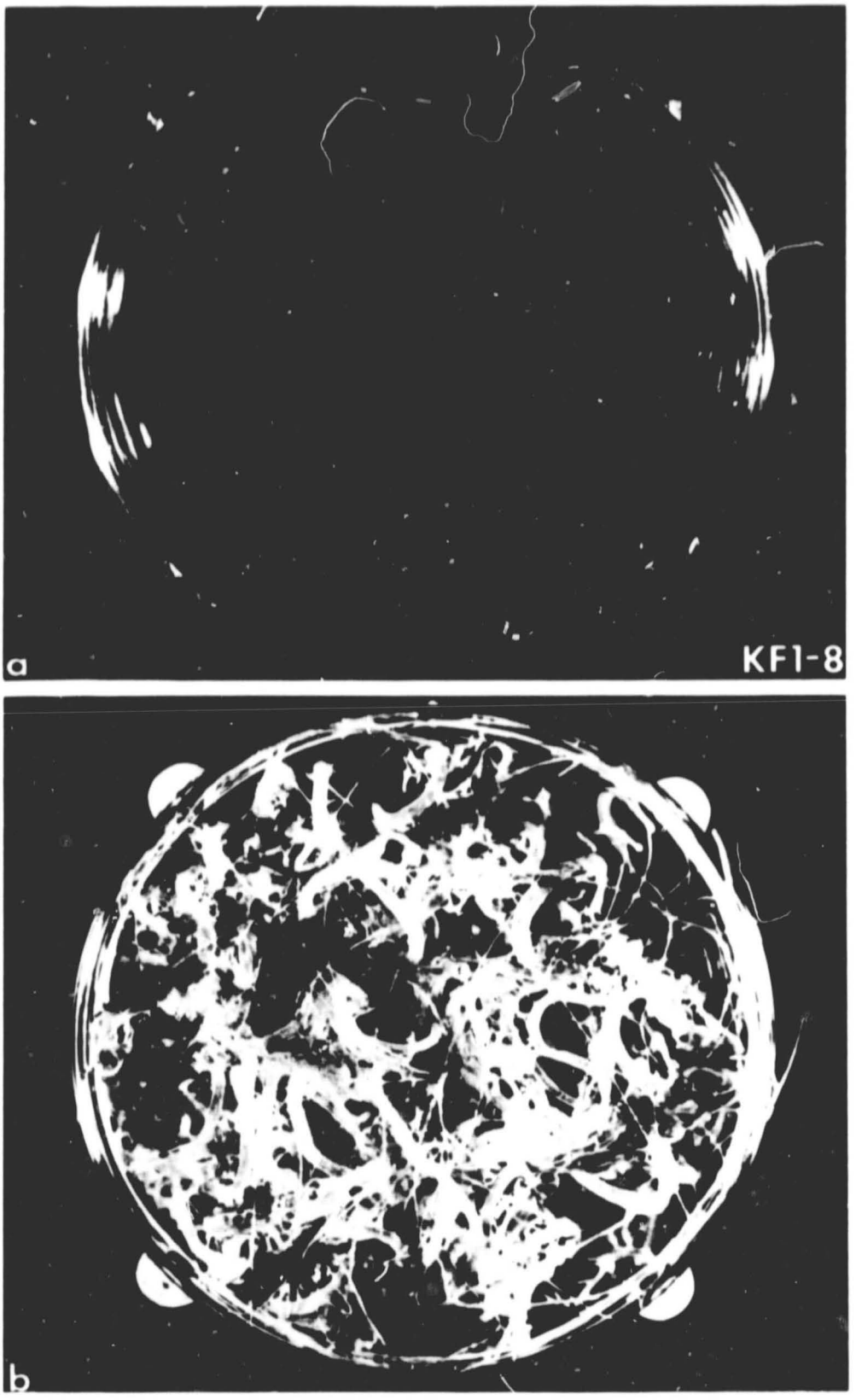

Figure 18

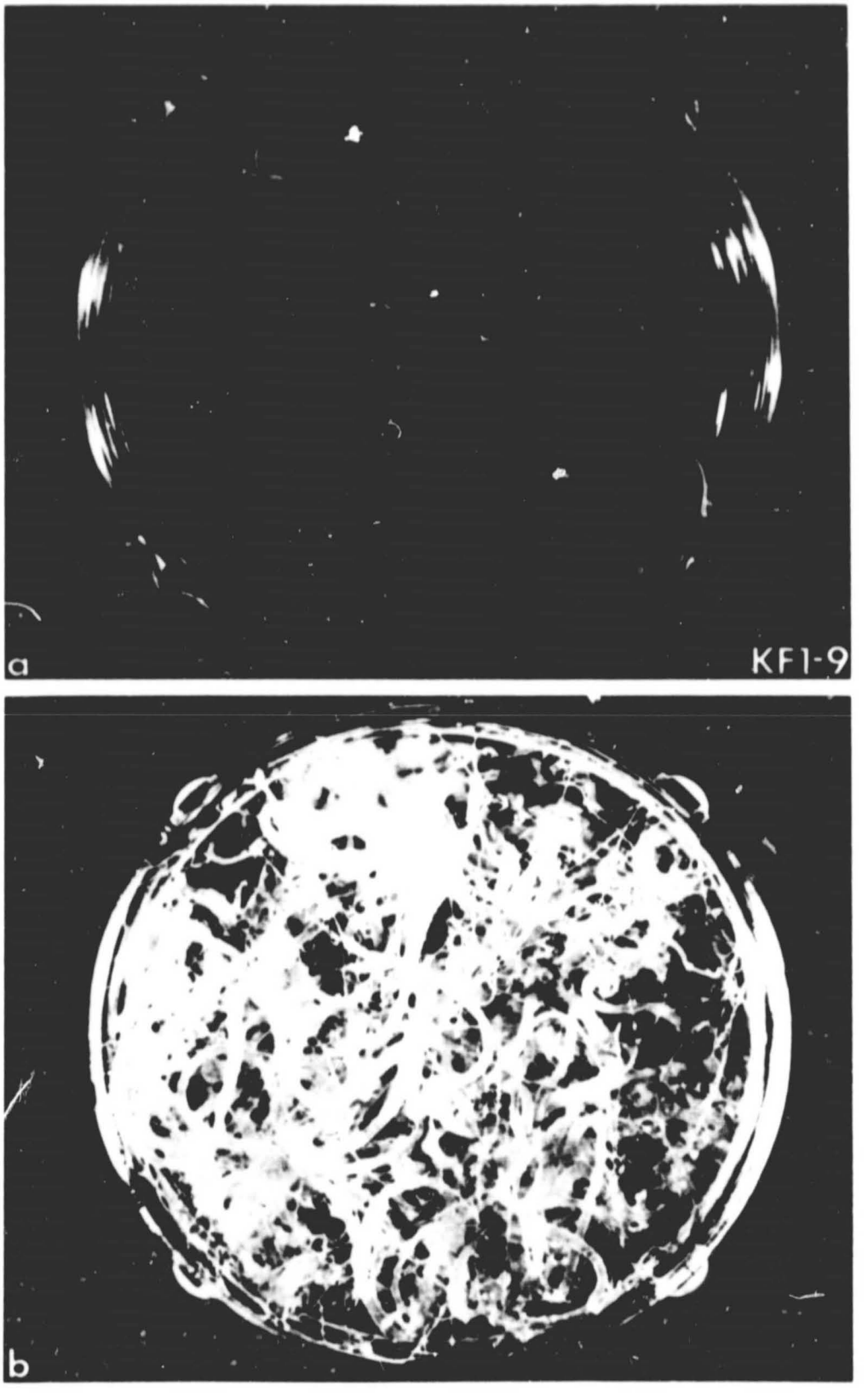

Figure 19

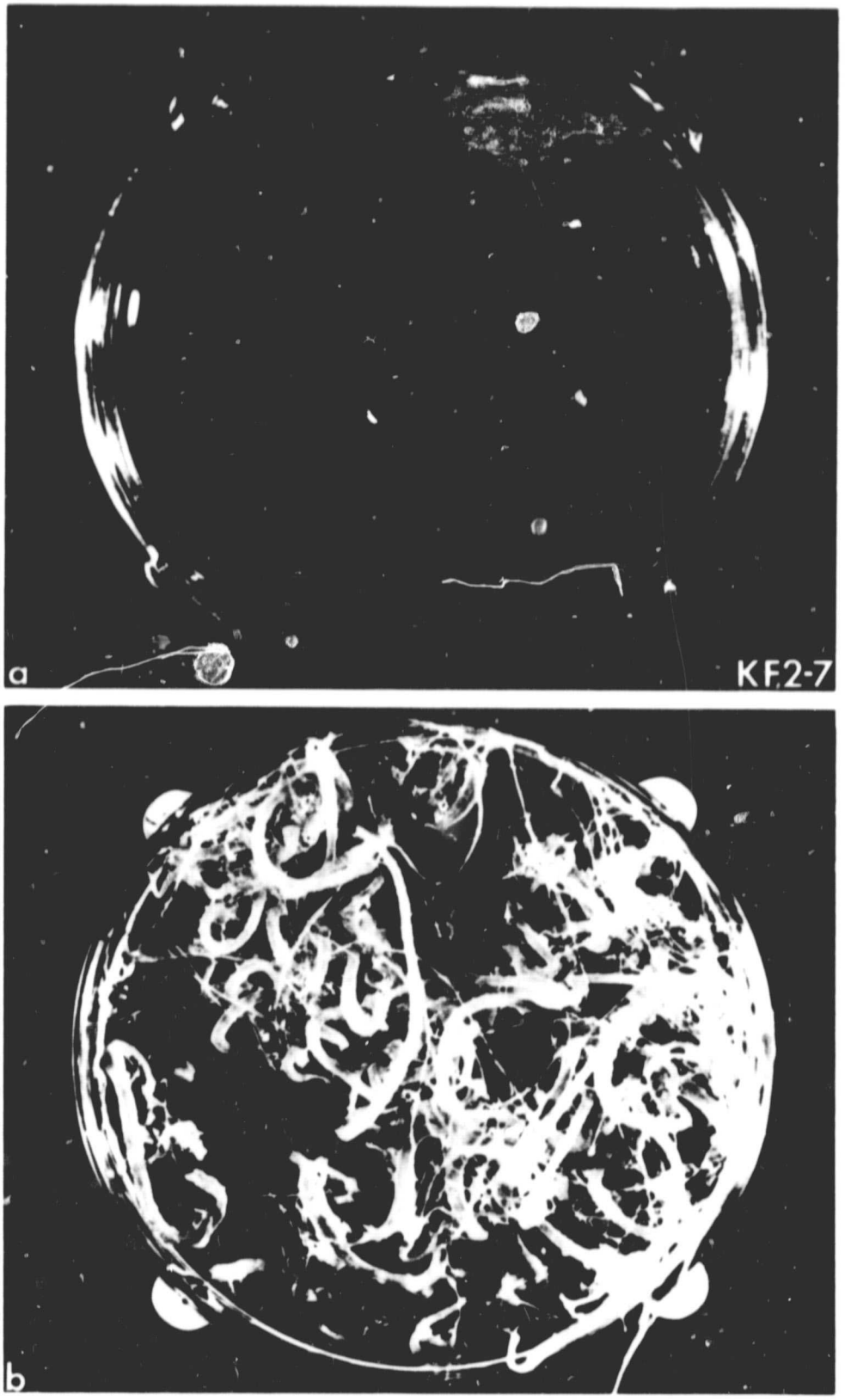

Figure 20

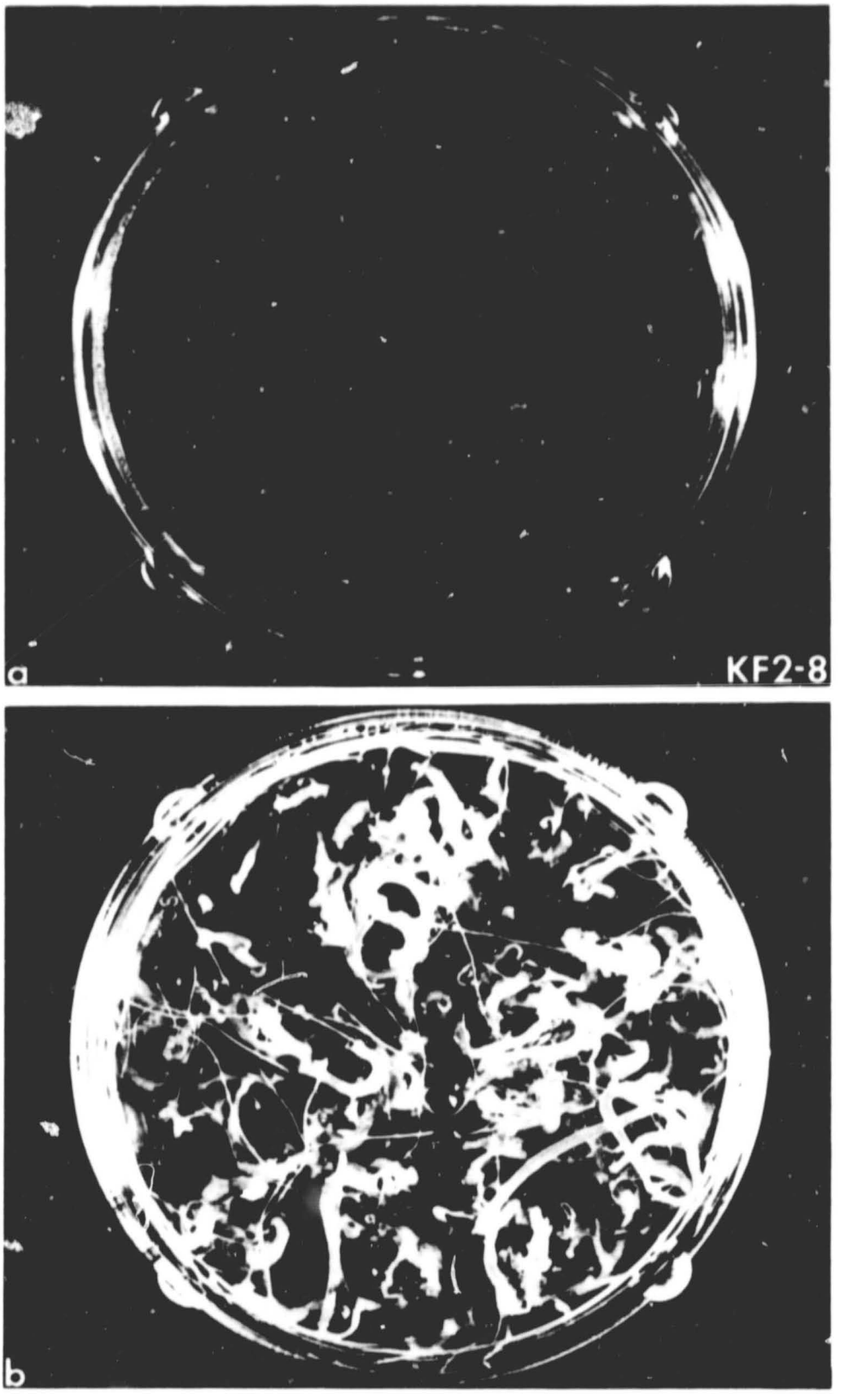

Figure 21

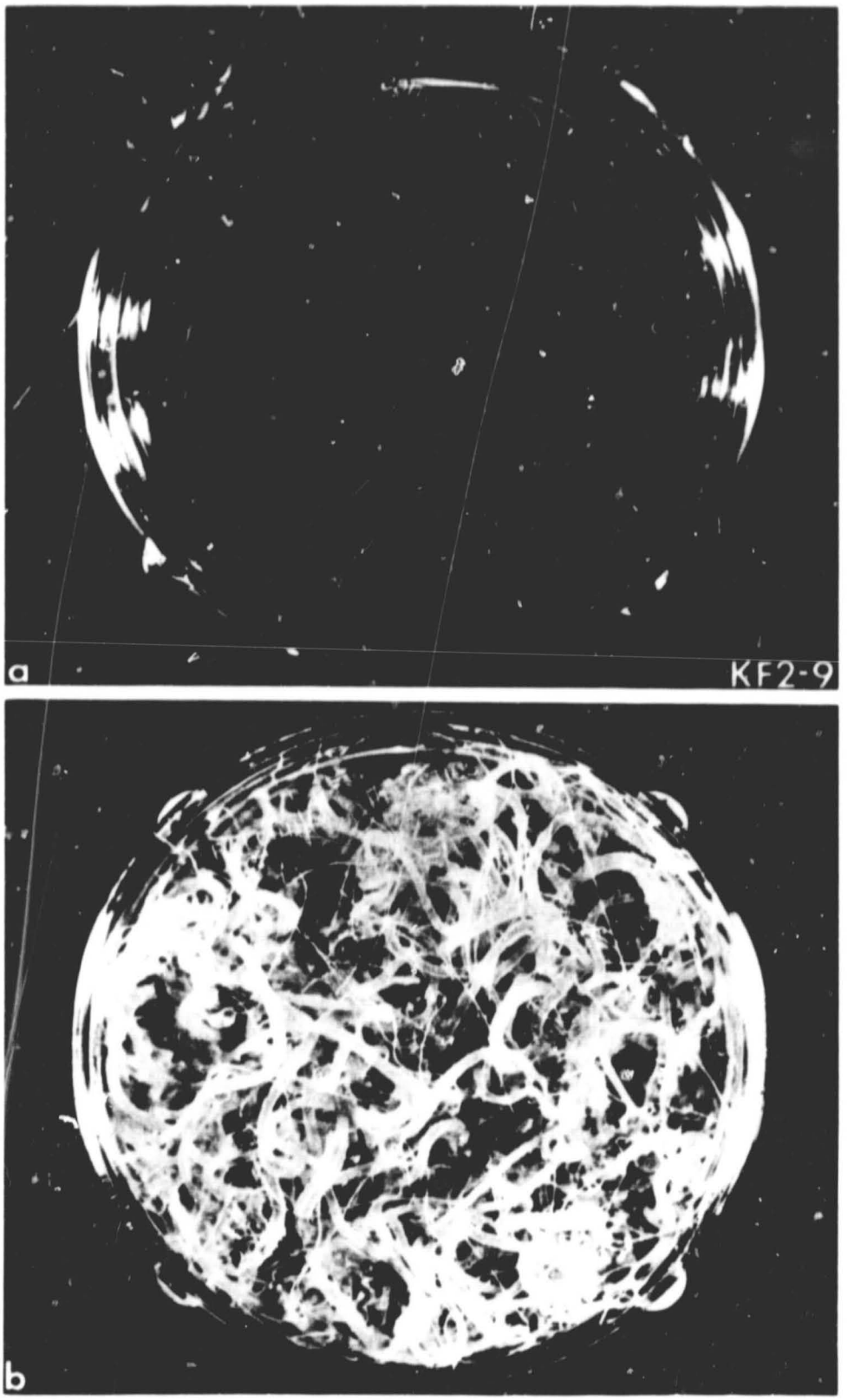

Figure 22

Fig. 23. Development of carrot from morphogenetically competent cells (sizes ranging between 38 and 74 μm) over the course of 23 days. Dishes were prepared on August 30, the same time as those destined for Cosmos 1129 and were maintained at 4°C until September 21 (day "0")--a total of 22 days. Dishes, of which these twelve are representative, were then placed in darkness at 25°C. Sample dishes were removed, examined and photographed every two days. The number in the lower right-hand corner of the panels indicates the length of time in days of growth at 25°C. This composite, in effect, shows photographically the time course of growth at a macro level. Size Scale: 50 mm diameter plastic petri dish.

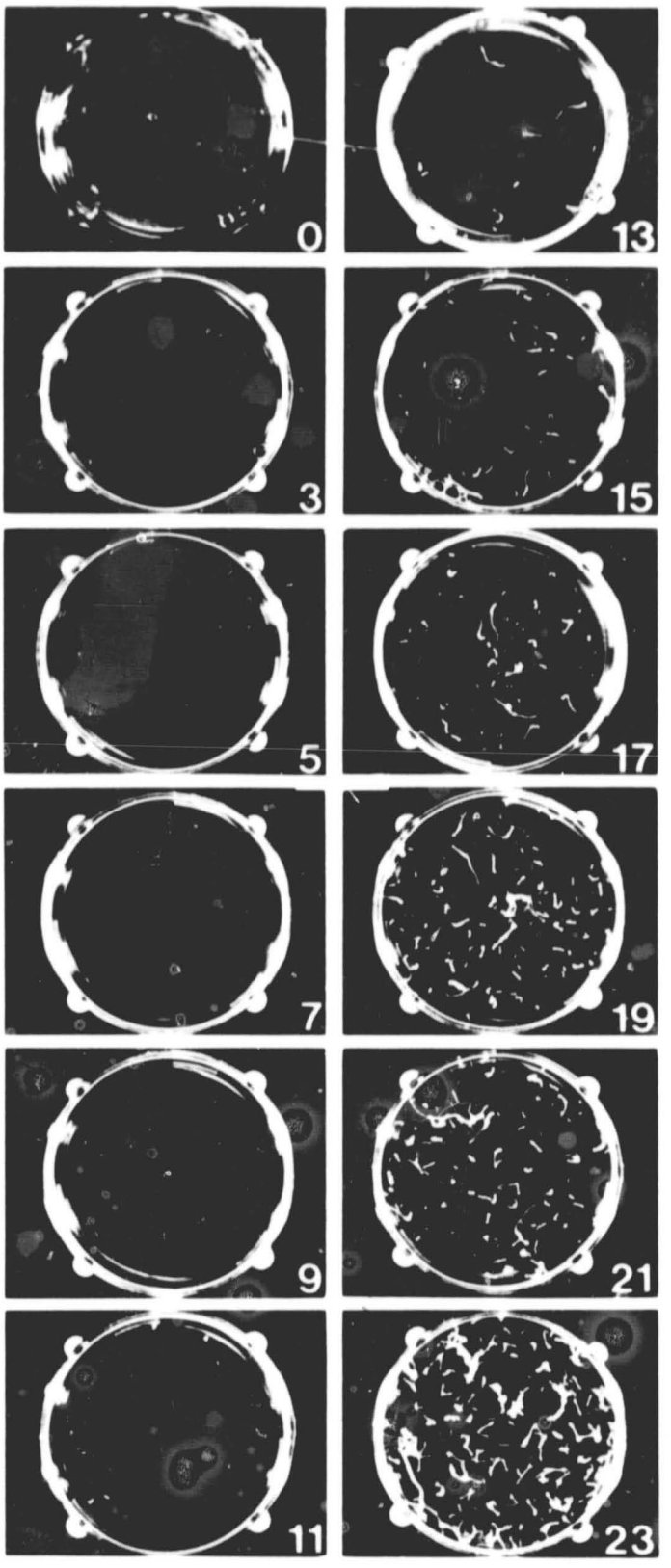

Figure 23

Fig. 24. Development of carrot from somatic embryos (sizes ranging between 406 and 864 μm) over the course of 23 days. Dishes were prepared on August 30, at the same time as those destined for flight on Cosmos 1129 and were maintained at 4°C until September 21 (day "0")--a total of 22 days. Dishes were then placed in darkness at 25°C. Sample dishes of which these are representative, were removed, examined and photographed every two days. The number in the lower left-hand corner of the panels with the petri dishes indicates the length of time in days of growth at 25°C. The opposite right-hand panels show the gross morphology of the plantlets which were mechanically freed from the agar by washing, etc. The composite on this and the following page, in effect, shows photographically the time course of growth at a macro level. Scale bar for the petri dishes and the embryos and plantlets: 1 cm.

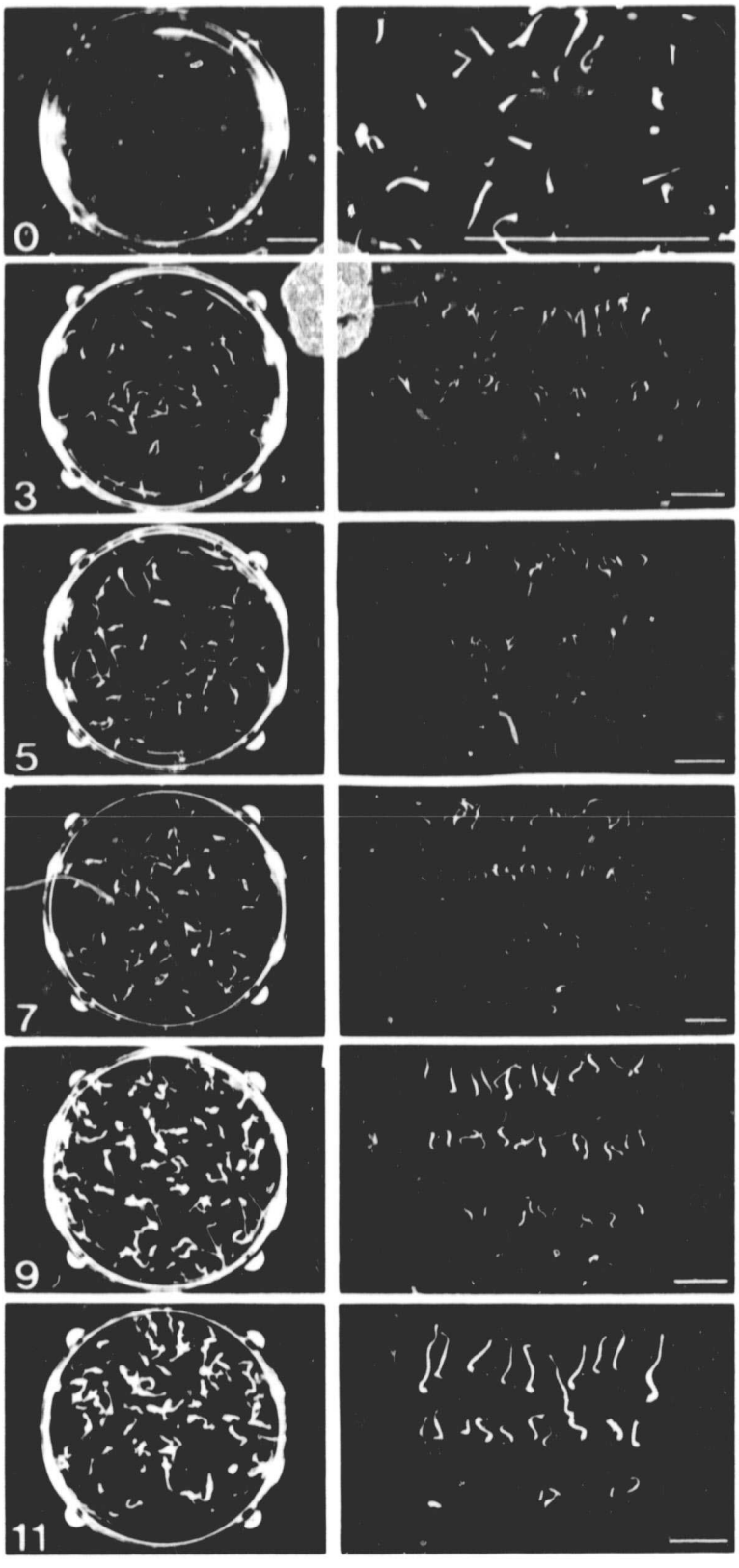

Figure 24

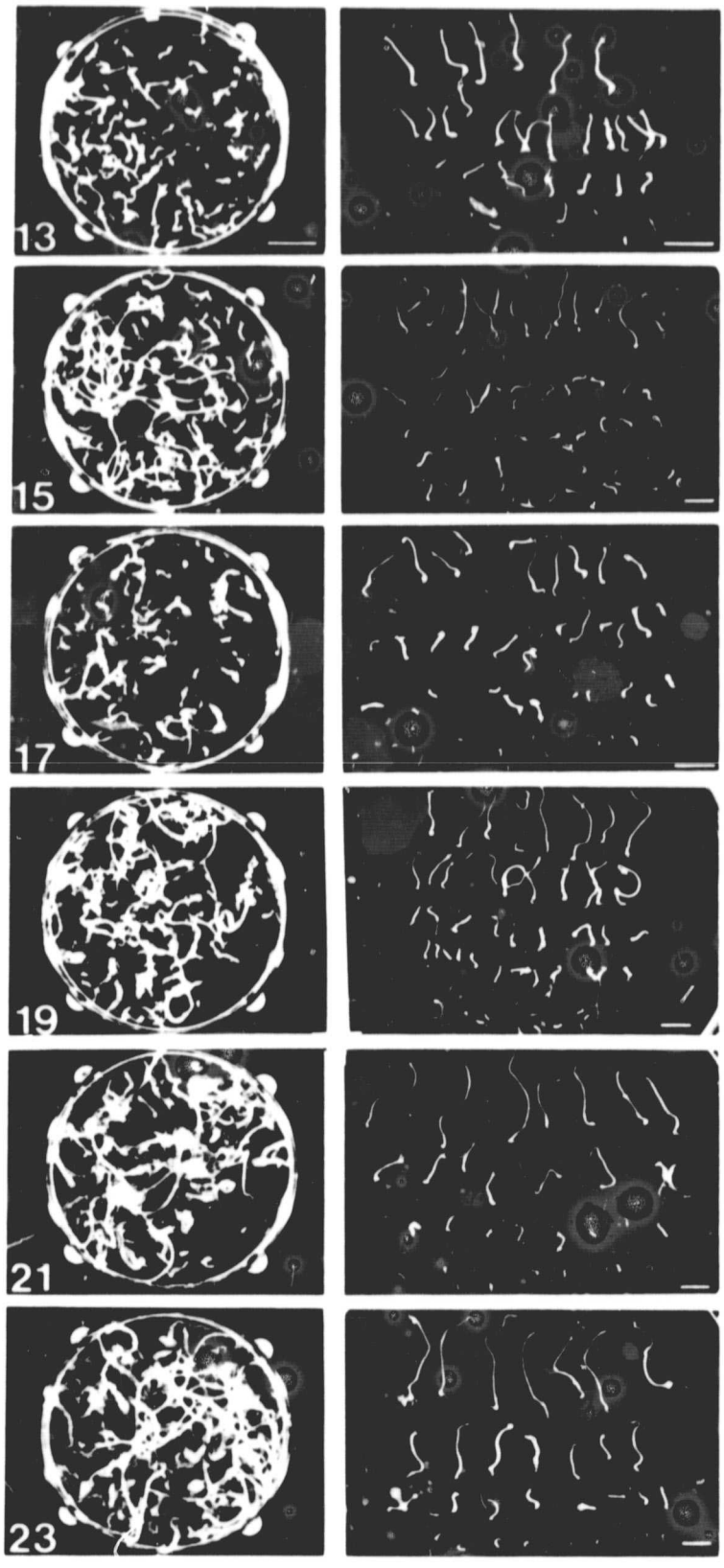

Figure 24

Fig. 25. Development of carrot from somatic embryos (sizes ranging between 234 and 406 μm) over the course of 23 days. Dishes were prepared on August 30, at the same time as those destined for flight on Cosmos 1129 and were maintained at 4°C until September 21 (day "0")--a total of 22 days. Dishes were then placed in darkness at 25°C. Sample dishes of which these are representative, were removed, examined and photographed every two days. The number in the lower left-hand corner of the panels with the petri dishes indicates the length of time in days of growth at 25°C. The opposite right-hand panels show the gross morphology of the plantlets which were mechanically freed from the agar by washing, etc. The composite on this and the following page, in effect, shows photographically the time course of growth at a macro level. Scale bar for the petri dishes and the embryos and plantlets: 1 cm.

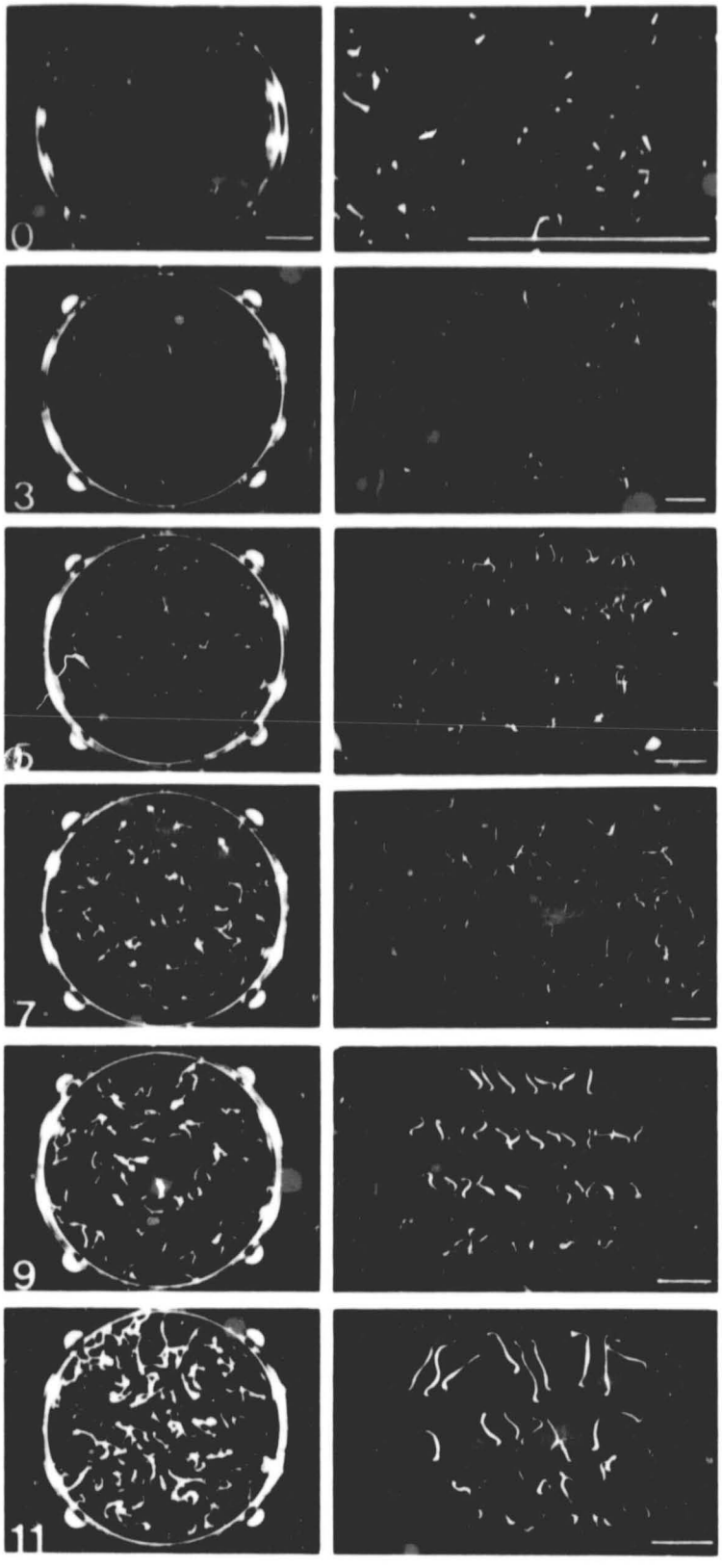

Figure 25

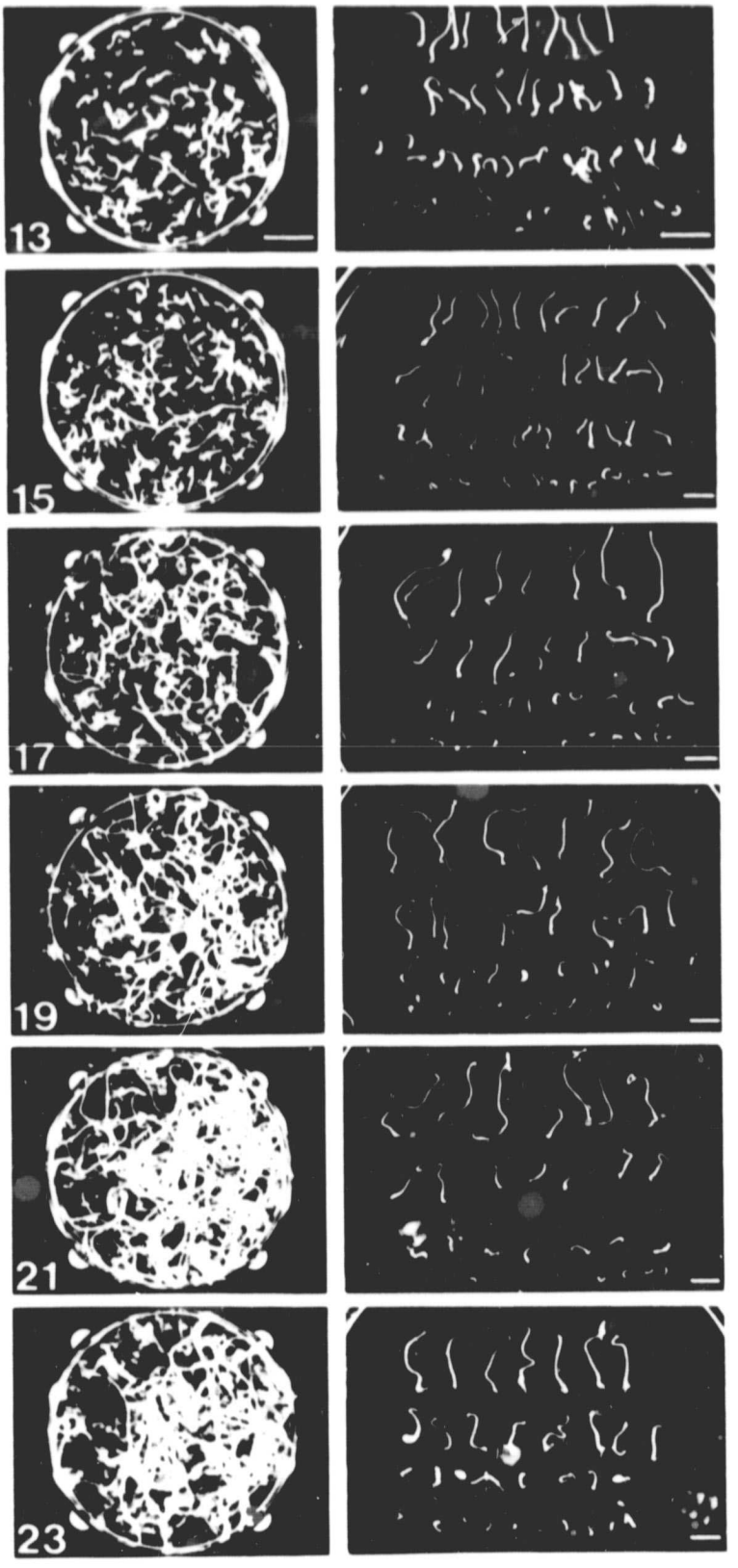

Figure 25

Fig. 26. Comparison of growth and development of a carrot plant from an embryo which grew in space and its exact ground control counterpart. The left-hand sequence (a through d) shows the growth of a somatic embryo (size range 406 to 864 μm) after removal from flight dish KF 1-4. The right-hand sequence (e through h) shows the growth of a somatic embryo from ground control dish KF 7-4. The length of time in days of growth using the date of the freshly removed embryo from the dishes as time "0", is shown in the lower right-hand corner of each panel. Scale bars: 1 cm.

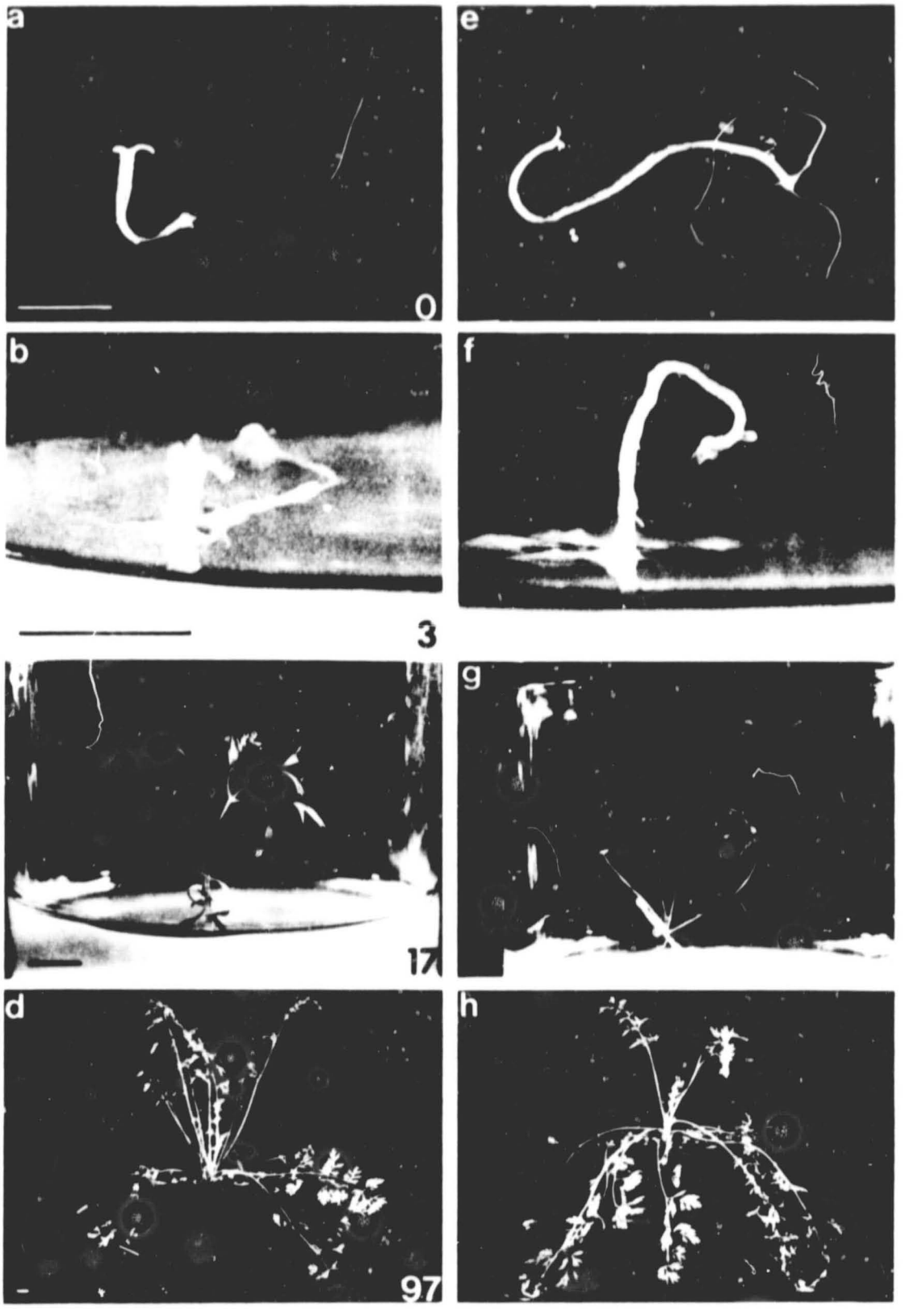

Figure 26

Fig. 27. Comparison of growth and development of a carrot plant from an embryo which grew in space and its exact ground control counterpart. The left-hand sequence (a through d) shows the growth of a somatic embryo (size range 234 to 406 μm) after removal from flight dish KF 1-7. The right-hand sequence (e through h) shows the growth of a somatic embryo from ground control dish KF 7-7. The length of time in days of growth using the date of the freshly removed embryo from the dishes as time "0", is shown in the lower right-hand corner of each panel. Scale bars: 1 cm.

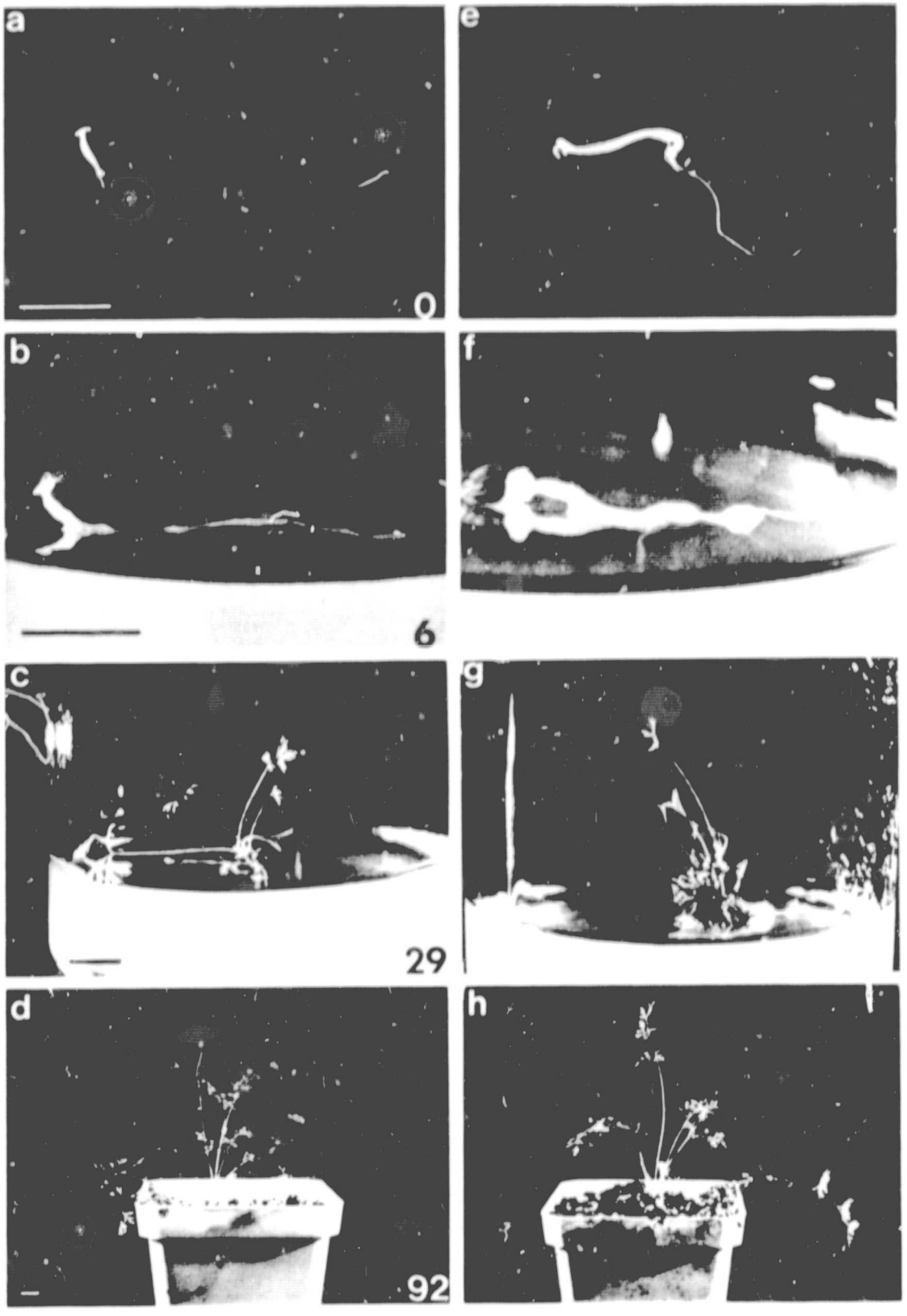

Figure 27

Fig. 28. Carrot development at near-0 g. Top row, representative stages of development exposed to the space environment. a, proembryonic cell clusters ranging between 38 and 74 μm; b, somatic embryos ranging between 406 and 864 μm; c, somatic embryos ranging between 234 and 406 μm; d,e, and f, dishes with carrot material at the stages shown at a,b, and c prepared for flight; g,h and i, dishes with embryos and plantlets after 18.5 days in flight. Scale bars: a-c 100 μm; d-i, 10 mm.

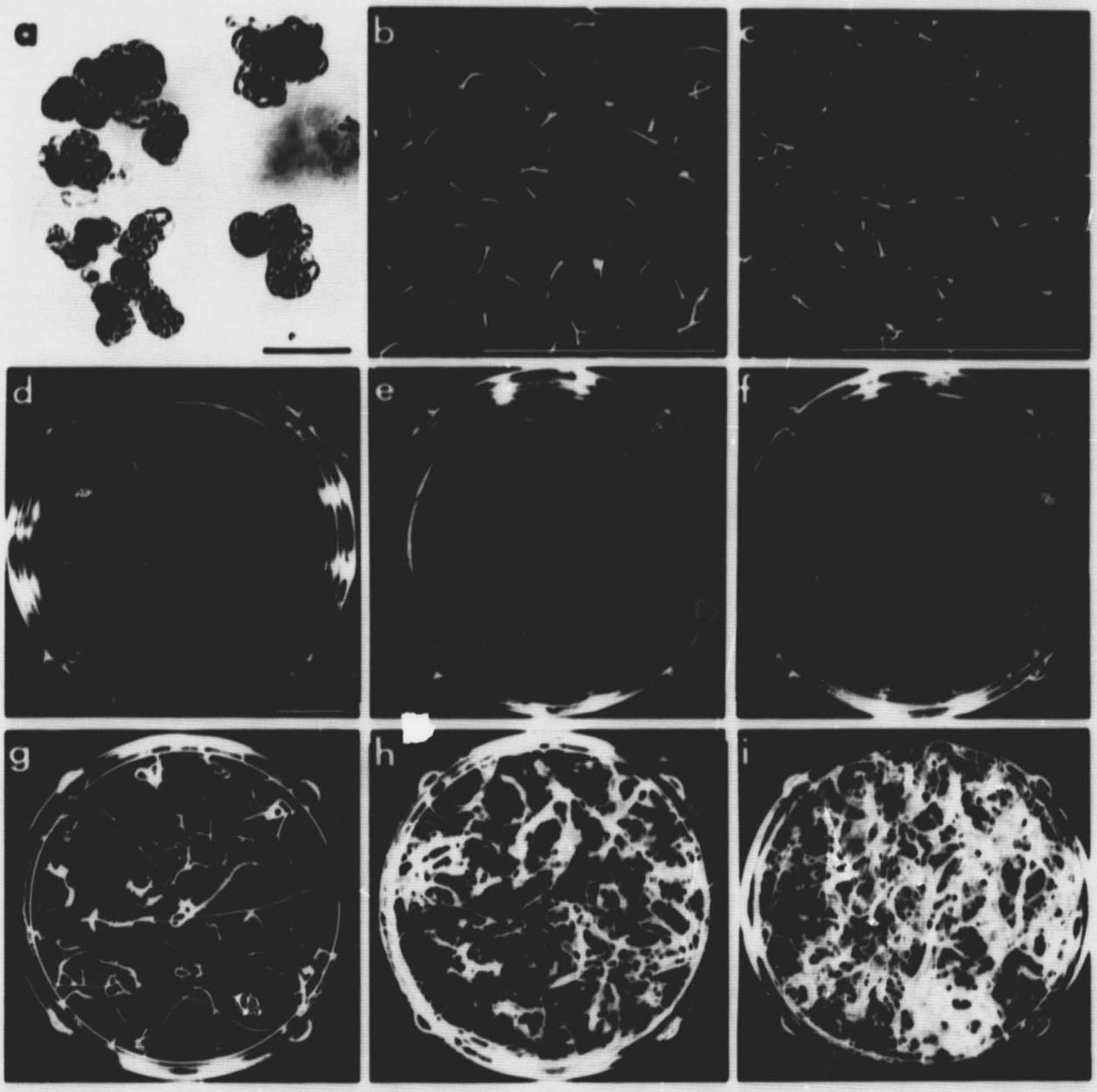

Figure 28

Fig. 2 . Carrot development at 1 g (ground controls). Top row, representative dishes with proembryonic cell clusters (a); b, somatic embryos ranging between 406 and 864 μm; and c, somatic embryos ranging between 234 and 406 μm; d,e and f, dishes with embryos and plantlets after 18.5 days on earth. Scale bars, 10 mm.

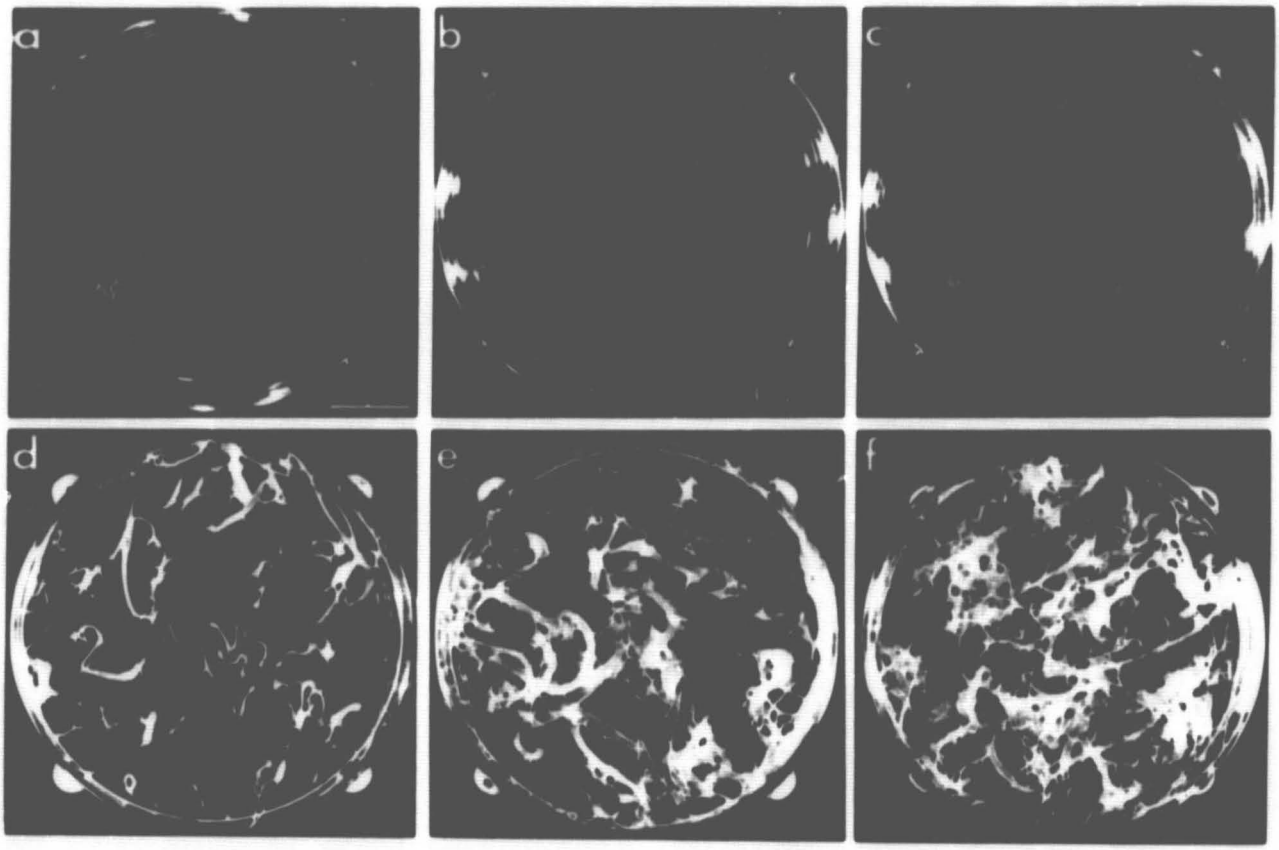

Figure 29

Cosmos 1129

Experiment K-309

SPACE RADIATION DOSIMETRY ABOARD COSMOS 1129: US PORTION OF EXPERIMENT K-309

Dr. E.V. Benton, Dr. R.P. Henke, A.L. Frank, C.S. Johnson,
R.M. Cassou, M.T. Tran and E. Etter
University of San Francisco

SUMMARY

Detector packets were placed aboard the Cosmos 1129 spacecraft for the purpose of measuring doses and particle fluences accumulated during the 18.56 day flight. Included were stacks of plastic nuclear track detectors for measurements of high-LET particles ($Z \geq 6$), fission-foil detectors for neutron measurements and thermoluminsecent detectors (TLDs) for measurement of total doses due to charged particles and gamma rays. Detectors were placed inside and outside the spacecraft hull. The high-LET particles registered are given as Z spectra and LET spectra and are translated into rem dose as a function of LET. The total accumulated doses for the particles (LET > 100 keV/μm) were 9.9 mrem inside and 25 mrem outside the spacecraft. The thermal, resonance and high-energy neutron doses were found to be 0.52, 7.4 and 125 mrem, respectively, and the interior TLD dose was 347 mrad.

I. INTRODUCTION

I.A. Experiment objectives

The purpose of Experiment K-309 is to provide a comprehensive picture of the radiation exposure experienced by the Cosmos 1129 spacecraft and its contents. The measurements include and distinguish between the low- and high-LET radiation components and also provide an approximate determination of the neutron exposure. The information gained from this experiment will be applicable to the assessment of spaceflight radiation standards, the study of the effects of the space radiation environment on man and other biological materials, operational support such as the total mission dose prediction, and the evaluation of the effectiveness of the radiation shielding deployed during the mission.

I.B. Experimental design

The experimental hardware consists of dosimetry packages deployed in two different locations. The most comprehensive measurements are accomplished by a 9.8 × 9.8 × 5.2 cm rectangular dosimetry package placed within the spacecraft. The contents of this package are shown schematically in Fig. 1. They consist of five stacks of plastic detectors oriented with equal stack volumes in the three orthogonal directions and four corner stacks containing an assortment of different detector types. The plastic stacks measure the high-LET primary cosmic-ray radiation component, and the corner stacks measure the low-LET and neutron radiation components.

In addition to the internal dosimetry package, there are four small cylindrical dosimetry packages, 4.0 cm diameter and 1.4 cm high, deployed on the exterior of the spacecraft. Three of these cylinders contain stacks

of intermixed plastic layers. The fourth contains TLD (thermoluminescent dosimeter) chips for low-LET dose measurements.

I.B.1. Interior plastic stacks

The plastic stacks in the interior module consist of alternating layers of three different detector types. A single repeat unit contains, in order, four layers of the plastic types, GE Lexan polycarbonate, American Acrylics CR-39, Lexan, and Kodak Pathé cellulose nitrate (CN), with respective nominal layer thicknesses of 190 μm, 1000 μm, 190 μm, and 100 μm. This sequence is repeated a sufficient number of times to comprise the entire thickness of each of the stacks. The arrangement of the plastic stacks along the three orthogonal directions is the preferred configuration because of the somewhat anisotropic response of the detectors (they respond to lower LET particles at normal incidence than at grazing incidence).

I.B.2. Exterior plastic stacks

The sequence of layers in the plastic stacks in the exterior packets differs from that of the interior stacks because the inclusion of a layer of the thick detector, CR-39, in each repeat unit would severely restrict the number of layers in the relatively thin stacks. Therefore the exterior stacks consist of alternating layers of Lexan and CN sandwiched between two layers of CR-39. One surface of each stack was exposed directly to the space environment except for a very thin evaporated layer of aluminum to reduce the UV exposure and temperature during the mission.

I.B.3. Corner stacks

The corner stacks in the experimental packages were designed to hold

both TLDs, for measuring the total absorbed dose, and particle radiator detectors, for measuring neutron fluences. The TLDs employed were TLD-700 (Li^7F) and TLD-200 (CaF_2). The particle radiators were of two types. Foils of B^{10} and Li^6F were used to produce He^4 particles by the (n,He^4) reaction. Cellulose nitrate plastic was sandwiched against the radiator foils to record He^4-particle tracks. Fission foils of Bi^{209}, Th^{232}, Np^{237} and U^{238} were used to produce fission fragments by the (n,f) reaction. Muscovite mica was used to record the tracks of the emitted fission fragments.

It was necessary to separate the radioactive fission foils from the TLDs in the experimental package in order to reduce the buildup of background gamma radiation doses in the TLDs as much as possible. The corner stacks, labeled A, B, C and D, were therefore built in two different configurations. Stacks A and C were designed to hold the fission foil detectors plus those using B^{10} foils. Stacks B and D were designed to hold the TLDs plus those detectors using Li^6F foils. Diagrams of the two configurations are shown in Figs. 2 and 3. Stacks A and C were composed of aluminum plates with alternate plates having milled holes of the proper sizes to contain the radiator detectors. Each stack contained two B^{10} foils of 1.0 mg/cm^2 thickness and 1.27 cm diameter on a 1.588 cm diameter titanium backing. One of these foils was shielded by 1.0-mm-thick plates of cadmium. Three foils each of Th^{232} and U^{238}, all of 1.27 cm diameter, were included. The Bi^{209} foil was rectangular and 1.27 by 3.81 cm in dimensions. The three preceding foil types were unbacked and mica detectors were placed against both foil surfaces. Two Np^{237} foils of 8 mg/cm^2 thickness and 1.27 cm diameter on a 1.588 cm diameter titanium backing completed the complement of foils.

Stacks B and D contained two foils each of Li^6F, 4.5 mg/cm^2 in thickness

and 1.588 cm in diameter, on a filter paper backing. One of these foils was shielded by 1.0-mm-thick cadmium. The remainder of the corner stacks were devoted to the TLDs. Plates having two slots, milled to accept three TLD chips each of 0.635 by 0.635 cm dimensions, were placed near the tops and bottoms and at the centers of the stacks. Each plate contained three chips each of Li^7F and CaF_2 TLDs.

I.B.4. Exterior TLD packets

The external TLD packets were designed to contain six TLD chips each of Li^7F and CaF_2 for total absorbed dose measurements outside the hull of the spacecraft. The diagram in Fig. 4 illustrates the packet configuration. The TLD chips were held in twelve square milled holes, 0.635 cm in dimensions, in an aluminum plate. The two TLD types were placed in alternate spaces and were spread, approximately equally, across the external packet dimension. An aluminum top plate, 0.318 cm thick, protected the TLDs from the external environment.

In Fig. 5 are shown the flight and the backup units. The large rectangular block marked F is the interior package which rests on the Soviet block of similar size. The aluminum flight container marked USA-USSR is shown at the right. The four circular exterior packets marked EF1,2,3 and TEF are the flight units, while the remainder are backup and laboratory test units.

II. MISSION PARAMETERS

The Cosmos 1129 mission utilized the standard high-inclination orbit ($i = 62.8$ deg) which is achieved by a high-latitude launch site. In terms of radiation exposure, this means that the spacecraft passed through regions of

relatively low geomagnetic shielding in the high-latitude portions of the orbit, which give rise to a fairly sizable low-energy component in the primary cosmic-ray spectrum. The other significant orbital elements are a minimum altitude of 226 km and a maximum altitude of 394 km. Cosmos 1129 was launched on 25 September 1979 and returned on 14 October 1979. The total time in orbit was 445 hours or 18.56 days.

Prior to the mission, the external detector packets from the K-309 experiment as well as from a number of other different experiments were housed in a specially designed mounting which has a cover to protect the experiments during launch and recovery, see Fig. 6. The cover was opened when the orbit was achieved. The covers were again closed prior to the return from orbit except in the case of one module which failed to close. This resulted in an unusually large heating of the detectors. Two of our exterior packets were mounted in this module, see Fig. 7. The heated packet with plastic detectors appeared to be relatively unaffected. The other packet, which housed the exterior TLD detectors, seems to have been seriously affected, however, making the measurement of the total external dose quite suspect. The remaining two external units were housed one each per container and survived the flight in good condition.

III. PROCESSING

III.A. Plastic stacks

Upon their return from the Soviet Union, the interior stacks were disassembled and the individual foils numbered. The outer foils on each stack were short-etched, both as a check and for preliminary fluence measurements. The bulk of the foils (CN, Lexan and CR-39) were then long-etched in preparation

for the automated HZE analysis. The outer layers of the spacecraft exterior plastic stacks were stripped off and short-etched as a check on fluence. The bulk of the layers from exterior stack #1 were long-etched. All flight plastics that were short-etched for purposes of checking fluence and condition were compared to their identical counterpart foils on the backup modules, which were all processed the same way. A summary of the etching parameters for the long-etched plastics is given in Table 1.

III.B. TLDs

The TLDs were pre-readout annealed at 100°C for 10 minutes, then read out with a Harshaw Model 2000 A+B TLD reader. The chips were then annealed by the standard procedure and exposed to a calibration source of Cs^{137} gamma rays. The calibrated exposures were then read out in the same way as the flight doses. The calibrations were used to convert the instrument output into absorbed dose equivalent for the TLDs. Each set of three TLDs from the corner stacks was handled independently. The Li^7F and CaF_2 TLDs from the exterior packets and the Li^7F TLDs from the individual badges were handled as sets. The TLDs from all the flight and backup packets returned were read out.

Since a high background dose appeared to be present on the TLDs, the flight packet corner stacks were repackaged with their complements of TLDs and radioactive foils. A preliminary two-week background measurement followed by another of 68 days duration were made. The TLDs were read out with calibrated dosimeters to yield the background exposures.

III.C. Thermal and resonance neutrons

The cellulose nitrate plastics from the B^{10} and Li^6F radiator detectors were etched in 6.25N NaOH solution at 40°C for 1 hr 40 min. The surfaces of

the plastics were then scanned under an optical microscope at 250X. All the flight samples were scanned plus samples from the backup packet to serve as backgrounds. The counted He^4 particle tracks were converted into track densities for each sample by appropriate area factors.

The track densities measured from the B^{10} and Li^6F radiators can be separated into those due to neutrons of energies below and above 0.3 eV. This can be seen from the cross sections shown in Fig. 8. The unshielded detectors are sensitive to all thermal and resonance neutrons present with efficiencies determined by the (n,He^4) cross sections of B^{10} and Li^6, which vary as $E_n^{-\frac{1}{2}}$. In the cadmium-shielded detectors, the thermal neutrons below 0.3 eV are absorbed out. The difference between the two yields the thermal neutron track densities while the shielded detectors yield the resonance neutron track densities.

The response of the 4.5 mg/cm^2 Li^6F detectors was previously found to be 4.90×10^{-3} tracks/thermal neutron, assuming isotropic neutrons and taking into account the self-shielding correction (Benton *et al.*, 1978). In a cross calibration, the response of the B^{10} detectors was found to be 1.46×10^{-2} tracks/thermal neutron.

The response of the Li^6F radiator detector to resonance neutrons has also been previously discussed (Benton *et al.*, 1978). It is necessary to assume a spectral shape for the neutrons in the resonance region (0.3 eV to 1 MeV) in order to derive an effective response. Since a moderated neutron spectrum assumes a shape approximately proportional to $\frac{1}{E_n}$, this is a reasonable estimate in the resonance region. The effective cross section is then

$$\sigma_R = \frac{\int_{E_0}^{E_{max}} \frac{\sigma(E_n)\, dE_n}{E_n}}{\int_{E_0}^{E_{max}} \frac{dE_n}{E_n}}$$

where

$$\sigma(E_n) = \frac{150.2}{E_n^{\frac{1}{2}}}$$

The resonance response can then be found from the thermal neutron response, where

$$R_R = R_{Th}\left(\frac{\sigma_R}{\sigma_{Th}}\right) ,$$

and $\sigma_{Th} = 950$ barns. By substitution

$$R_R = 5.89 \times 10^{-6} \frac{\int_{0.3}^{10^6} \frac{150.2\, dE_n}{E_n^{\frac{3}{2}}}}{\int_{0.3}^{10^6} \frac{dE_n}{E_n}}$$

$$R_R = 8.85 \times 10^{-4} \frac{\left[-2\, E_n^{-\frac{1}{2}}\right]_{0.3}^{10^6}}{\left[\ell n\, E_n\right]_{0.3}^{10^6}}$$

$$R_R = 2.15 \times 10^{-4} \text{ tracks/neutron.}$$

For the B^{10} foils, σ_{Th} is 4017 barns and

$$\sigma_{E_n} = \frac{635}{E_n^{\frac{1}{2}}} .$$

The calculation gives

$$R_R = 6.02 \times 10^{-4} \text{ tracks/neutron.}$$

It should be noted that the thermal neutron responses, R_{Th}, which were used in these calculations were the 2π responses, that is, without a self shielding factor. Since the radiator foils are more transparent to the resonance neutrons, the self-shielding correction is not appropriate.

III.D. High-energy neutrons

The high-energy neutron fluences (E_n > 1 MeV) are derived from the fission foil/mica detectors. The mica samples from these detectors were etched in 50% HF solution for 50 min. Prior to use, the samples had been etched for 2 hr. This was sufficient to etch out the fossil tracks to a size much larger than the flight tracks and to avoid any background contribution from these tracks. The etched samples were scanned under an optical microscope at 250X and the track densities determined. The flight samples and sufficient backup samples for background measurements were scanned.

The fission foil detectors are sensitive to both neutrons and protons of the energies found in space. Protons are the dominant primary particles in orbital flights and, thus, can be expected to produce the majority of the fission fragment tracks found on the mica samples. The neutrons are secondary particles whose main mode of production is through interactions between the

protons and nuclei of elements composing the spacecraft and its contents. The (n,f) and (p,f) cross sections are not well enough known or distinct enough to permit an unfolding procedure to be applied to the measurements. Also, the errors associated with the counting statistics are too great for unfolding methods to apply. As in a previous report (Benton *et al.*, 1978), the neutron and proton contributions to track densities were separated by making some assumptions concerning the spectral shapes of the two components and by using some comparative orbital measurements of protons and neutrons by activation foils.

IV. RESULTS

As the initial results of the K-309 experiment were processed, it became apparent that an unusual and unexpected radiation exposure had occurred which exceeded the exposure resulting from the cosmic rays and trapped radiation. This radiation contamination was manifested as a much higher than expected dose to the ground control dosimeters and a much larger than expected fluence of very low-energy particles as experienced in the plastic detectors. Although this phenomenon is not fully understood, a considerable amount of testing has been employed to elucidate it. The results of these tests will be described in a later section. The impact of this radiation contamination on the results obtained in the plastic dosimeters and the neutron dosimeters appears to be minimal, but the total dose measurements from the TLDs seem to have been seriously affected.

IV.A. Plastic dosimeter results

The long-etched detector layers were read out using our standard auto-

mated-HZE procedures (Henke *et al.*, 1979). The parameters of the read out procedure are given in Table 1. The measured track positions from the superimposed layers of each of the five interior HZE-particle stacks are shown in Fig. 9a-e. In each of the stacks a 4 cm × 4 cm area was scanned. The corners were excluded because of the distorted etching conditions around the layer mounting holes and to remove the portion of each layer which had been scribed with the layer number. The total active scanning area of each layer (after the corners were excluded) is 13.61 cm^2. Many of the 6467 measured track positions in Fig. 9 are seen to be aligned in rows. These rows indicate heavier particle events for which sequential registration occurs in a number of layers of the stack.

The measured track positions for the exterior stack are shown in Fig. 10. The intersection of a square with the circular sample area was scanned. The total area of this scan region is 8.01 cm^2. In the Lexan layers, it was necessary to exclude certain areas, such as around the mounting holes and the regions where the layers were numbered, because of etch artifacts. In the CN, only the actual areas of the mounting and position fiducial holes were excluded. Thus, the active area on each of the 27 Lexan and 27 CN layers are 3.27 cm^2 and 7.95 cm^2, respectively. In these areas, there are 76 and 2620 measured tracks, respectively.

The coincident events seen in Figs. 9 and 10 were identified by tracing the measured track positions from layer to layer (Henke *et al.*, 1979). The particle trajectories so identified having three or more position measurements per particle are shown in Figs. 11 and 12. These scatter plots give $\sin \alpha \sqrt{2 - 2 \sin \delta}$ vs. $\cos \alpha \sqrt{2 - \sin \delta}$ for each of the particle trajectories in each of the three orthogonal interior stacks in Fig. 11 and for the

exterior stack in Fig. 12. The parameters α and δ are the particle azimuthal and dip angles, respectively, (the dip angle is the angle made between the trajectory and the plane of the coordinate system). The travel direction along the trajectory has not been identified in these plots.

The functional form for the coordinates in Figs. 11 and 12 has been chosen so that equal solid angles are mapped into equal areas on the plot. Moreover, the boundaries in each orthogonal direction correspond to the constraints,

$$-1 < \frac{\cos \alpha}{\tan \delta} < 1 \qquad (1)$$

and

$$-1 < \frac{\sin \alpha}{\tan \delta} < 1 \qquad (2)$$

With the above constraints, the trajectories shown in Fig. 11 give full coverage of the 4π steradians of solid angle with no overlap. The coverage of the exterior trajectories in Fig. 12 is $4\pi/3$ steradians. Aside from some slight deviations, the plotted interior point densities seem to be quite uniform, indicating that the cosmic-ray beam was nearly isotropic in spite of anisotropic shielding. The exterior densities are peaked toward the normal.

The average particle fluences obtained in the interior CN, CR-39 and Lexan detectors, respectively, are 6.1 ± 0.1, 2.2 ± 0.2 and 0.26 ± 0.02 particles/cm^2. The averages were taken over most of the measured layers with an approximately equal representation from each of the three orthogonal directions. Because of the LET-dependent dip-angle cutoffs in each of the detector materials, these fluences represent a weighted integral over the LET spectrum of the particles.

The weighting factor, or kernel of the integral, is the effective solid-angle projection-factor window as a function of particle LET. Using this concept, it is possible to compute an effective LET cutoff for a given combination of particle selection criteria, detector calibration parameters (the calibration is the relationship of the cone angle of an etched track in the plastic to the particle LET), and detector processing parameters. If an isotropic power function LET spectrum is assumed, it is possible to compute rigorous particle fluence using the true dip angle dependent LET cutoff of the detector. The effective LET is the value of LET for which the same computed particle fluence is obtained by assuming no registration below the cutoff value and 100% registration above it (at all dip angles). This effective value of the LET cutoff is reasonably insensitive to the assumed exponent in the power function LET spectrum. The values (LET in water equivalent units) are 102, 214 and 675 keV/μm, respectively, in CN, CR-39 and Lexan as processed for the measured particle fluences given above. The CR-39 cutoff should be assumed to be approximate since the calibration relationship on which it is based is a tentative one.

Similarly, the exterior particle fluences are 0.86 ± 0.10 and 12.2 ± 0.2 for Lexan and CN, respectively and the corresponding LET values are 636 and 101 keV/μm in water. In this case, there is no CR-39 result since the CR-39 layers were not long-etched and the coverage of solid angle cannot be considered to be isotropic.

The high-LET portion of the LET spectrum can be constructed using the measured particle fluences and their respective effective LET cutoffs. The effective LET cutoffs correspond to a measured planar fluence, that is, the

fluence that would be seen by a planar detector with 100% efficiency above the effective cutoff LET. Because of the average projection factor (averaged over all solid angles) of ½, the effective solid angle seen by each of the detector stacks is 2π. Therefore, the integral LET spectrum for a given effective LET cutoff is the corresponding fluence divided by 2π. The integral LET spectrum points are shown in Fig. 13. The least squares fit power function representation of the spectra,

$$\frac{d^2N}{dA\ d\Omega} > LET = \begin{cases} 1882\ LET^{-1.636} & \text{interior} \\ 1496\ LET^{-1.440} & \text{exterior} \end{cases}$$

are shown as straight lines in the log-log plot. Their negative derivatives, the differential LET spectra, are therefore given by

$$\frac{d^3N}{dA\ d\Omega\ dLET} = \begin{cases} 3079\ LET^{-2.636} & \text{interior} \\ 2154\ LET^{-2.440} & \text{exterior} \end{cases} \tag{3}$$

The high-LET particle dose and REM dose can be obtained by integrating Eq. (3). The dose contributed by particles with energy loss rates higher than LET is given by

$$D > LET = 2.013 \times 10^{-6} \int_{LET}^{\infty} L \frac{d^3N}{dA\ d\Omega\ dLET}(L)\ dL$$

$$= \begin{cases} 0.0097\ LET^{-0.636}\ \text{rads} & \text{interior} \\ 0.0099\ LET^{-0.440}\ \text{rads} & \text{exterior} \end{cases} \tag{4}$$

with LET in keV/μm H_2O. Using an interpolated form of the ICRU recommended quality factor,

$$QF = \begin{cases} LET^{0.58} & 53 < LET < 175 \\ 20 & LET \geq 175 \end{cases} \quad (5)$$

the REM dose is given by

$$REM > LET = \begin{cases} 0.1107\ LET^{-0.056} - 0.0756 & 100 < LET < 175 \\ 0.195\ LET^{-0.636} & LET \geq 175 \end{cases} \quad (6a)$$

for the interior spectrum and

$$REM > LET = \begin{cases} 0\ 0842 - 0.0310\ LET^{0.140} & 100 < LET < 175 \\ 0.197\ LET^{-0.440} & LET \geq 175 \end{cases} \quad (6b)$$

for the exterior spectrum. The coefficient of the integral, 2.013×10^{-6}, includes the 4π steradian solid-angle factor and the conversion from keV/μm-cm^2 to rads. Equations (4) and (6) can be expected to apply in the approximate interval 100 < LET < 1000 keV/μm in water. The dose and REM doses are shown plotted in Fig. 14.

IV.A.1. Z spectra

The atomic number, Z, and particle stopping point have been computed for

each of the particles identified in the tracing process. This was accomplished using a least-squares fit of a model event to the measured track opening areas as a function of the distance along the trajectory as described in Henke *et al.* (1979).

From the total population of computed particles, those events which have potential of having accurately determined Z values have been selected to assemble the Z spectrum. The selection criteria are that the particle must 1) have at least 3 measurable etched-through tracks, 2) stop in the stack, and 3) have at least one measured track with an area less than 0.5 of the maximum area achievable by an extremely high-LET particle in the same trajectory. The measured Z spectrum assembled according to the selection criteria above are shown in Fig. 15. The results of the three different detector types are considered separately in the Z analysis procedure and then combined in the Z spectrum histogram.

The measured Z spectra are converted to absolute units by dividing by the appropriate geometric factor, which is consistent with the above selection criteria. The geometric factor is the product of stack volume (water equivalent) times solid angle available for capturing a particle as a function of Z. Because of the complexity of the scanned volume of the stack and the selection criteria, the geometric factor was determined using a Monte Carlo technique. For each value of Z, a population of particles with a known density of random stopping points and random isotropically distributed space angles was generated. The same selection criteria applied to the real particle events were applied to these simulated events to determine the geometric factor. The geometric factors so determined are shown in Fig. 16 for the interior stacks and in Fig. 17 for the exterior stacks. The geometric factors shown in-

clude the contribution from all three detector types.

The absolute Z spectra are shown in Fig. 18. They are expressed in particles stopping per unit stack volume per solid angle per Z. These units rather than the more conventional units of particles per area per solid angle per energy are employed because of the limited number of events, the lack of knowledge of the shielding distribution for the interior detectors, and because they relate more directly to the measured distribution and are applicable at the point of measurement.

IV.B. Neutron dosimetry

The track densities counted on the CN plastics from the B^{10} and Li^6F radiator detectors are given in Table 2. At the bottom of the table are the average track densities which can be related to thermal and resonance neutrons. The fluences of the neutrons in these energy ranges can be calculated by using the responses which were given earlier for the two detector types. The thermal neutron fluence accumulated during the flight was $4.65 \pm 0.22 \times 10^5$ neutrons/cm^2 as measured by the Li^6F detectors and $5.52 \pm 0.14 \times 10^5$ neutrons/cm^2 as measured by the B^{10} detectors. The resonance fluence was $1.35 \pm 0.32 \times 10^6$ neutrons/cm^2 as measured by the Li^6F detectors and $1.41 \pm 0.13 \times 10^6$ neutrons/cm^2 as measured by the B^{10} detectors. The errors given are derived from the counting statistics only. It can be seen that the backgrounds counted on the plastics were rather high and were nearly twice as high for the Li^6F radiators as for the B^{10} radiators. This may be explained from an apparent accumulation of radon gas in the detector packet during the time it was assembled. As explained in Section IV.D.1 of this report, a spurious background track density was found on the plastic stack detectors which suggested that the agent was a gaseous He^4 particle emitter which diffused down to the detec-

tors from the edge of the stack. There was no residual radioactivity present. This indicates an isotope of radon was present. In the B^{10}/CN and $Li^{6}F$/CN detectors, the radiators were pressed tightly against the plastic track recorders, allowing little active volume for radon to accumulate in. However, the $Li^{7}F$ foils, pressed onto their paper backings, were rather porous while the thin B^{10} foils, plated onto their titanium backings, were much less so. This caused the radon to produce background tracks at different rates in the two cases.

The difference in thermal neutron fluences measured by the two detectors appears to be significant. This does not necessarily indicate detector inaccuracy since there can be no certainty that the detectors encountered the same number of thermal neutrons. One of the B^{10} detectors had a thermal component of track density which was 28% higher than the other. This may not be unusual for spatial variations of thermal neutrons.

The track densities counted on the mica samples from the fission foil radiators are given in Table 3. The track densities from the two corner stacks are approximately the same except in the case of the Np^{237} detectors where a significant discrepancy exists. As compared with the Cosmos 936 track densities, there has been a relative shift in foil track densities. The Bi^{209} track densities are smaller although this is not statistically significant. The Th^{232} foils are significantly lower while the U^{238} foils are higher. The latter finding is also not statistically significant.

The track densities from the foils of each type have been averaged in Table 4. The neutron fluences were calculated from the measured values as was done previously but with improved cross sections for the (n,f) and (p,f) reactions. The improvement was made possible by a recent paper on these reactions (Lomanov *et al.*, 1979). The neutron and proton cross sections are plotted

in Figs. 19 and 20, respectively. Since the Bi^{209} (n,f) and (p,f) cross sections are equal, to within the known accuracies, the cross section appears only on the proton graph.

In order to separate the fractions of track densities which are due to neutron and proton interactions, it is necessary to have their spectral shapes and relative magnitudes. Since none of the detectors on the flight measure these quantities independently, it is necessary to approximate them by relying on other appropriate measurements and calculations.

Proton spectra have been measured on other Earth orbit missions by nuclear emulsions. A typical example are the Biosatellite III measurements which have been reported (Hewitt *et al.*, 1972). For a representative neutron spectrum a calculated differential spectrum of cosmic-ray-induced atmospheric neutrons has been used (Merker, 1973). The spectra for a series of air pressure altitudes was calculated from 0 to 700 g/cm^2. The 0 g/cm^2 case, which gives the the hardest spectrum, was used. This calculation should yield the most reasonable approximation of the situation aboard a spacecraft. The production modes for neutrons are similar in the two cases. The relative proton and neutron spectra are plotted in Fig. 21.

Numerical integrations were made to determine the efficiencies of the detectors for the above neutron spectrum for energies above 1 MeV and for the proton spectrum for energies above 17 MeV. The sensitivity of thick fission foil detectors have been measured to be 1.16×10^{-5} tracks/neutron-barn (Pretre *et al.*, 1968). The sensitivity for a nucleon spectrum, therefore, depends on the effective cross section of the detector to the spectrum which is given by

$$\sigma_e = \int_0^\infty \sigma(E)\, N(E)\, dE$$

where $\sigma(E)$ is the energy dependent cross section and $N(E)$ is the normalized nucleon spectrum. The calculated efficiencies are given in Table 5.

The relative abundances of protons and neutrons were obtained by using Skylab measurements of neutron and proton fluences (Fishman, 1974). These were made simultaneously by activation foil methods on an orbital spaceflight where conditions should approximate those on Cosmos 1129. Fluxes of 2.3 protons/cm^2-sec between 30 and 100 MeV and 0.96 neutrons/cm^2-sec between 3 and 15 MeV were measured. For the spectral shapes of the nucleons assumed in this report, these values would convert into fluxes of 7.85 protons/cm^2-sec > 17 MeV and 3.94 neutrons/cm^2-sec > 1 MeV. Using these proportions, the neutron and proton fluences accumulated by the four fission foil detectors are given in Table 6. The average values are very close to those found on the Cosmos 936 flight. The neutron fluence was found to be 2.1×10^6 cm^{-2} and the proton fluence 4.3×10^6 cm^{-2}. Due to the assumptions made in calculating the fluences, the errors may be quite large but are probably less than an order of magnitude.

IV.C. TLD results

The results of the TLD measurements in the corner stacks are given in Table 7. The nine TLD chips of each type in the corner stacks have been averaged. The numbers represent equivalent Cs^{137} gamma-ray absorbed doses as determined by calibration.

Several things are evident from the measured doses. 1) The background test yielded doses much less than those found in the backup stacks. 2) The ratios between the Li^7F doses and between the CaF_2 doses for the backup package and the background test are much different, with that for CaF_2 being higher. These two facts indicate that the backup package was exposed to a

source of radiation not attributable to the fission foils in the package, and that this additional radiation was characteristically different from that produced by the fission foils. The CaF_2 TLDs have an enhanced response to higher LET radiation, compared to Li^7F. The additional radiation could, therefore, have included a significant low-energy (<100 keV) gamma-ray component and/or particles of $Z > 1$. 3) The scatter in the measured doses from the backup stacks show that the additional radiation was nonuniform in some unknown manner. One Li^7F dose is about 50% higher than the other, while the difference between the CaF_2 doses is only 6%. It can be seen from the background tests that the internal background is quite uniform, as expected from the symmetrical arrangement of the stacks. 4) It follows that neither the backup stack or background test exposures represent valid backgrounds for the measured flight doses. Since both the flight and backup stacks were apparently subjected to the additional radiation exposure, a rough background can be assumed from the backup doses. However, the scatter in the measurements make the results subject to large and unknown errors. It can be seen that, for the CaF_2 doses, backup stack B has a greater value than flight stack B, while for the D stacks, the flight dose is considerably higher. For the Li^7F doses, the variation is less but still quite large.

The subtraction of the average of all backup stack doses which were measured from the average of all the flight doses gives a net dose for the Cosmos 1129 flight of 347 mrad equivalent. Due to the background uncertainties, the accuracy of this number is estimated to be ±50%

The doses measured by the external detectors are given in Table 8. The flight detectors were heated and partially annealed during the spacecraft descent. The doses found are therefore not valid. It is seen that substan-

tial backgrounds were accumulated in the detector packets which were not used.

IV.D. Investigation of the radiation contamination problem

When the outer layers of the plastic stacks (both interior and exterior, flight and backup) were processed by a short etch, it was found that short tracks (~30 μm) were liberally distributed over all the plastics. The tracks were observed to be primarily multiply emitted, with the source appearing to be sitting on or near the plastic surface. As some of these surfaces were interior to the stack, it seemed at first glance to indicate gaseous diffusion and nuclear decay of some contaminant. The tracks were consistent in every way with those produced by He^4 particles.

At this point, a survey was taken to determine the nature of the contaminant. The stack end pieces from all stacks, flight and backup, were fluence-mapped on the side of the plastic that was interior to the stack. If contamination was by slow gaseous diffusion, then the edges would have higher fluence than the center of each piece. In every case, this was determined to be the case. No radioactivity remained on the plastics after disassembly. Only radon gas would seem to have the properties discovered in the contaminant.

The TLD results also suggest that a source of radiation was present, other than the gamma rays from the fission foils, which was contributing to background. Since the high fluences of He^4-particle tracks found on the plastic detectors were apparently from an isotope of radon, the flight materials were tested for radon emission. The radioactive foils used in the Cosmos 1129 measurements were, therefore, sealed in small boxes with samples of CR-39 track recording plastic. The two items were arranged in the boxes so that no particles emitted from the surfaces of the fission foils could reach the CR-39.

Only radionuclei diffusing into the air in the box could irradiate the track recorders. After exposures of two weeks, the CR-39 samples were etched and scanned for tracks. The average track densities from the Np^{237} and U^{238} exposures were 3 and 4 tracks/mm^2, respectively, the average track density from the Th^{232} exposures was 68 tracks/mm^2. Only the Th^{232} foils need consideration as significant sources of radon.

That isotope of radon from the thorium chain is Rn^{220}, called thoron. It has a half-life of 55 seconds. It seemed questionable as to whether thoron from the Th^{232} could have been a significant background source. The foils were flown on Cosmos 936, contained in a plastic stack, without obvious effects. Also, it has been shown that the short half-life of thoron limits its ability to diffuse through thin plastic membranes (Fleischer *et al.*, 1979). The time of diffusion through a thin permeable membrane is much longer than 55 seconds. Also flown aboard Cosmos 1129 were some TLD badges, sealed in polyethylene, which included plastic sheet. These plastic track detectors were also found to have a high density of He^4 particle tracks on their surfaces. The permeability of the polyethylene to thoron was checked by a repeat of the exposures of CR-39 in a sealed box containing Th^{232} foils. In this exposure, two CR-39 samples were present. One was sealed inside a cavity formed of polyethylene sheet taken from the same roll as that used with the badges. After a two week exposure, the CR-39 samples were etched and scanned. The uncovered sample contained a similar high density of He^4-particle tracks as in the previous exposures. The covered sample was free of tracks except for the normal low density which a track recorder collects during storage periods from Rn^{222} in the ambient air. Since thoron could not have diffused into the sealed badges, this suggests that the longer-lived isotope, Rn^{222}, may have been present with the

detector packets in rather high concentrations sometime after the assembly.

As a separate check, the background track density deriving from the thoron which issues from the Th^{232} fission foils was measured during the background test exposures for the plastic detectors comprising the HZE stacks. Unused samples of CR-39 and CA-80-15 plastics were included in the reassembled flight package. After the 68 day exposure period, and disassembly, they were processed in a standard way and the track densities were counted in the regions where the maximum numbers of tracks were found, which is near the edges of the sheet. The track densities found were 300 cm^{-2} on the CR-39 and 200 cm^{-2} on the CA-80-15. In comparison, after the 118 day exposure of the original flight and backup packages, the maximum track densities counted were about 5×10^4 cm^{-2}. The maximum track densities were found where an air gap existed next to the plastic surface. The air gaps served as pockets which radon could build up in. A similar air gap existed near the top edges in the background test exposures. The reassembled detector packages were sealed in polyethylene during the background test so the thoron produced within the package could not have diffused away. It is not possible to say how the spurious exposure occurred.

IV.E. Summary of results of neutron and TLD measurements

During the Cosmos 1129 flight, the following quantities were measured with the neutron and TLD detectors. The thermal neutron fluence was found to be 5.1×10^5 cm^{-2}. This is an average of the levels at the four corner stack positions. The individual measurements indicate that differences of about ±20% in thermal neutron exposure took place around the box. The absolute accuracy of the fluence is about ±20% also, due mainly to uncertainties in the

energy distribution in the thermal region. This converts to a flux of 0.318 neutrons/cm^2-sec for the 18.56 day flight. The resonance neutron (0.3 eV to 1 MeV) fluence was found to be 1.4×10^6 cm^{-2}. This converts to a flux of 0.87 neutrons/cm^2-sec. The error limits for this value are estimated to be -30% to +50%, due mainly to the assumption of a $\frac{1}{E}$ spectral shape in this region. The high-energy fluence was found to be 2.1×10^6 cm^{-2}. This converts to a flux of 1.3 neutrons/cm^2-sec. The assumptions made in the associated calculations allow an error of an order of magnitude in this number but it is the same as found for Cosmos 936 and compares reasonably well with other measurements made under similar conditions (Quist *et al.*, 1974). The thermal, resonance and high-energy neutron fluences correspond to doses of 0.52, 7.4 and 125 mrem, respectively, or a total of 133 mrem. The TLD measurements yielded an average dose of 347 mrads. The estimated error for this value is ±50% and results from an uncertainty in the correct background subtraction for the dosimeters due to an unexplained spurious irradiation of all the detectors.

ACKNOWLEDGMENTS

This joint US-USSR experiment was performed as part of a US-USSR biological satellite program. In order to achieve a thorough understanding of the results, an exchange of data and subsequent analysis and discussions will be necessary. The authors would like to thank Dr. K. Souza, NASA-Ames Research Center, for his valuable help during all phases of the experiment. The assistance given by Dr. E.E. Kovalev and his group is also gratefully acknowledged.

REFERENCES

Benton E.V., Cassou R.M., Frank A.L., Henke R.P. & Peterson D.D. (1978) Space radiation dosimetry on board Cosmos 936: US portion of Experiment K-206. *Final Report, NASA Contract No. NAS2-9504.*

Fishman, G.J. (1974) Neutron and proton activation measurements from Skylab. *AIAA Paper No. 74-1227, AIAA/AGU Conference on Scientific Experiments of Skylab*, Huntsville, Alabama.

Fleischer R.L., Giard W.R., Mogro-Compero A., Turner L.G., Alter H.W. & Gingrich J.E. (1979) Dosimetry of environmental radon: methods and theory for low-dose, integrated measurements. *General Electric Report No. 79CRD263*, Schenectady, N.Y.

Henke, R.P., Benton E.V. & Cassou R.M. (1979) A method of automated HZE-particle Z-spectra measurement in plastic nuclear track detectors. Paper presented at the 10th International Conference on Solid State Nuclear Track Detectors, Lyon, France.

Hewitt J.E., Schaefer H.J. & Sullivan J.J. (1972) Radiation exposure during the Biosatellite III primate flight. *Health Phys.* 23, 461-468.

Lomanov, M.F., Shimchuk G.G. & Yakovlev R.M. (1979) Solid state detectors of fission fragments for the rem-dose measurement of mixed proton and neutron radiation. *Health Phys.* 37, 677-686.

Merker, M. (1973) The contribution of galactic cosmic rays to the atmospheric neutron maximum dose equivalent as a function of neutron energy and altitude. *Health Phys.* 25, 524-527.

Pretre S., Tochilin E. & Goldstein N. (1968) A standardized method for making neutron fluence measurements by fission fragment tracks in plastics. *Proc. 1st Int'l Congr. Radiation Protection*, Rome.

Quist T.C., Furst M., Burnett D.S., Baum J.H. & Peacock C.L. Jr. (1974) Spacecraft-produced neutron fluxes on Skylab--preliminary report. Division of Geological and Planetary Science, California Institute of Technology, Pasadena, California 91125.

TABLE 1. ETCHING AND MEASURING PARAMETERS

	Interior stacks			Exterior stack	
Detector type	Lexan	CR-39	CN	Lexan	CN
Average layer thickness (μm)	187.3	1029	100.2	191.1	98.5
Etch temperature (°C)	60*	70	40	60	40
NaOH normality	6.25	6.25	2.5	6.25	2.5
Etch time (hours)	171.9*	236.0, 218.0**	103.8, 92.5**	77.7	86.3
Average fraction of layers removed	0.785	0.831	0.630	0.777	0.620
Magnification (linear pixels/mm)	38.6	38.6	100	50	170
Minimum area detected (sq. pixels)	1.5	1.5	0.5	0.5	0.5
Measured particle fluence (cm^{-2})	0.26 ± 0.02	2.2 ± 0.2	6.1 ± 0.1	0.86 ± 0.01	12.2 ± 0.2
Effective LET_∞ cutoff (keV/μm H_2O)	675	214	102	636	101
Integral spectrum (particles/cm^2-ster > LET_∞ cutoff)	0.042 ± 0.004	0.35 ± 0.04	0.97 ± 0.02	0.137 ± 0.016	1.94 ± 0.04

*Some of etch at lower temperature because heater broke during etch

**Etched in two halves

TABLE 2. TRACK DENSITIES COUNTED FROM THE Li^6F/CN AND B^{10}/CN DETECTORS

Corner stack	Radiator	Shielding	Tracks/mm^2
AF	B^{10}	none	84.5 ± 2.5
	B^{10}	1 mm Cd	13.8 ± 0.8
BF	Li^6F	none	35.5 ± 1.2
	Li^6F	1 mm Cd	13.8 ± 0.7
CF	B^{10}	none	104.8 ± 2.7
	B^{10}	1 mm Cd	14.4 ± 0.8
DF	Li^6F	none	37.7 ± 1.4
	Li^6F	1 mm Cd	13.8 ± 0.7
Background	Li^6F		10.9 ± 0.4
	B^{10}		5.6 ± 0.5
$E_n < 0.3$ eV	(Li^6F)		22.8 ± 1.1
$E_n > 0.3$ eV	(Li^6F)		2.9 ± 0.7
$E_n < 0.3$ eV	(B^{10})		80.6 ± 2.0
$E_n > 0.3$ eV	(B^{10})		8.5 ± 0.8

TABLE 3. RESULTS OF COUNTING FROM FISSION FOIL/MICA DETECTORS

Corner stack	Radiator	Tracks/cm^2
AF	Bi^{209}	5.3 ± 1.1
		6.5 ± 1.2
	Th^{232}	42.2 ± 6.1
		41.3 ± 6.0
		38.6 ± 5.8
		36.0 ± 5.6
		35.1 ± 5.6
		41.3 ± 6.0
	Np^{237}	727. ± 24
		709. ± 24
	U^{238}	211. ± 14
		205. ± 13
		192. ± 13
		204. ± 13
		190. ± 13
		155 [damaged mica]
CF	Bi^{209}	7.6 ± 1.3
		7.1 ± 1.3
	Th^{232}	40.0 ± 5.9
		42.1 ± 6.1
		38.6 ± 5.8
		49.2 ± 6.6
		47.4 ± 6.5
		29.0 ± 5.0

(continued)

Table 3. continued

Corner stack	Radiator	Tracks/cm^2
	Np^{237}	880 ± 27
		862 ± 26
	U^{238}	212 ± 14
		200 ± 13
		195 ± 13
		231 ± 14
		202 ± 13
Backgrounds	Bi^{209}, Th^{232}	0
		0
		0.9 (1 track)
		0
		0
		0
		1.8
		0
		1.8
		0
		0.9
	Np^{237}	558 ± 21
		609 ± 22
	U^{238}	84 ± 9
		112 ± 10
		115 ± 10

TABLE 4. SUMMARY OF FISSION FOIL/MICA MEASUREMENTS

Foil	Corner stack	Tracks/cm^2	Average
Bi^{209}	AF	5.4 ± 1.1	6.2
	CF	6.9 ± 1.2	
Th^{232}	AF	38.6 ± 2.7	39.6
	CF	40.6 ± 6.6	
N^{237}	AF	135 ± 23	212
	CF	288 ± 25	
U^{238}	AF	97 ± 16	101
	CF	104 ± 19	

TABLE 5. EFFICIENCY FACTORS FOR THE FISSION FOIL DETECTORS FOR THE SELECTED NEUTRON (E_n > 1 MeV) AND PROTON (E_p > 17 MeV) SPECTRA IN TRACKS/NUCLEON

Radiator foil	Neutron spectrum	Proton spectrum
Bi^{209}	7.73×10^{-7}	1.69×10^{-6}
Th^{232}	6.73×10^{-6}	9.28×10^{-6}
Np^{237}	2.26×10^{-5}	1.94×10^{-5}
U^{238}	1.47×10^{-5}	1.76×10^{-5}

TABLE 6. NEUTRON (>1 MeV) AND PROTON (>17 MeV) FLUENCES CALCULATED FOR THE FISSION FOIL DETECTORS

Fission foil	Neutron fluence (cm^{-2})	Proton fluence (cm^{-2})
Bi^{209}	1.5×10^6	3.0×10^6
Th^{232}	1.6×10^6	3.1×10^6
Np^{237}	3.5×10^6	6.9×10^6
U^{238}	2.0×10^6	4.1×10^6
Average	2.1×10^6	4.3×10^6

TABLE 7. TLD MEASUREMENTS FROM THE CORNER STACKS

Stack	mrad equivalent Li^7F	mrad equivalent CaF_2	Explanation	
BF	1290	2093	flight stacks	68.2 day assembly
DF	1387	2624	flight stacks	
BB	1057	2186	backup stacks	
DB	707	2055	backup stacks	
B	586	810	background test	68 day assembly
D	585	817	background test	

TABLE 8. TLD MEASUREMENTS FROM EXTERNAL DETECTORS

	mrad equivalent		
Detector	Li^7F	CaF_2	Explanation
TEF	593*	899*	flight detector
TEB	324	751	backup detector
TET	286	636	"test" detector

*The TLDs were partially annealed by heat during the spacecraft descent.

FIGURE CAPTIONS

1. Schematic diagram of interior dosimetry package. The plastic stacks, labeled A-E, measure the HZE radiation component and the corner packages measure the low-LET and neutron radiation components. Also shown are the coordinate systems for the HZE stacks.
2. Dimensions of corner stacks A & C.
3. Dimensions of corner stacks B & D.
4. External TLD stack (1).
5. Photograph of flight and backup units both internal and external.
6. One of the containers used to house the external package after the flight with the lid open.
7. The container which housed two of the external packages showing extensive heat damage.
8. Cross sections of some reactions in the thermal neutron range.

9a-e. Measured particle track positions on the interior stacks A-E, respectively. In each of the figures, all of the positions measured in all of the layers of the stacks are superimposed on the x-y plane. The coordinates are shown in Fig. 1.

10. Measured particle track positions for the exterior stack.

11a. Projection of particle trajectories from the combined interior stacks A and C. The points represent the intersection of the particles with the z=1 plane if the trajectories were translated to pass through the coordinate system origin. The scale has been appropriately reduced at the periphery of the plot, however, to map equal solid angles in the trajectory angle space into equal areas on the plot to facilitate an estimation of the degree of isotropy of the beam. The azimuthal angle,

α, of the trajectory is measured counter-clockwise from the x axis and the dip angle, δ, is measured upward (toward +z) from the x-y plane. The direction of particle travel is not taken into account.

11b. Projection of particle trajectories from the combined interior stacks B and D.

11c. Projection of particle trajectories from interior stack E.

12. Projection of particle trajectories for the exterior stack.

13. Integral LET spectra. The solid line is a weighted least-squares fit of a power function to the three points measured in the three different-sensitivity interior detectors, CN, CR-39 and Lexan. The exterior spectrum, shown by the dashed line, is determined from the exterior CN and Lexan detector results.

14. Integral dose and REM dose. The dose and REM dose due to particles with energy loss rates greater than LET (shown as the abscissa) are plotted.

15. Measured Z spectra. This representation uses the sum of narrow gaussian curves, each with an area of one and centered on an individual measurement of Z. This approach avoids some of the arbitrariness in the bin placement that accompanies the use of a standard histogram.

16. Geometric factor for the interior stacks.

17. Geometric factor for the exterior stacks.

18. Absolute Z spectra.

19. Neutron fission cross sections of three fission foil isotopes.

20. Proton fission cross sections of four fission foil isotopes.

21. The assumed neutron and proton spectra used in calculating the high-energy neutron fluence.

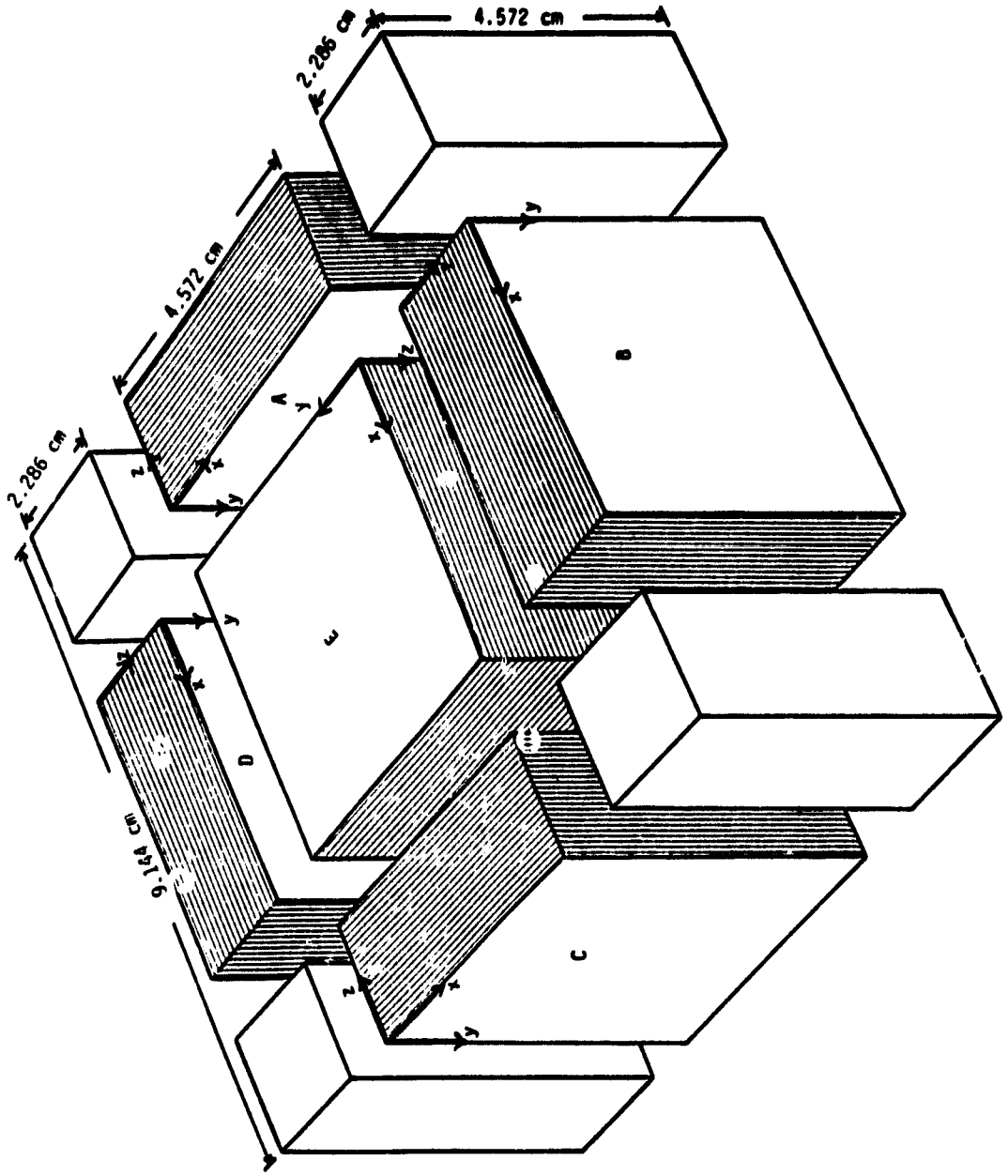

Figure 1

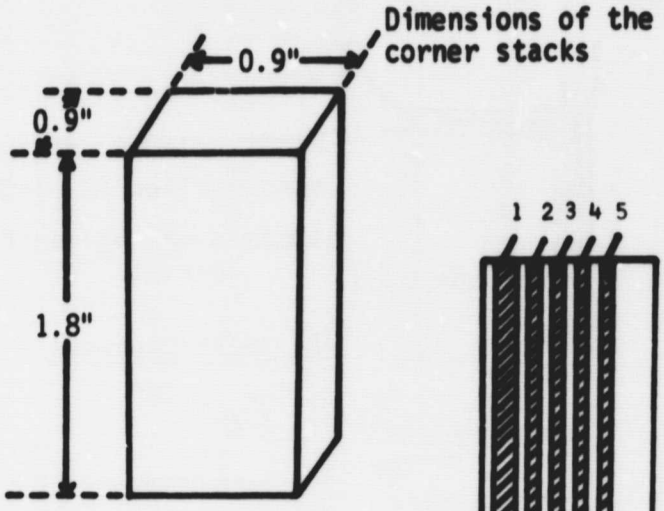

solid Aℓ plates
milled Aℓ plates

Side view of corner stacks A and C

Plate thicknesses

1 1/8"
2-5 1/16"
front plate 1/16"
separation plates 1/16"
back plate 0.210"

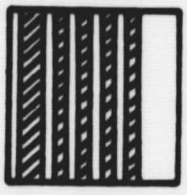

Top view of corner stacks A and C

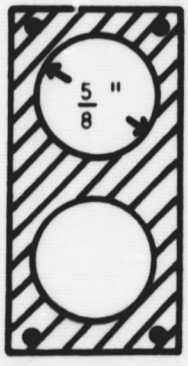

Plates 1 & 5
1 (top) B^{10}/CN
(bottom) Cd/B^{10}/CN/Cd
5 mica/Np^{237}/mica

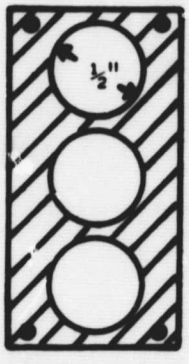

Plates 2 & 3
2 mica/Th^{232}/mica
3 mica/U^{238}/mica

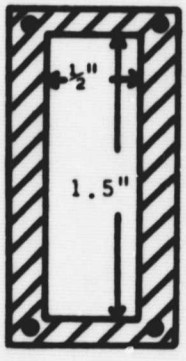

Plate 4
mica/Bi^{209}/mica

Top views of milled plates

Figure 2

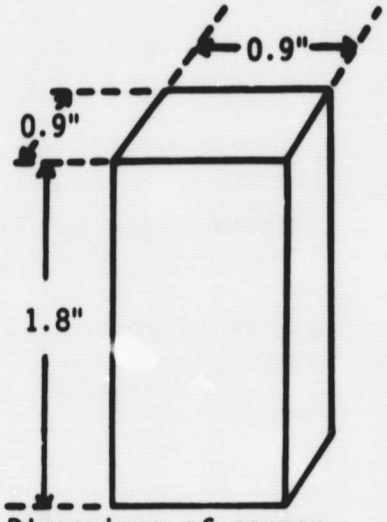

Dimensions of corner stacks

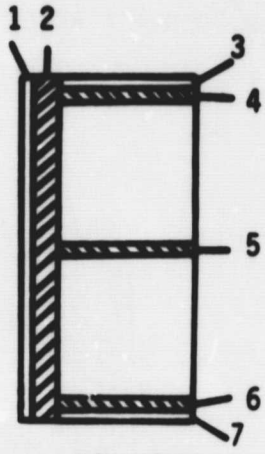

side view

solid Aℓ plates
milled Aℓ plates
areas milled from plates

Plate thicknesses

1,3-7 1/16"
2 1/8"

top view

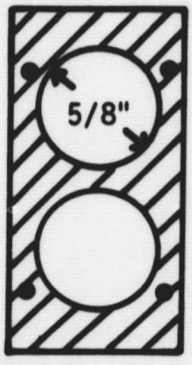

Plate 2

(top) Li^6F/CN
(bottom) Cd/Li^6F/CN/Cd

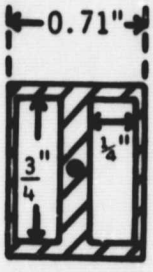

Plates 4-6

(left) Li^7F TLDs
(right) CaF_2 TLDs

Figure 3

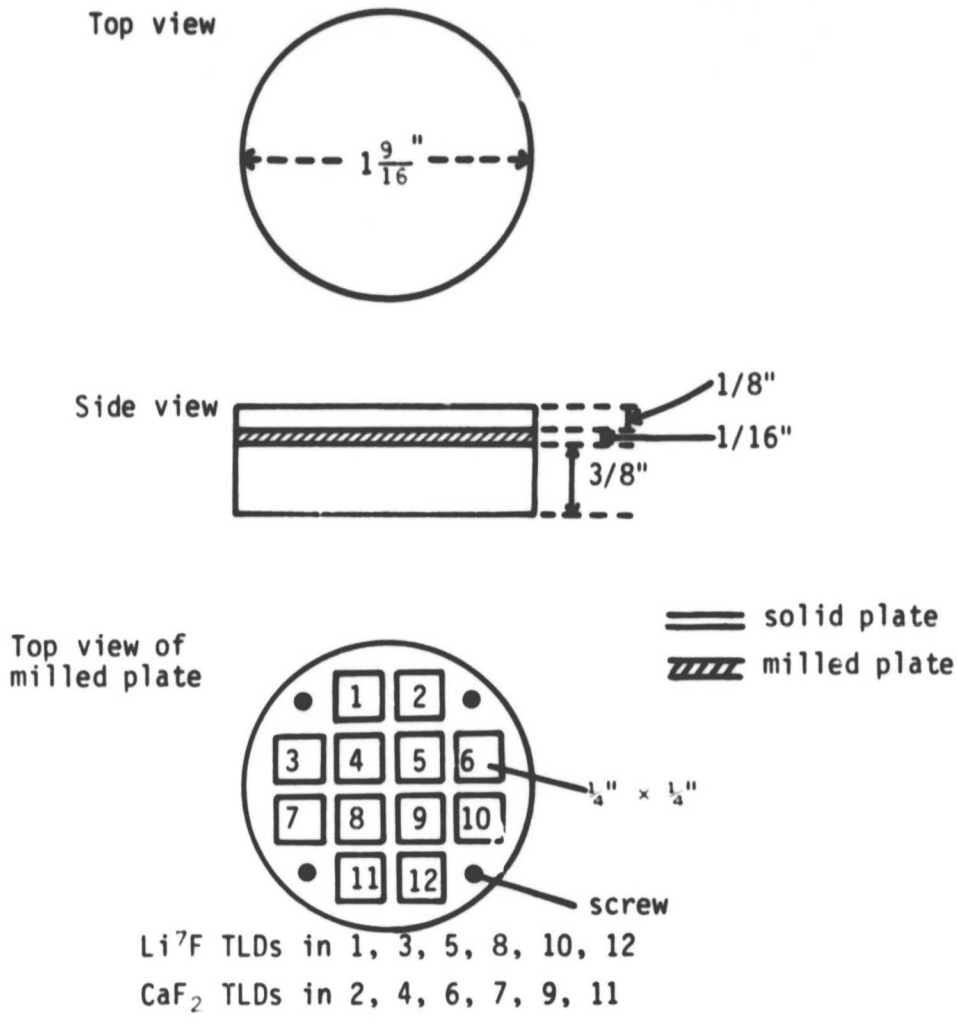
Top view
1 9/16"
Side view
1/8"
1/16"
3/8"
solid plate
milled plate
Top view of
milled plate
1
2
3
4
5
6
7
8
9
10
11
12
1/4" × 1/4"
screw
Li7F TLDs in 1, 3, 5, 8, 10, 12
CaF2 TLDs in 2, 4, 6, 7, 9, 11

Figure 4

USA
USSR
INTEGRITY

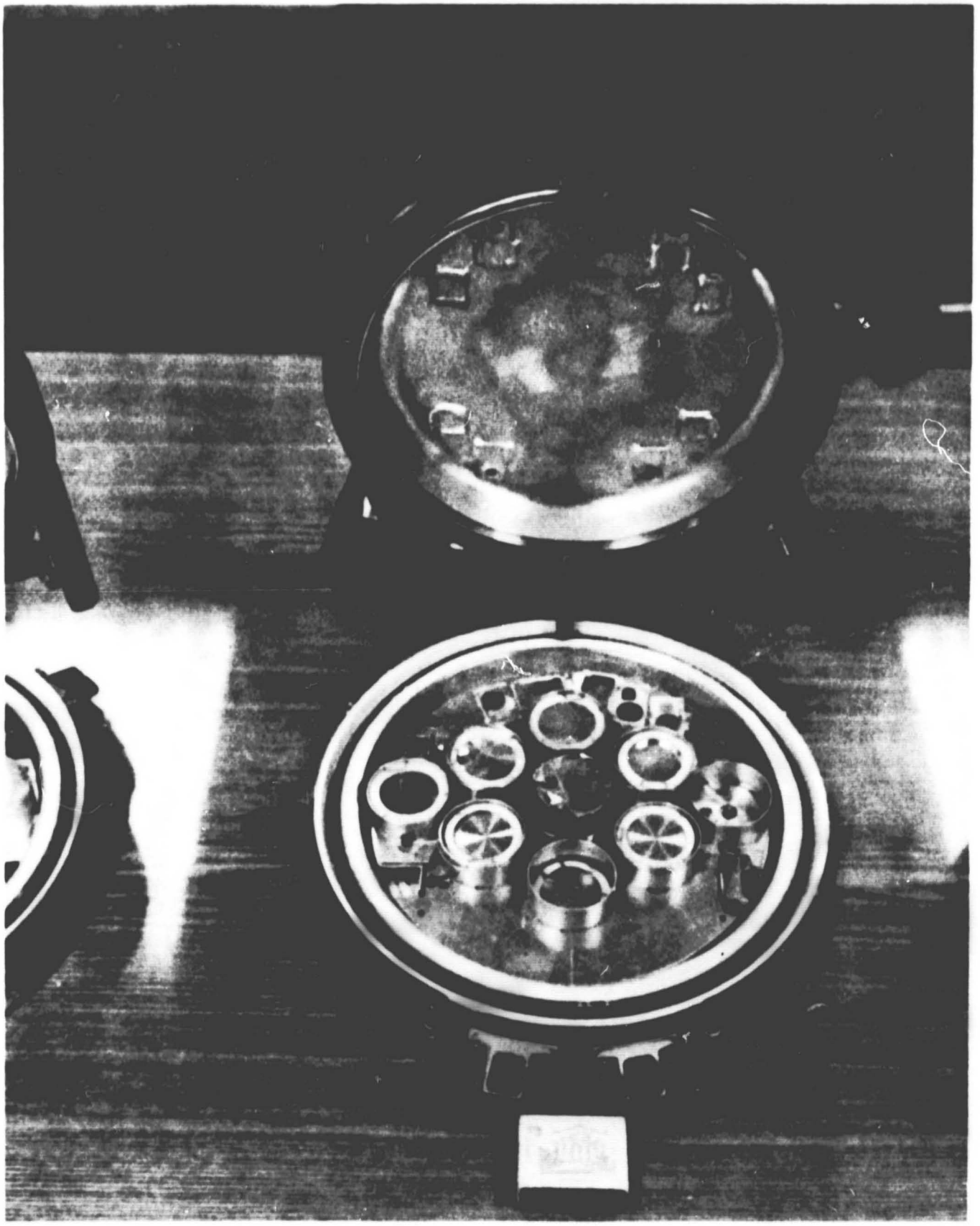

Figure 6

Figure 7

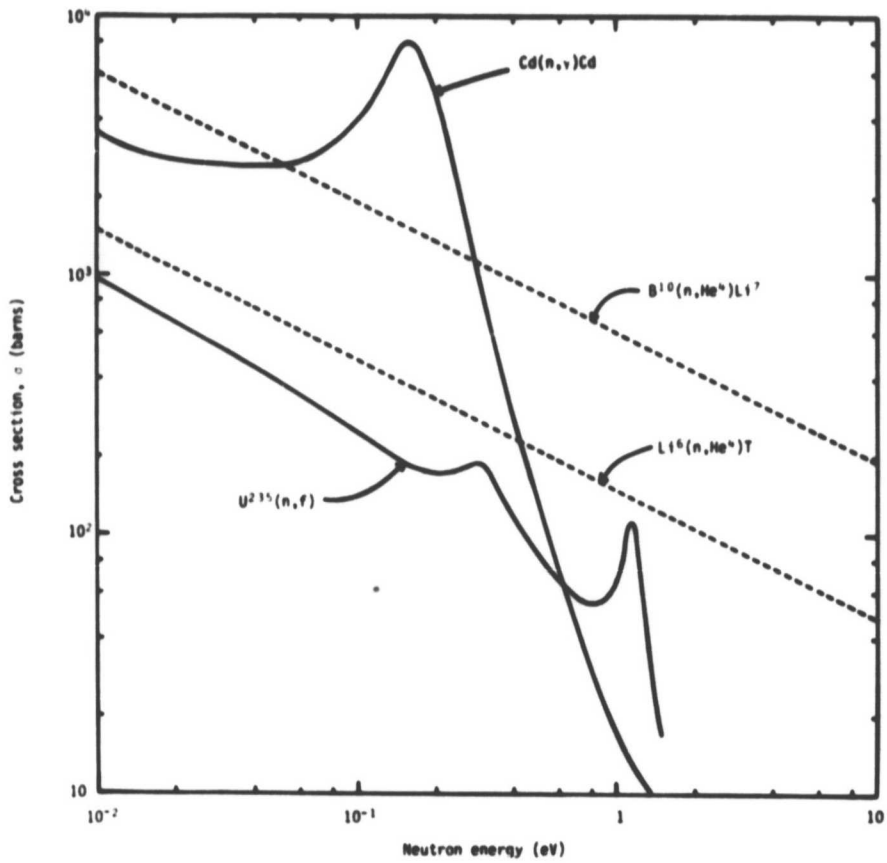
Cd(n,γ)Cd
B10(n,He4)Li7
Li6(n,He4)T
U235(n,f)
Cross section, σ (barns)
Neutron energy (eV)
10
10²
10³
10⁴
10⁻²
10⁻¹
1
10

Figure 8

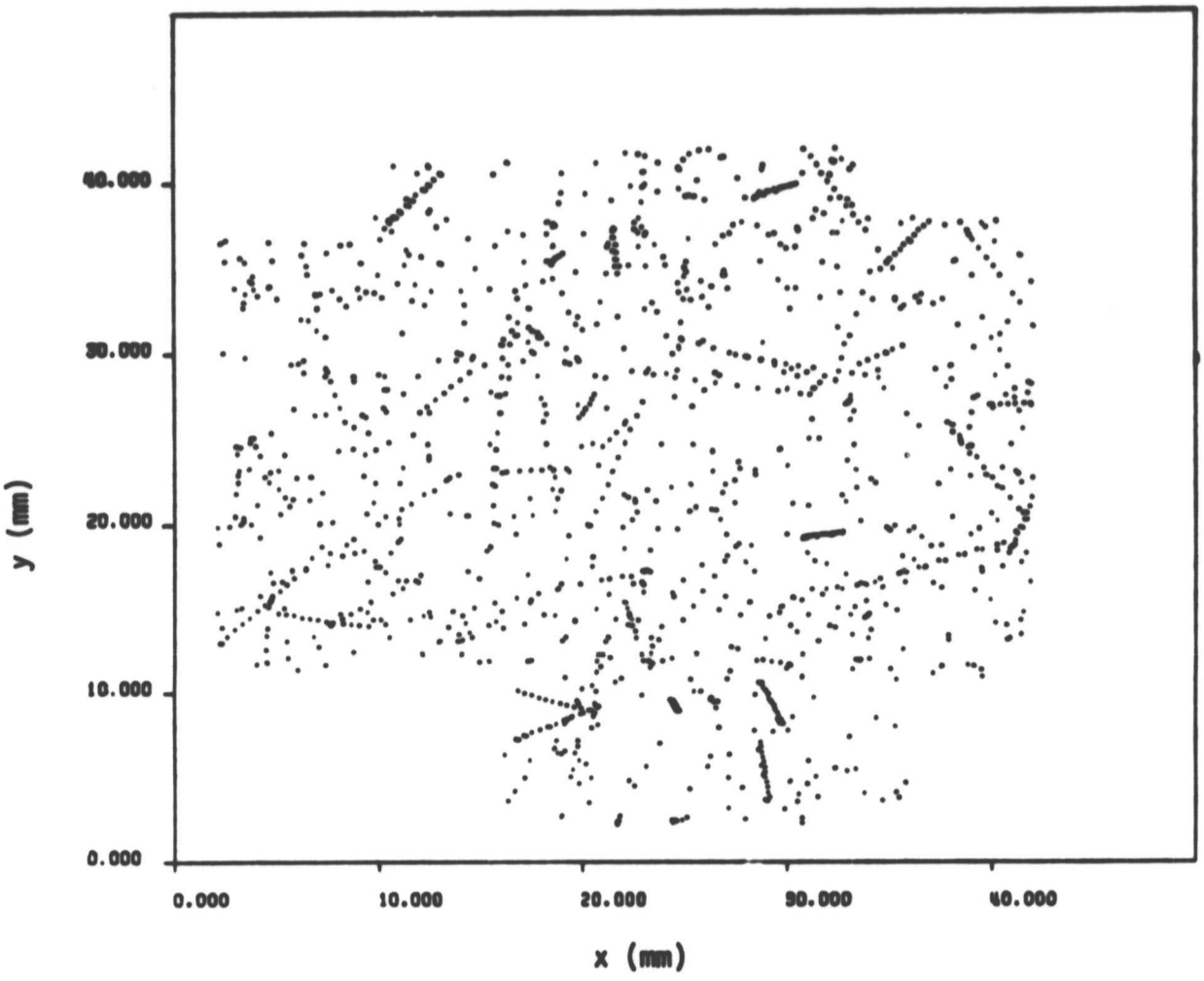
40.000
30.000
20.000
10.000
0.000
y (mm)
0.000
10.000
20.000
30.000
40.000
x (mm)

Figure 9a

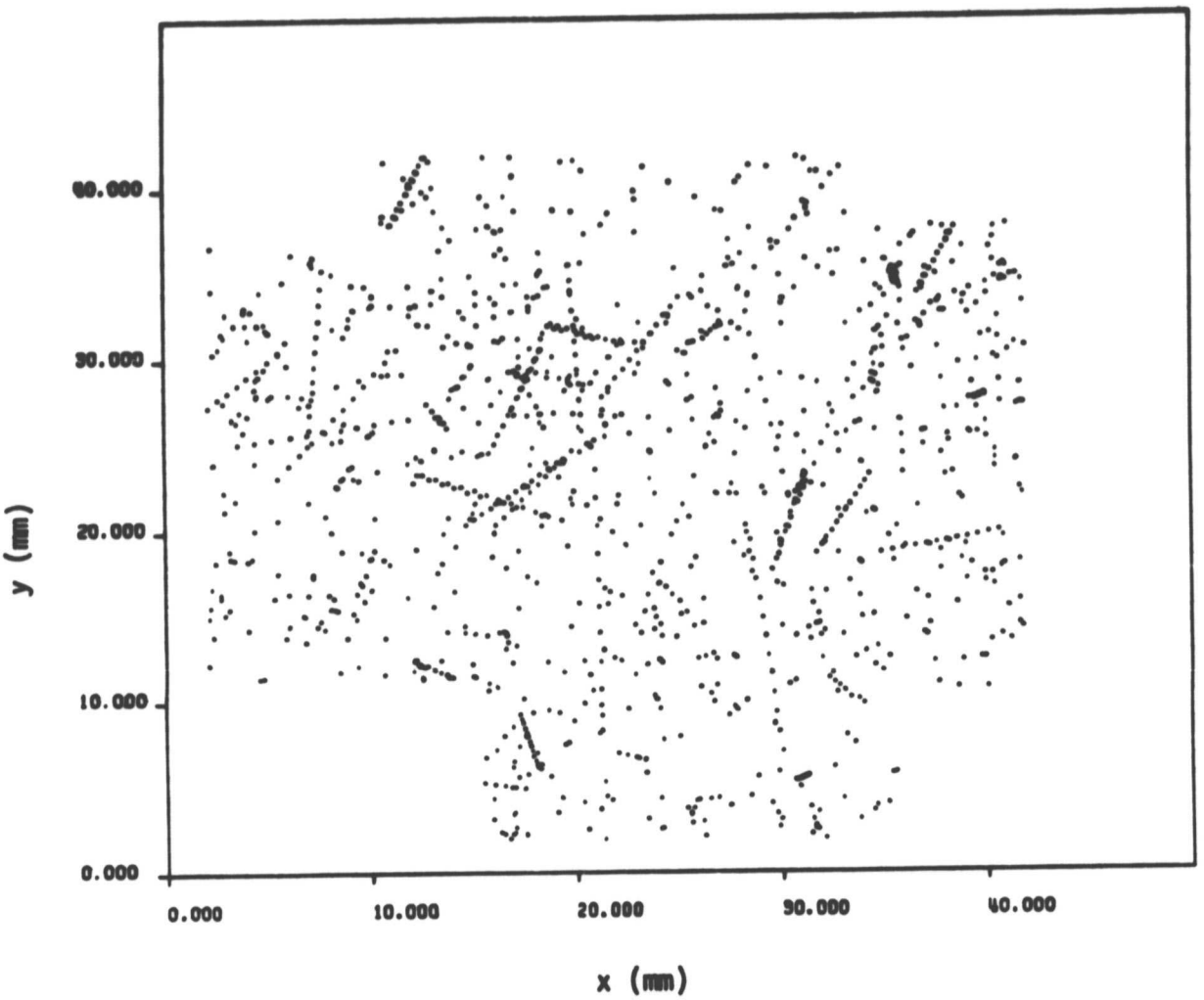

Figure 9b

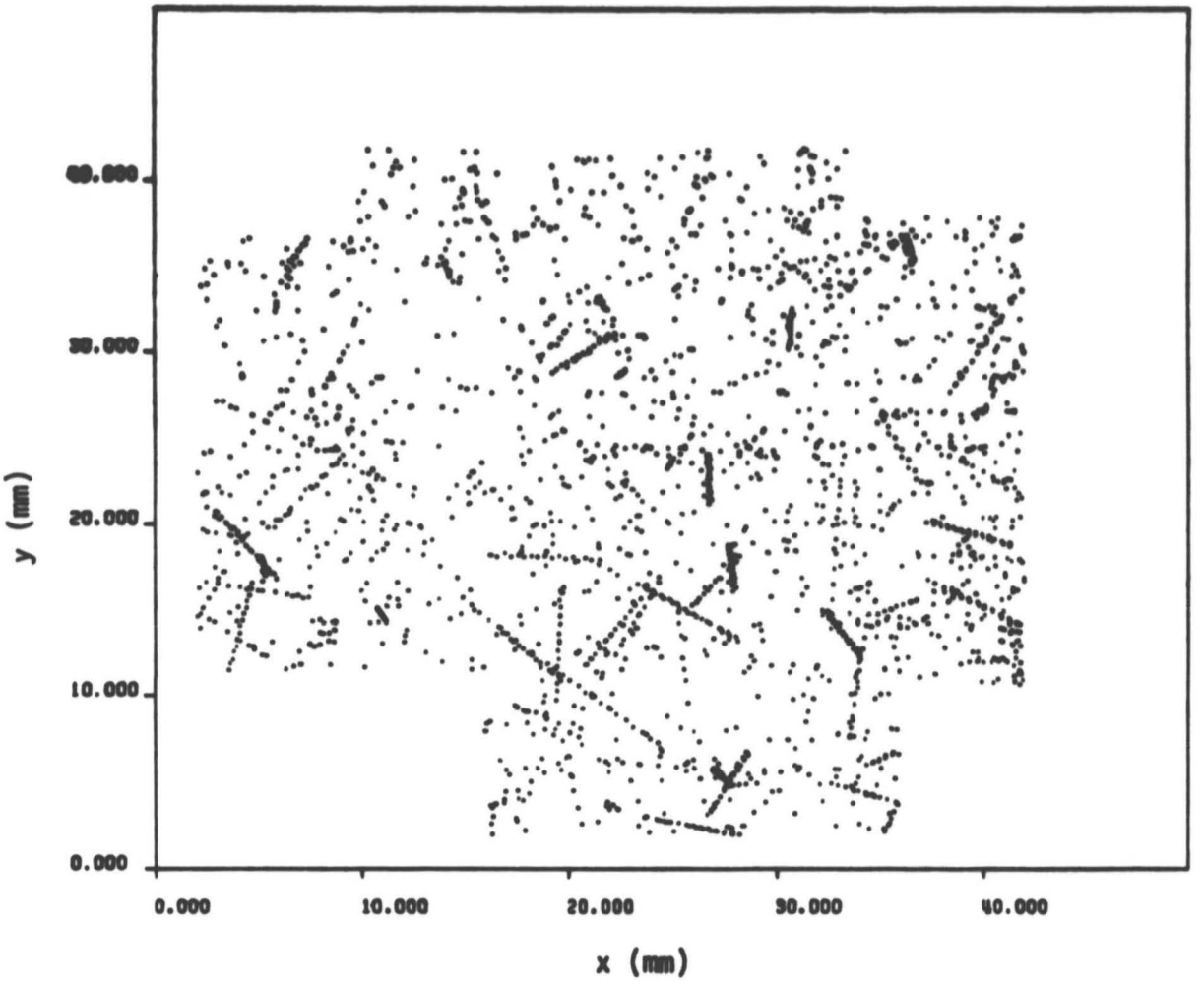

Figure 9c

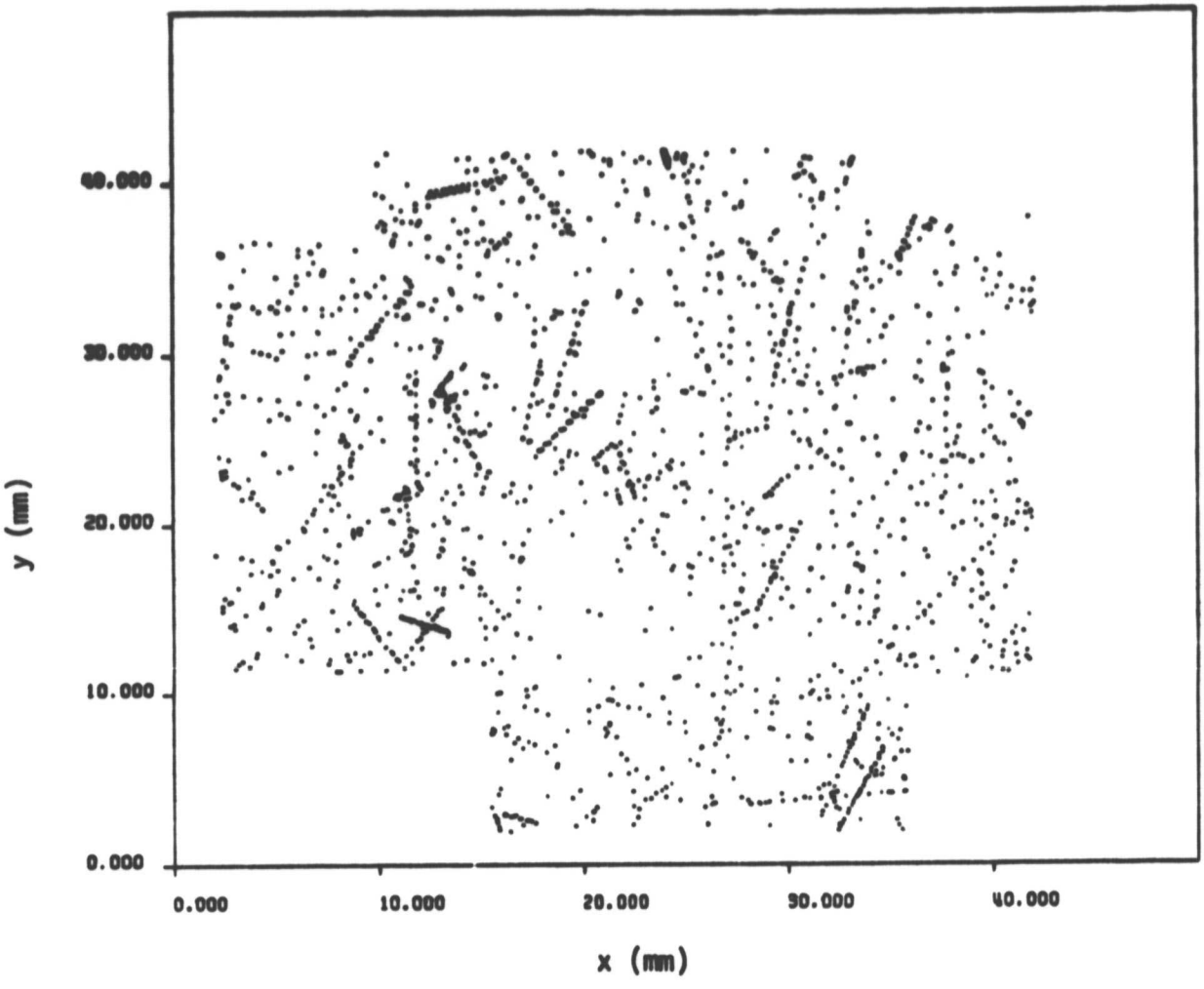
40.000
30.000
20.000
10.000
0.000
y (mm)
0.000
10.000
20.000
30.000
40.000
x (mm)

Figure 9d

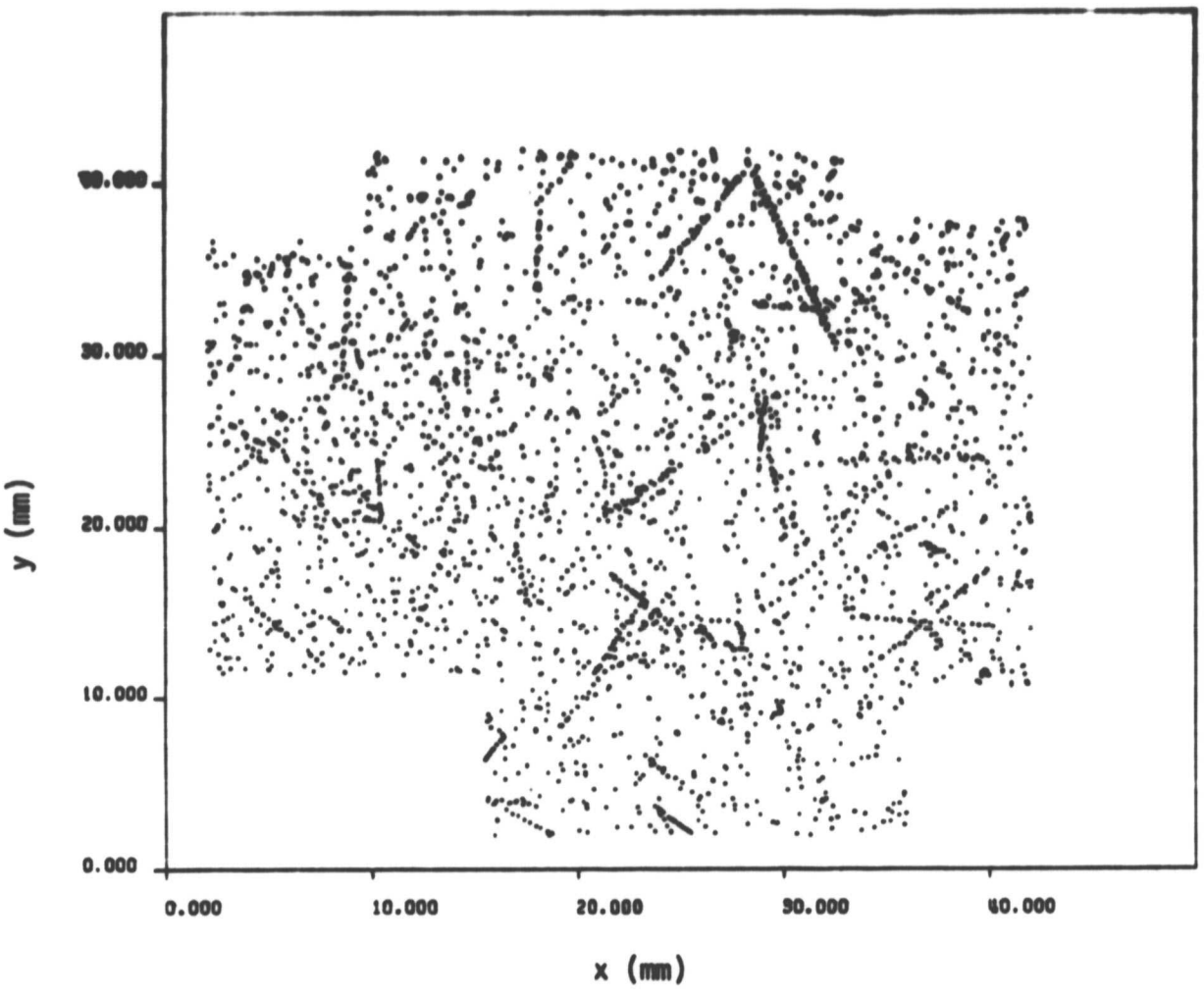

Figure 9e

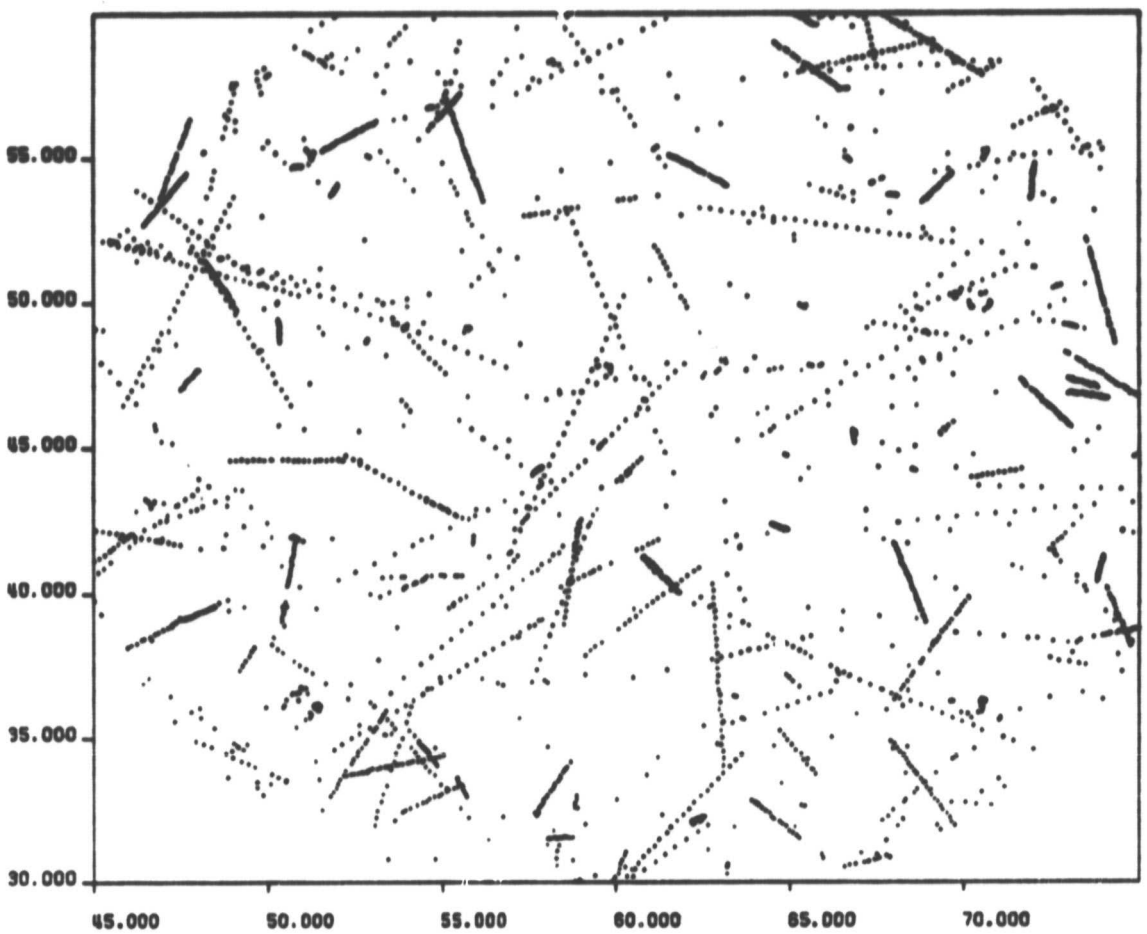
55.000
50.000
45.000
40.000
35.000
30.000
45.000
50.000
55.000
60.000
65.000
70.000

Figure 10

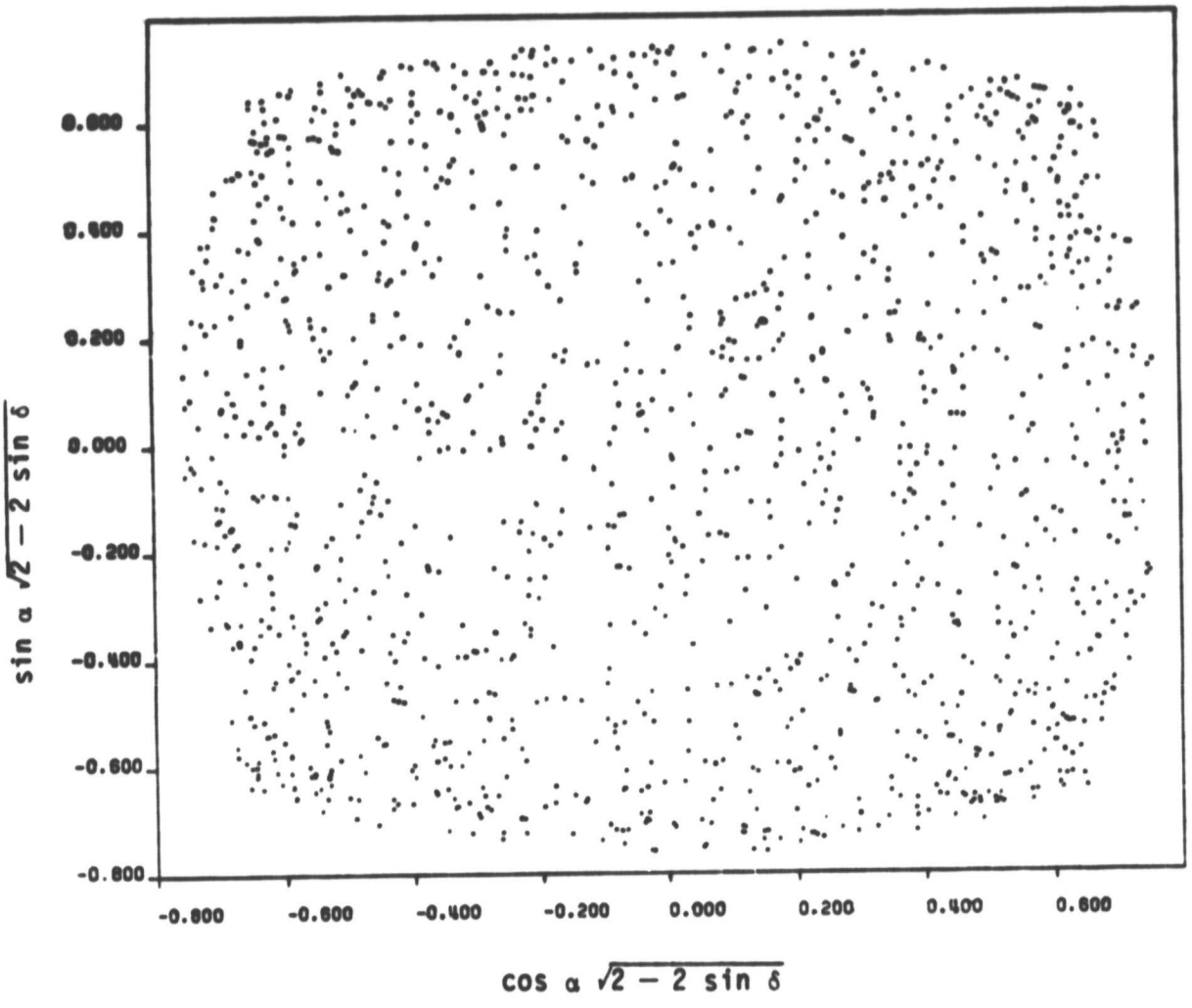
0.800
0.600
0.400
0.000
-0.200
-0.400
-0.600
-0.800
-0.800
-0.600
-0.400
-0.200
0.000
0.200
0.400
0.600
sin α √2 − 2 sin δ
cos α √2 − 2 sin δ

Figure 11a

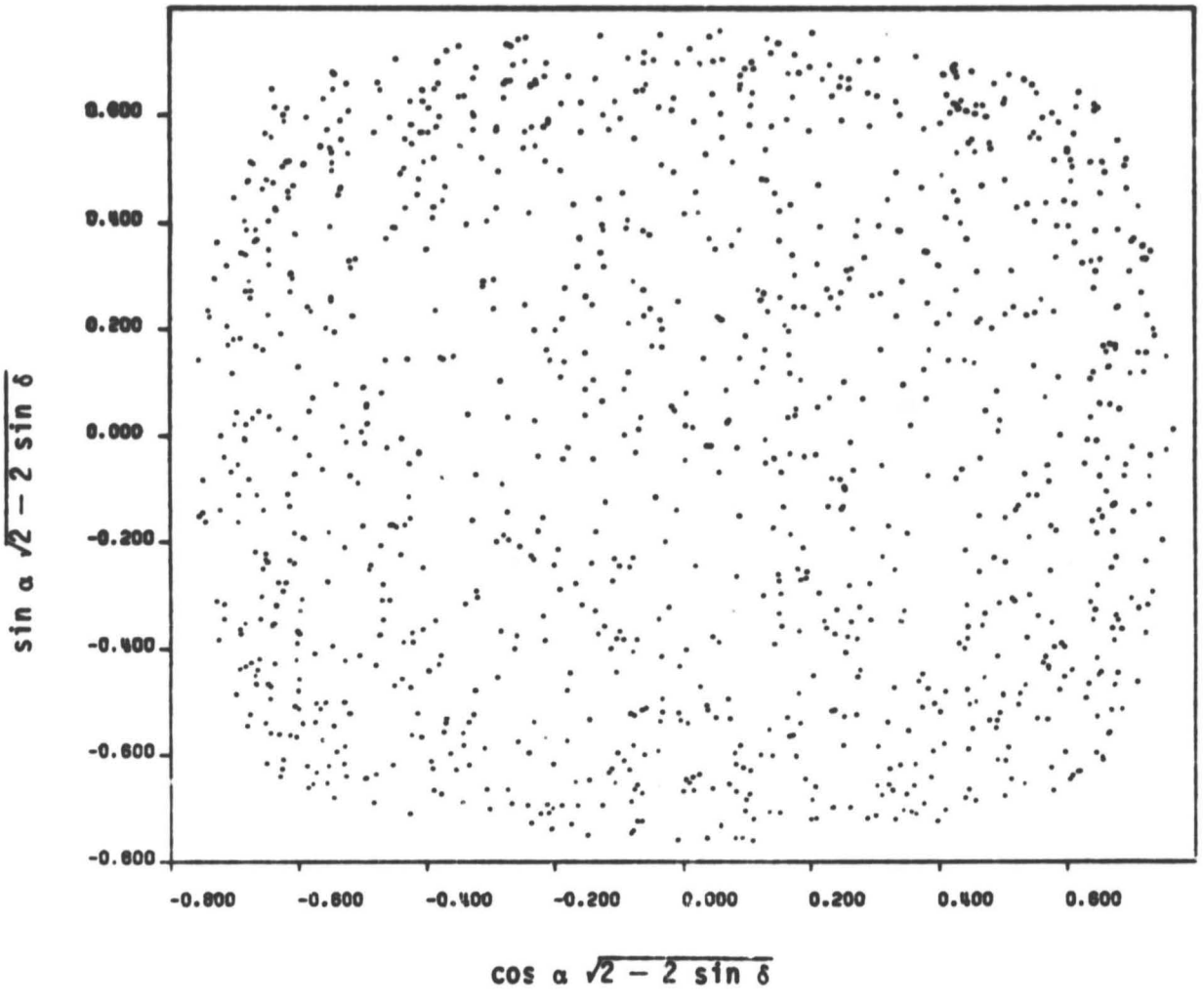

Figure 11b

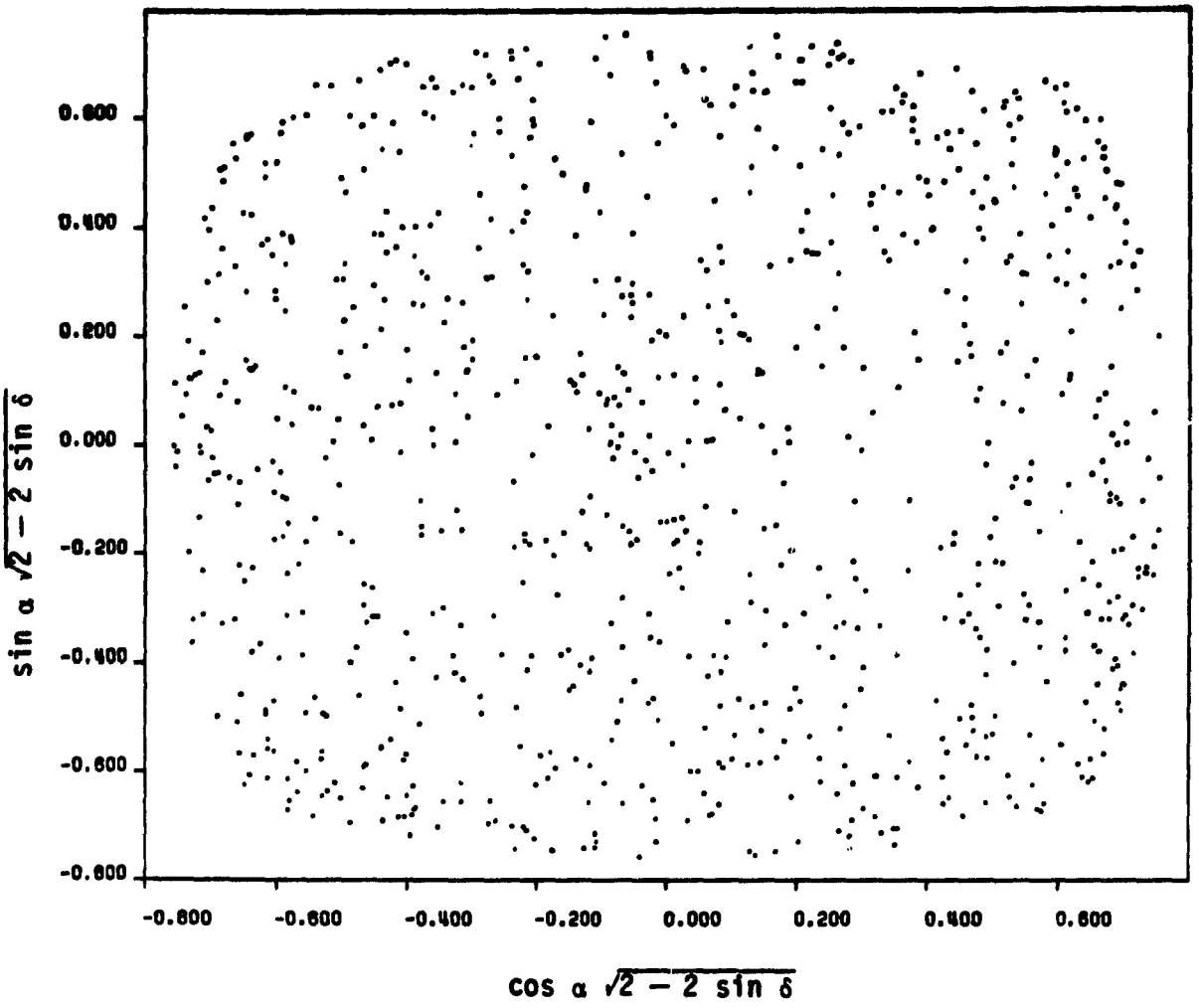
0.800
0.400
0.200
0.000
-0.200
-0.400
-0.600
-0.800
-0.800
-0.600
-0.400
-0.200
0.000
0.200
0.400
0.600
sin α √2 − 2 sin δ
cos α √2 − 2 sin δ

Figure 11c

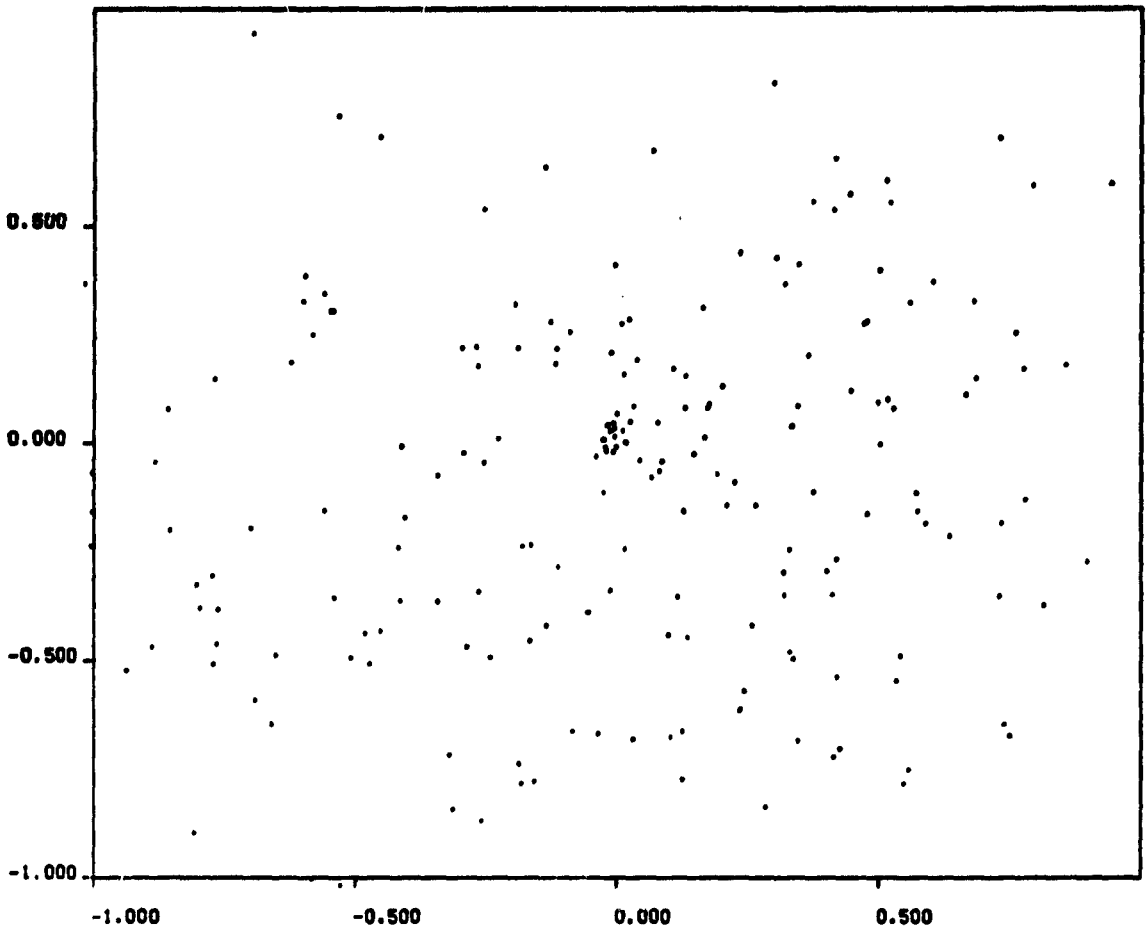

Figure 12

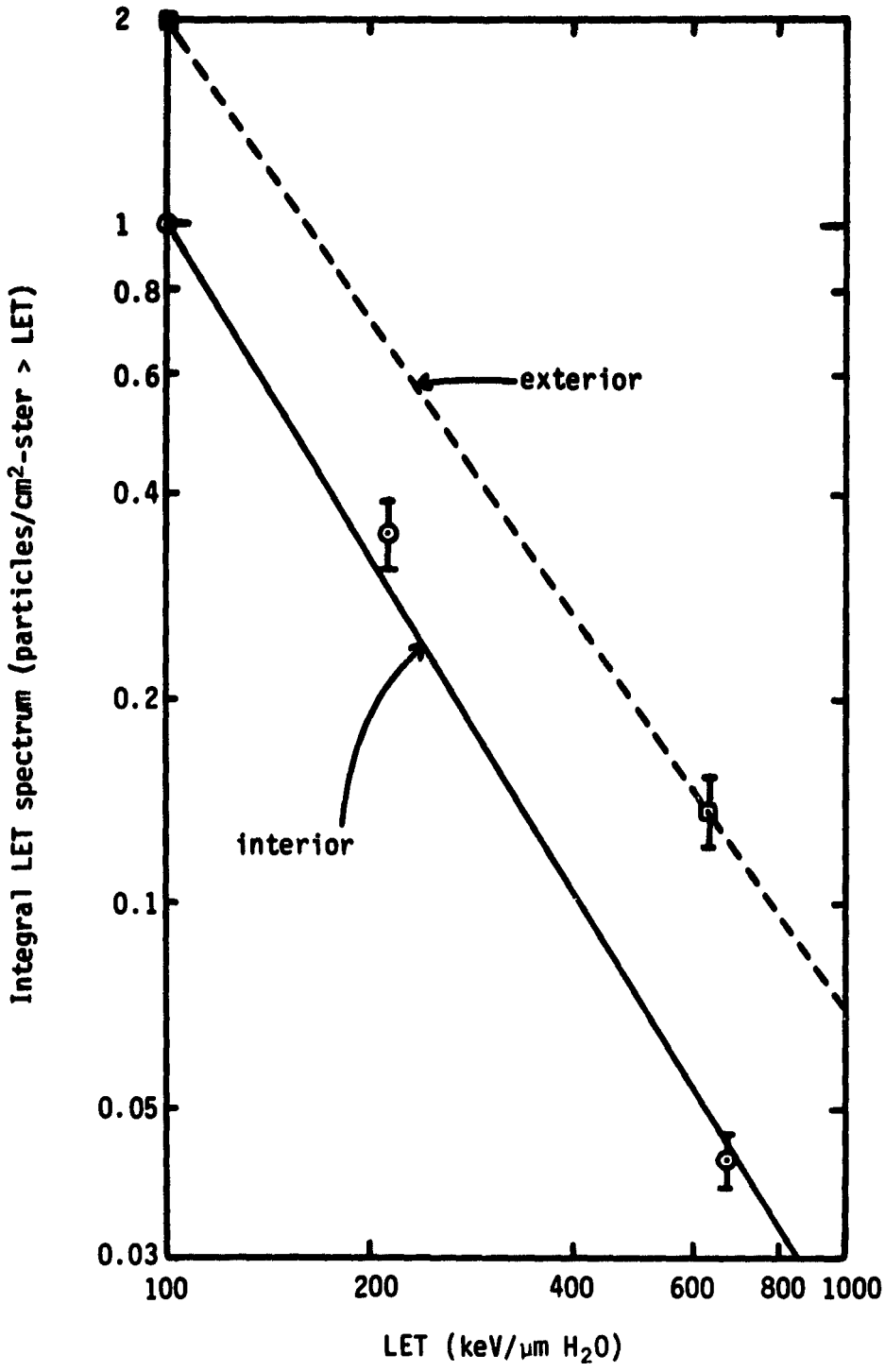
2
1
0.8
0.6
0.4
0.2
0.1
0.05
0.03
100
200
400
600
800
1000
exterior
interior
Integral LET spectrum (particles/cm²-ster > LET)
LET (keV/μm H₂O)

Figure 13

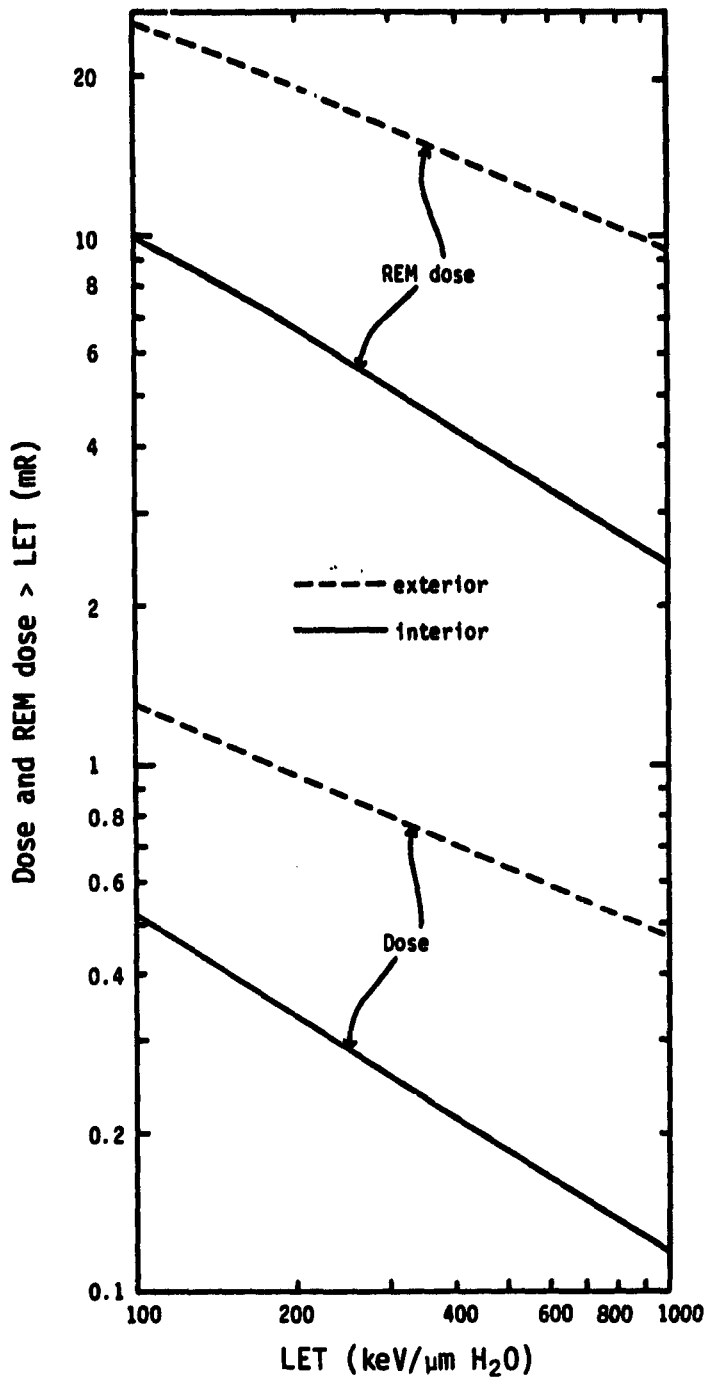
Dose and REM dose > LET (mR)
20
10
8
6
4
2
1
0.8
0.6
0.4
0.2
0.1
REM dose
exterior
interior
Dose
100
200
400
600
800
1000
LET (keV/μm H2O)

Figure 14

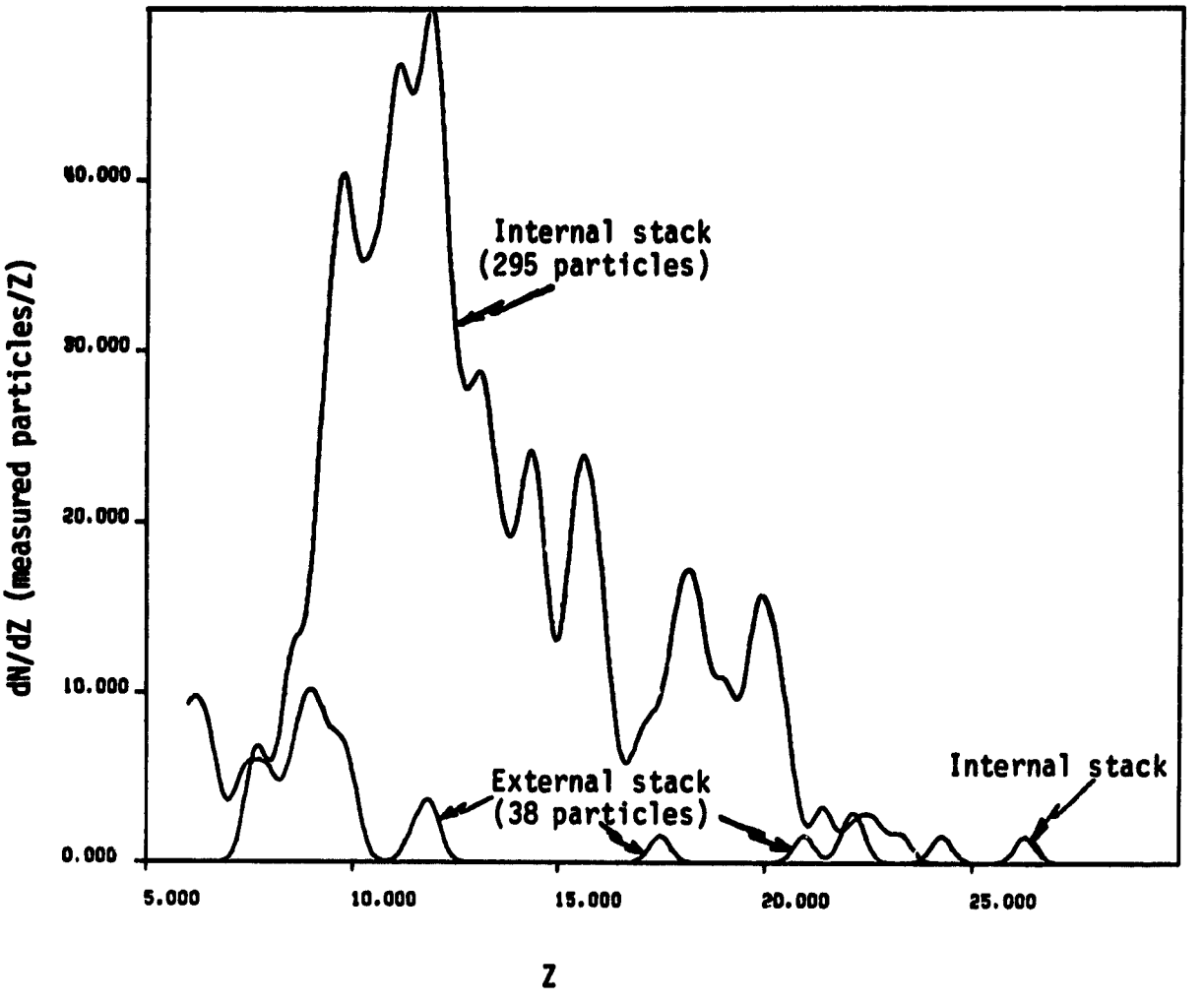
40.000
30.000
20.000
10.000
0.000
dN/dZ (measured particles/Z)
Internal stack
(295 particles)
External stack
(38 particles)
Internal stack
5.000
10.000
15.000
20.000
25.000
Z

Figure 15

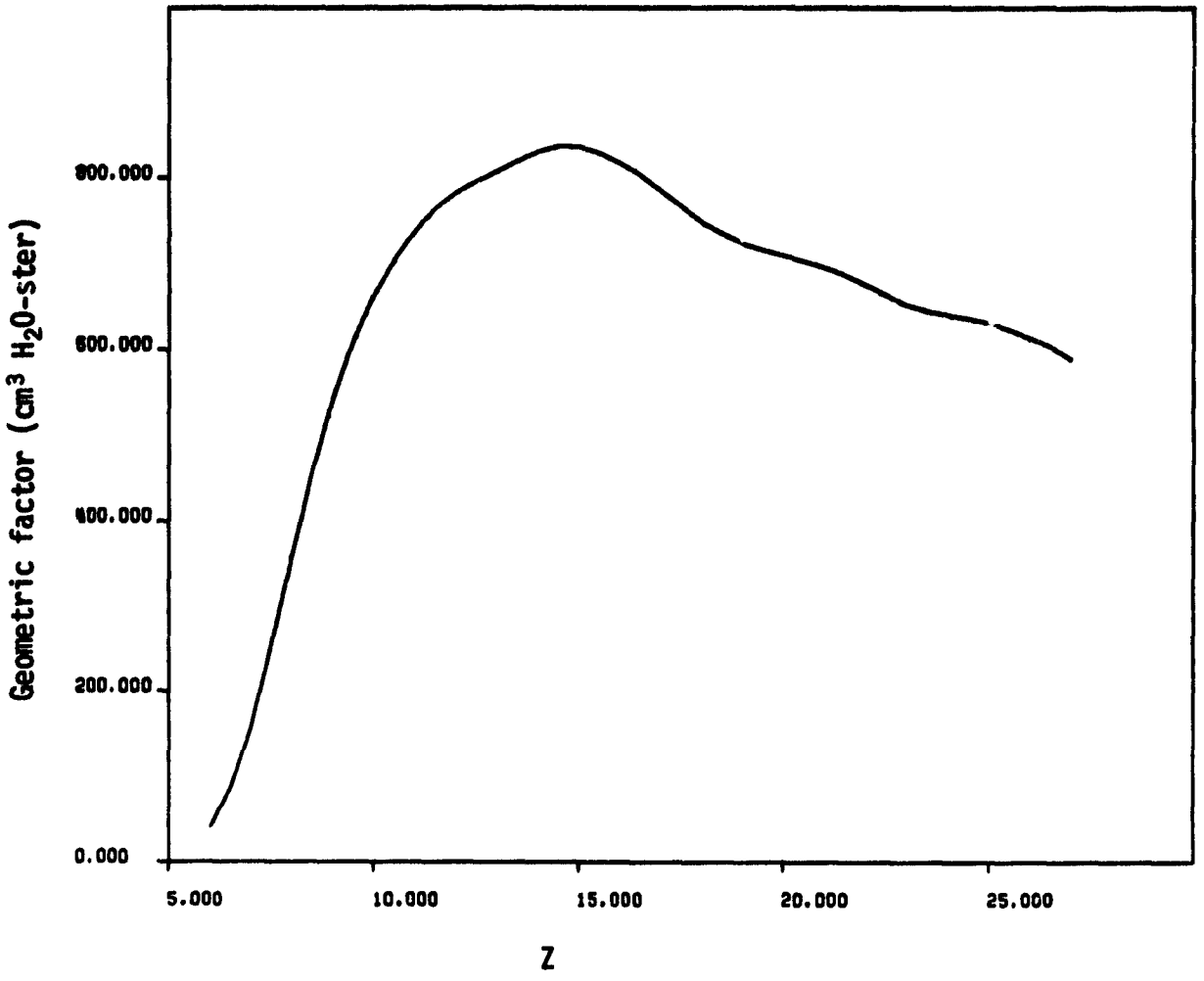
Geometric factor (cm³ H₂O-ster)
800.000
600.000
400.000
200.000
0.000
5.000
10.000
15.000
20.000
25.000
Z

Figure 16

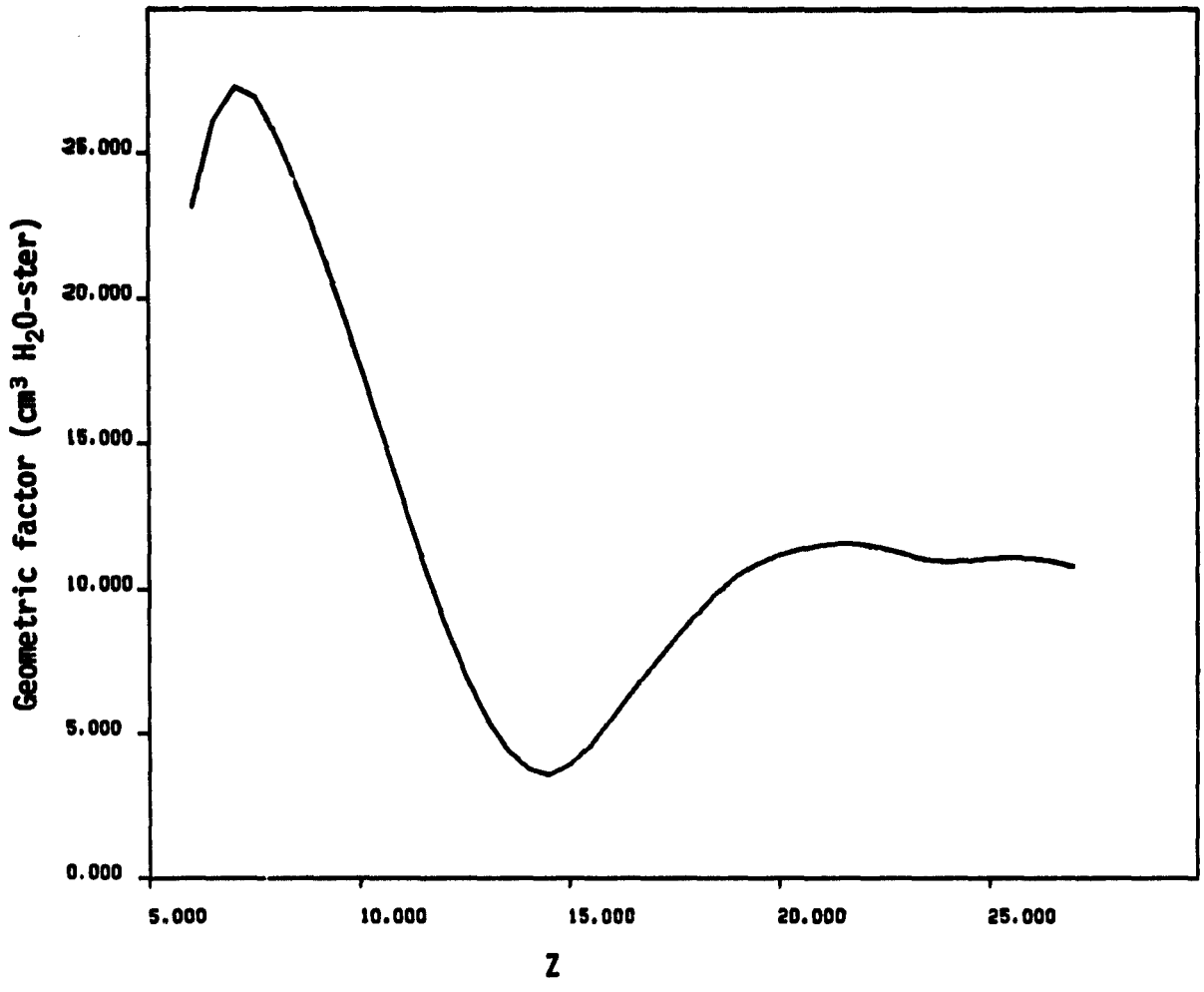

Figure 17

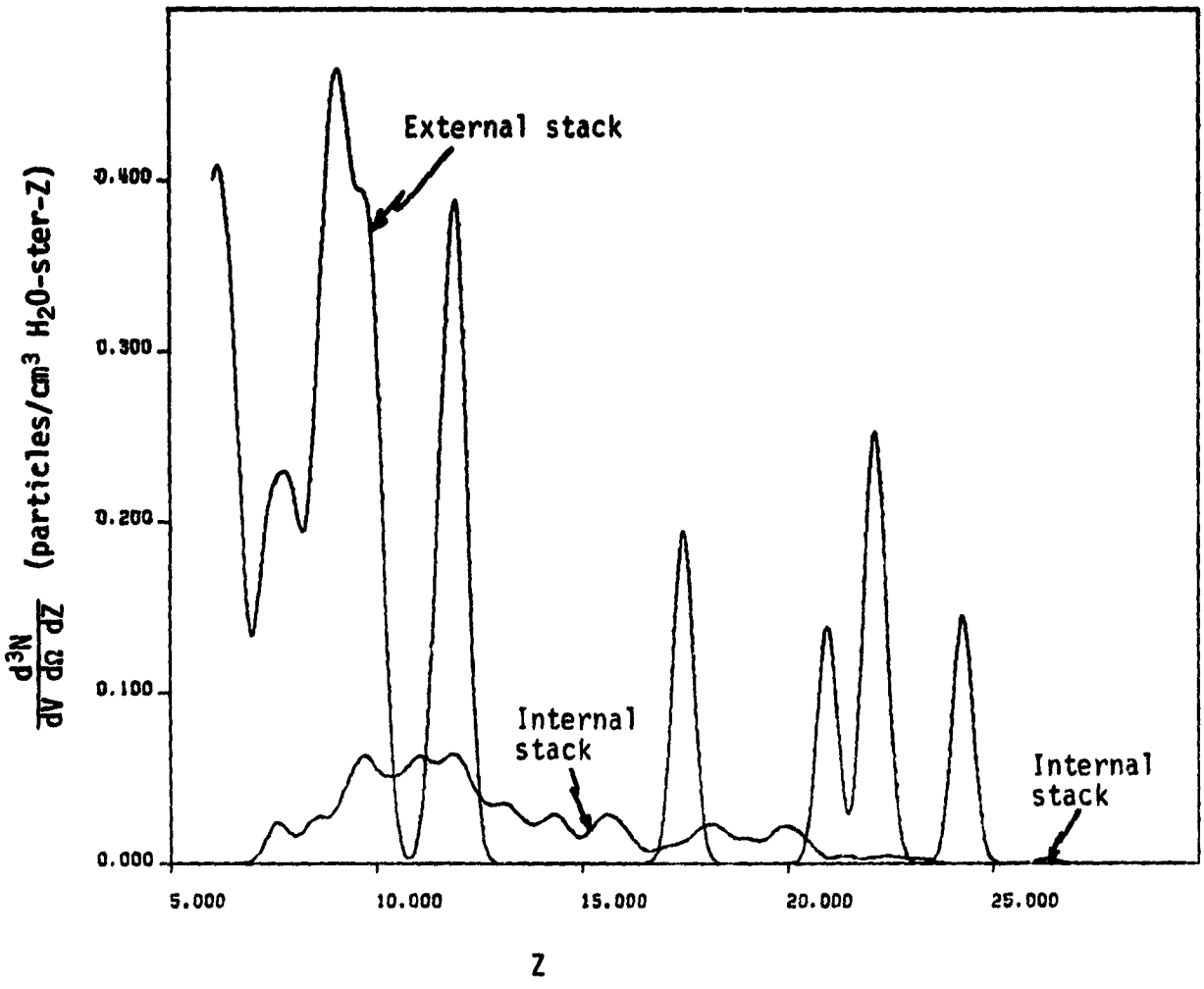
External stack
Internal stack
Internal stack
0.400
0.300
0.200
0.100
0.000
5.000
10.000
15.000
20.000
25.000
Z
$\frac{d^3N}{dV\,d\Omega\,dZ}$ (particles/cm^3 H_2O-ster-Z)

Figure 18

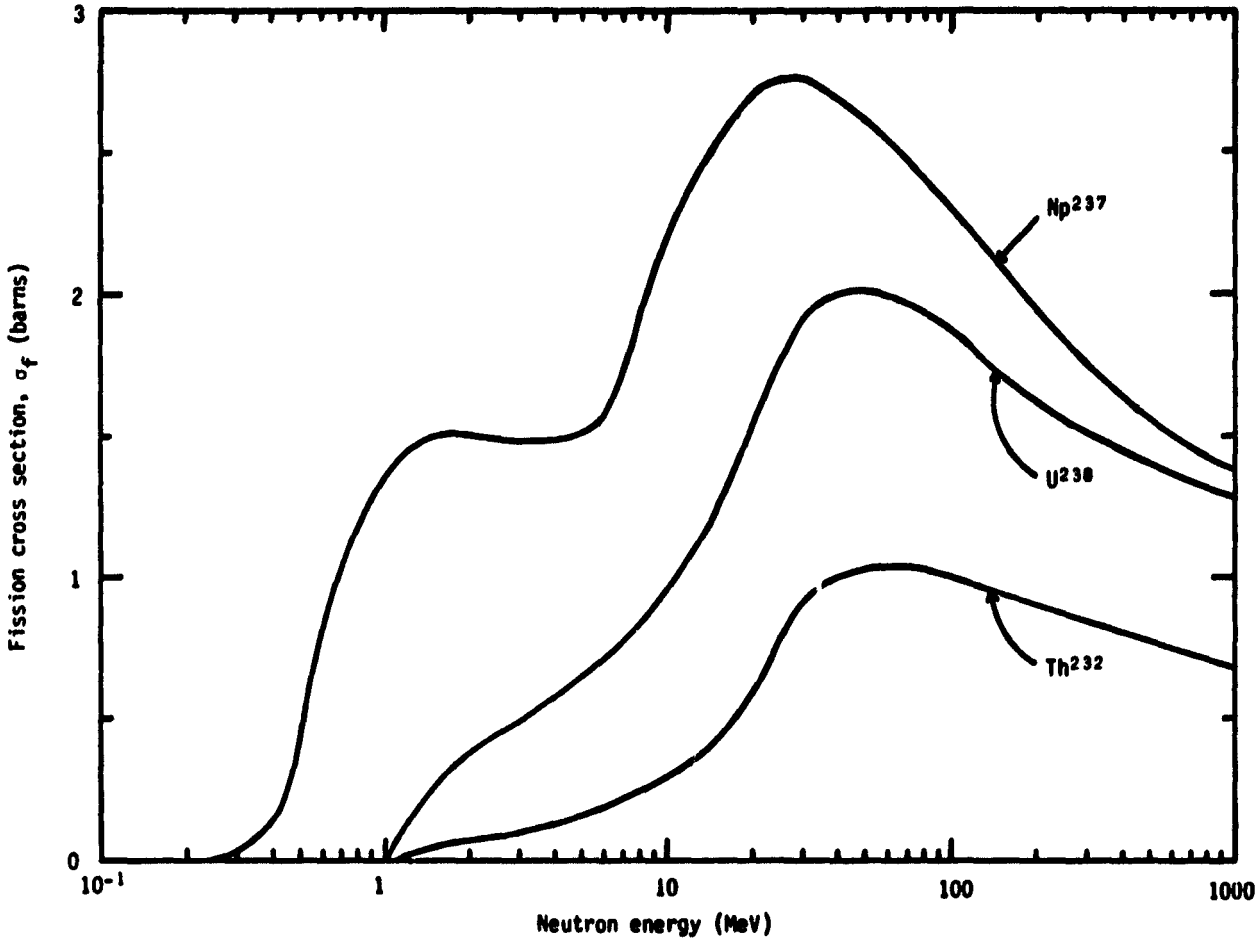
3
2
1
0
Fission cross section, σ_f (barns)
10^{-1}
1
10
100
1000
Neutron energy (MeV)
Np^{237}
U^{238}
Th^{232}

Figure 19

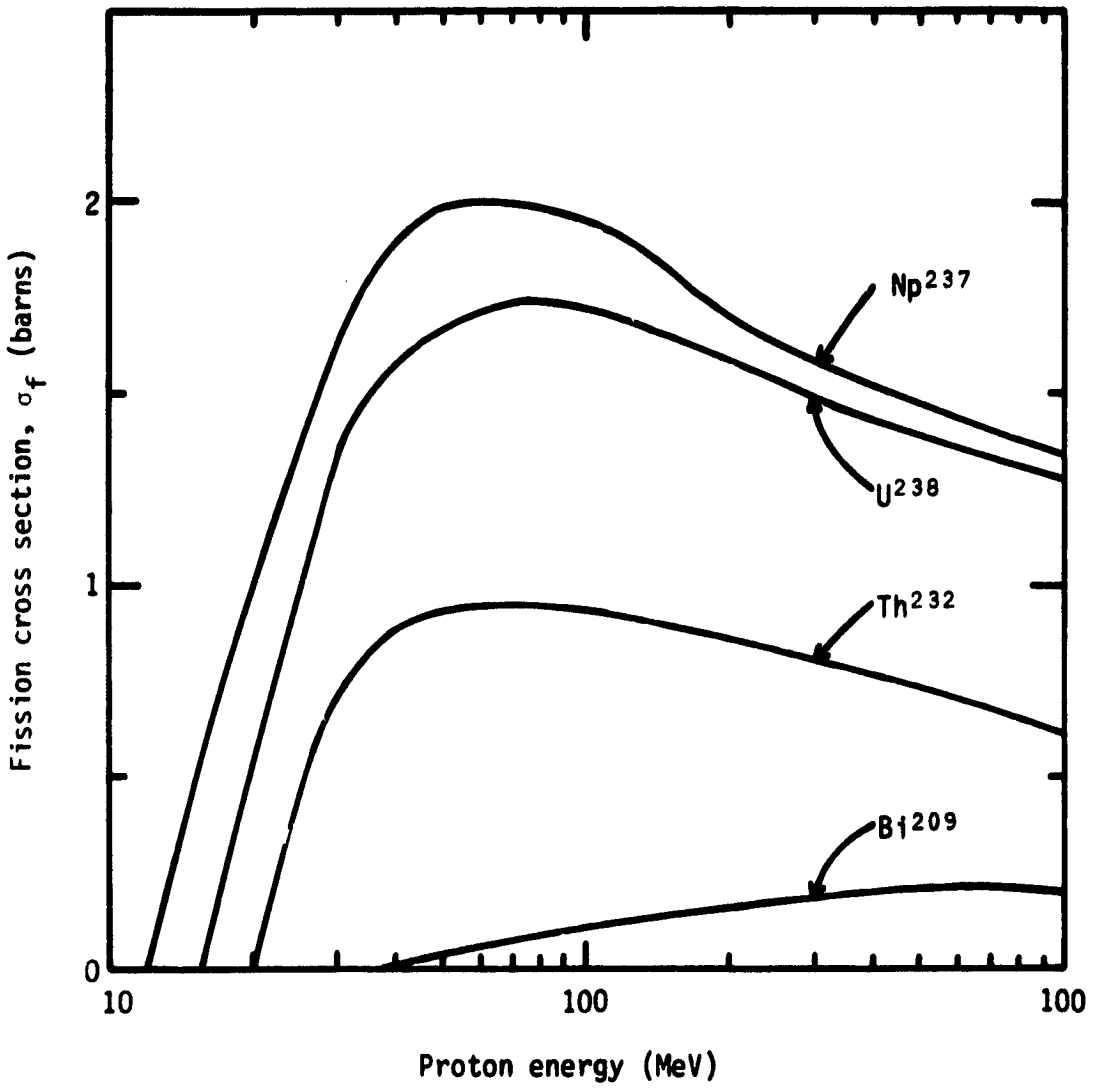
Fission cross section, σ_f (barns)
2
1
0
10
100
100
Proton energy (MeV)
Np^{237}
U^{238}
Th^{232}
Bi^{209}

Figure 20

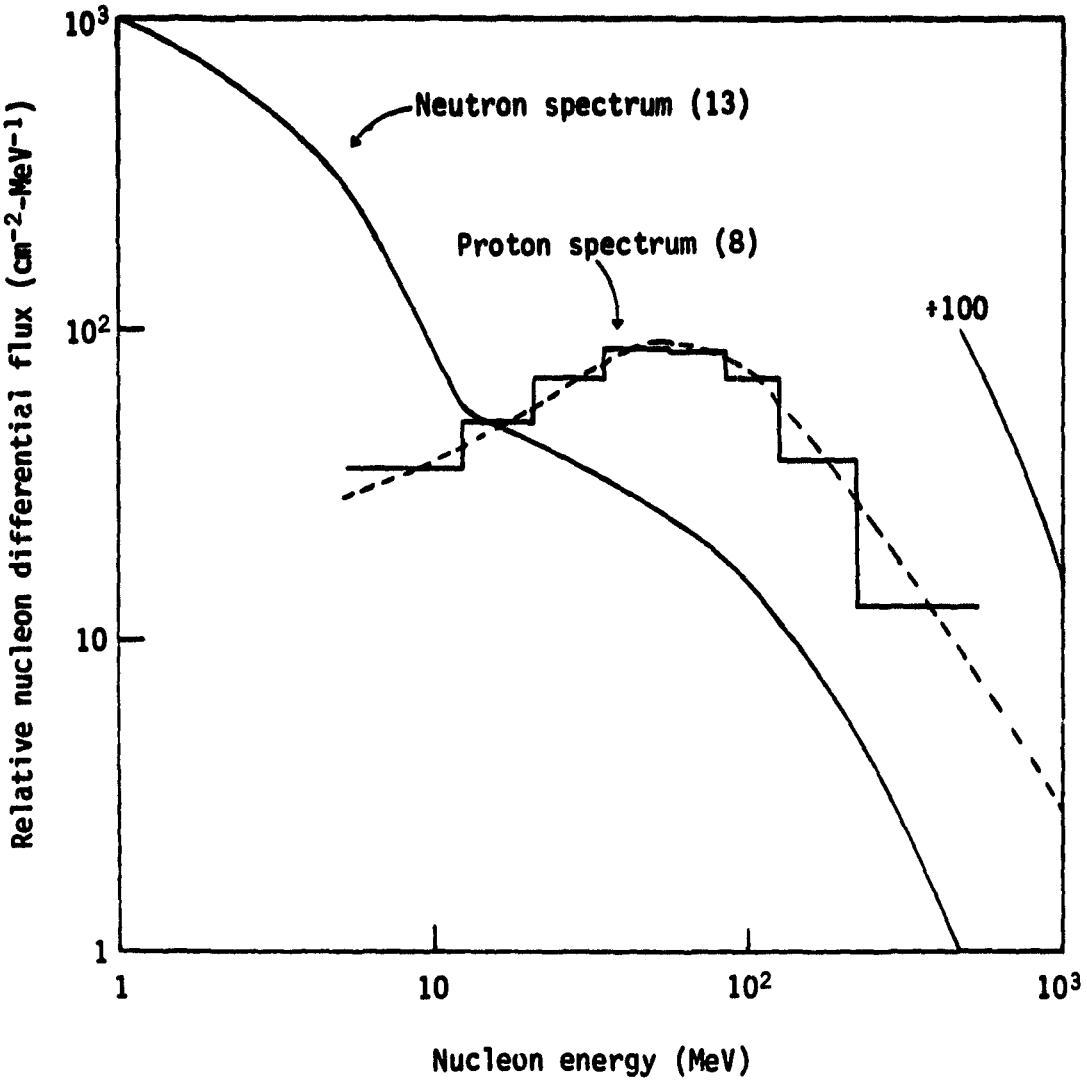

Figure 21

1. Report No.	2. Government Accession No.	3. Recipient's Catalog No.
NASA TM-81288		

4. Title and Subtitle	5. Report Date
FINAL REPORTS OF U.S. PLANT AND RADIATION DOSIMETRY EXPERIMENTS FLOWN ON THE SOVIET SATELLITE COSMOS 1129	May 1981
	6. Performing Organization Code

7. Author(s)	8. Performing Organization Report No.
Milton R. Heinrich and Kenneth A. Souza (eds.)	A-8572
	10. Work Unit No.
	805-91-01

9. Performing Organization Name and Address	11. Contract or Grant No.
Ames Research Center, NASA Moffett Field, Calif. 94035	
	13. Type of Report and Period Covered
12. Sponsoring Agency Name and Address	Technical Memorandum
National Aeronautics and Space Administration Washington, D.C. 20546	14. Sponsoring Agency Code

15. Supplementary Notes

16. Abstract

On September 25, 1979, the Soviet Union launched Cosmos 1129, an unmanned spacecraft carrying biology and physics experiments from 9 countries, including both the Soviet Union and the United States. The launch marked the third time the Soviet Union has flown U.S. experiments aboard one of its unmanned spacecraft — the first being Cosmos 782 in November 1975 and the second, Cosmos 936 in August 1977. All three flights have carried a variety of biological species and remained in orbit approximately 19 days. Aboard Cosmos 1129 were (1) 30 young male Wistar SPF rats used for a wide range of physiological studies; (2) experiments with plants, fungi, insects, and mammalian tissue cultures; (3) radiation physics experiments; (4) a heat convection study; (5) a rat embryology experiment in which an attempt was made to breed 2 male and 5 female rats during the flight; and (6) fertile quail eggs used to determine the effects of spaceflight on avian embryogenesis. After 18.5 days in orbit, the spacecraft landed in central Asia where a Soviet recovery team began experiment operations within a few hours of landing. Specimens for U.S. experiments were initially prepared at the recovery site or in Moscow and transferred to U.S. laboratories for complete analyses. An overview of the mission focusing on preflight, on-orbit, and postflight activites and the final reports of U.S. plant and radiation dosimetry experiments aboard Cosmos 1129 are presented.

17. Key Words (Suggested by Author(s))	18. Distribution Statement
Space biology Weightlessness Aerospace medicine	Unlimited STAR Category - 51

19. Security Classif. (of this report)	20. Security Classif. (of this page)	21. No. of Pages	22. Price*
Unclassified	Unclassified	194	$15.50

*For sale by the National Technical Information Service, Springfield, Virginia 22161